

AN ABSTRACT OF THE THESIS OF

Yo-Hsin Huang for the degree of Master of Science

in Chemistry presented on June 23, 1986

Title: The Photochemistry of Some Polyhalobenzenes

Abstract approved: Redacted for Privacy
Dr. Peter K. Freeman

The photodechlorination of fluoropentachlorobenzene was carried out by irradiation at 254 nm in acetonitrile and in hexane in the presence of triethylamine. The observed regiochemistries are rationalized in terms of C-Cl bond fission in the radical anion formed by electron transfer from the triethylamine. Two possible bent transition states are proposed in accordance with the negative chemical ionization mass spectrum of the fluoropentachlorobenzene.

The mode of bond fission in the radical anions of hexafluorobenzene, hexachlorobenzene, and tri-, tetra-, and pentafluorobenzene(s) was also studied using negative chemical ionization mass spectrometry. In order to determine the stability of the aryl anion generated from bond fission in the parent radical anion, an attempt was made to detect any further decomposition of the aryl

anion by analyzing the negative chemical ionization mass spectra of the following compounds: azobenzene, 2,2'-3,3',5,5',6,6'-octachloroazobenzene, 2,6-dichlorobenzophenone, 2,6-dichloro-2',4',6'-trimethylbenzophenone, benzoyl peroxide, and 2,2',6,6'-tetrachlorobenzoyl peroxide.

The photolysis of pentafluorobenzene at 254 nm in acetonitrile has been carried out by Freeman et al.,¹¹ wherein the formation of defluorination products, as well as the formation of at least four unidentified high molecular weight isomers with m/e 298 was observed. Thus, the same photolysis experiment was repeated in order to identify the high molecular weight isomers. In addition to the defluorination products, six isomers of octafluorobiphenyl were formed, whose mass spectra indicated the presence of four fluorines on each benzene ring, rather than three on one and five on the other. In order to identify these six isomers, synthesis of the appropriate octafluorobiphenyls was carried out using the Ullmann reaction. The six octafluorobiphenyl isomers formed in the photolysis mixture were then identified by comparing their gas chromatographic retention times and mass spectra with those of the synthesized compounds. A mechanistic scheme is proposed for the formation of the six octafluorobiphenyl isomers.

The Photochemistry of Some Polyhalobenzenes

by

Yo-Hsin Huang

A THESIS

submitted to

Oregon State University

In partial fulfillment of
the requirements for the
degree of

Master of Science

Completed June 23, 1986

Commencement June 1987

APPROVED:

Redacted for Privacy

Professor of Chemistry in charge of major

Redacted for Privacy

Head of Department of Chemistry

Redacted for Privacy

Dean of Graduate School

Date thesis is presented June 23, 1986

Typed by Violet Jonas for Yo-Hsin Huang

ACKNOWLEDGMENT

I would like to thank Professor Peter K. Freeman for his guidance throughout my graduate studies. I would like to thank Dr. Violet Jonas and Dr. Ramanujan Srinivasa for their helpful suggestions. I would like to thank Lorenz Siggel for his valuable friendship, encouragement, and concern, with whom I spent many hours both in and out of the lab, and for the knowledge and experience he shared with me, and for the patience he showed in answering my numerous questions. I would like to thank Brian Arbogast for his work in running the gas chromatograph-mass spectrometer, and Rodger Kohnert for his work in running the ^1H , ^{13}C , and ^{19}F NMR spectra and exact masses during the course of my research.

I also wish to thank my fiancée, Ms. Shu-Chih Tang, and my parents for their emotional support and their love, which have sustained me more than I can say.

TABLE OF CONTENTS

INTRODUCTION	1
RESULTS AND DISCUSSION	24
The Regiochemistry of Photodechlorination of Fluoropentachlorobenzene	24
Negative Chemical Ionization Mass Spectral Study of Bond Fission in Hexafluorobenzene and Hexachlorobenzene	36
Negative Chemical Ionization Mass Spectral Study of Bond Fission in Polyfluorobenzenes	42
The Detection of Further Decomposition of the Aryl Anion	46
Identification of the Octafluorobiphenyls Formed in the Photolysis of Pentafluoro- benzene	57
EXPERIMENTAL	66
General	66
Preparation of Fluoropentachlorobenzene (<u>8</u>)	67
Preparation of 1-Fluoro-2,3,4,5-tetrachloro- benzene (<u>9</u>)	68
Preparation of 1-Fluoro-2,3,5,6-tetrachloro- benzene (<u>11</u>)	69
Photolysis of Fluoropentachlorobenzene (<u>8</u>) in Acetonitrile in the Presence of Tri- ethylamine and Product Analysis	70
Photolysis of Fluoropentachlorobenzene (<u>8</u>) in Hexane in the Presence of Triethyl- amine and Product Analysis	73

Negative Chemical Ionization Mass Spectrometric Study of Fluoropentachlorobenzene (8)	74
Negative Chemical Ionization Mass Spectrometric Study of Hexafluorobenzene and Hexachlorobenzene	75
Negative Chemical Ionization Mass Spectrometric Study of Polyfluorobenzenes	75
Detection of Further Decomposition of the Aryl Anion Using Negative Chemical Ionization Mass Spectrometry	76
Preparation of 2,2',3,3',5,5',6,6'-Octafluoroazobenzene (29)	77
Preparation of 2,6-Dichlorobenzophenone (32)	78
Preparation of 2,6-Dichloro-2',4',6'-trimethylbenzophenone (35)	80
Preparation of 2,2',6,6'-Tetrachlorobenzoyl Peroxide (41)	80
Preparation of 2,2',3,3',4,4',5,5'-Octafluorobiphenyl (50)	82
Preparation of 2,2',3,3',4,4',6,6'-Octafluorobiphenyl (51)	82
Preparation of 2,2',3,3',4,4',5,6'-Octafluorobiphenyl (53)	83
Preparation of 2,2',3,3',4,5,5',6'-Octafluorobiphenyl (54)	84
Preparation of 2,2',3,3',4,5',6,6'-Octafluorobiphenyl (55)	85
Preparation of 2,2',3,3',5,5',6,6'-Octafluorobiphenyl (52)	86
Photolysis of Pentafluorobenzene (45) in Acetonitrile in the Absence of Triethylamine	87

APPENDICES

		91
Appendix I.	GC-MS Data for Photoproducts of Fluoropentachlorobenzene	91
Appendix II.	¹³ C-NMR Spectra of the Octa- fluorobiphenyls <u>50</u> - <u>55</u>	92
Appendix III.	¹⁹ F-NMR Spectra of the Octa- fluorobiphenyls <u>50</u> - <u>55</u>	105

LIST OF FIGURES

FIGURE	Page
1. A concise energy level diagram showing transitions between excited states and the ground state.	2
2. Orbital interactions of AB collision pairs and A*B collision complexes.	5
3. Plot of $1/\phi$ versus the reciprocal of the triethylamine concentration for the photolysis of pentafluorobenzene in acetonitrile.	18
4. Plot of $1/\phi$ versus the reciprocal of the pentafluorobenzene concentration for the photolysis of pentafluorobenzene in acetonitrile.	20
5. The negative chemical ionization mass spectrum of 2,6-dichlorobenzophenone (<u>32</u>).	51
6. The negative chemical ionization mass spectrum of 2,6-dichloro-2',4',6'-trimethylbenzophenone (<u>35</u>).	52
7. ^{13}C -NMR spectrum of 2,2',3,3',4,4',5,5'-octafluorobiphenyl (<u>50</u>).	93
8. ^{13}C -NMR spectrum of 2,2',3,3',4,4',6,6'-octafluorobiphenyl (<u>51</u>).	95
9. ^{13}C -NMR spectrum of 2,2',3,3',5,5',6,6'-octafluorobiphenyl (<u>52</u>).	97
10. ^{13}C -NMR spectrum of 2,2',3,3',4,4',5,6'-octafluorobiphenyl (<u>53</u>).	99
11. ^{13}C -NMR spectrum of 2,2',3,3',4,5,5',6'-octafluorobiphenyl (<u>54</u>).	101
12. ^{13}C -NMR spectrum of 2,2',3,3',4,5',6,6'-octafluorobiphenyl (<u>55</u>).	103

FIGURE		Page
13.	^{19}F -NMR spectrum of 2,2',3,3',4,4',5,5'-octafluorobiphenyl (<u>50</u>).	106
14.	^{19}F -NMR spectrum of 2,2',3,3',4,4',6,6'-octafluorobiphenyl (<u>51</u>).	108
15.	^{19}F -NMR spectrum of 2,2',3,3',5,5',6,6'-octafluorobiphenyl (<u>52</u>).	110
16.	^{19}F -NMR spectrum of 2,2',3,3',4,4',5,6'-octafluorobiphenyl (<u>53</u>).	112
17.	^{19}F -NMR spectrum of 2,2',3,3',4,5,5',6'-octafluorobiphenyl (<u>54</u>).	114
18.	^{19}F -NMR spectrum of 2,2',3,3',4,5',6,6'-octafluorobiphenyl (<u>55</u>).	116

LIST OF TABLES

TABLE	Page
1. Solvent Effects on The Rate of Product Formation in the Photolysis of Various Haloarenes in the Presence of Triethylamine.	10
2. Photolysis of Polychlorobenzenes in Acetonitrile with TEA Present.	13
3. Sensitized Photolysis of Polychlorobenzenes in Acetonitrile with TEA present.	14
4. Results Obtained for the Photolysis of Fluoropentachlorobenzene in the Presence of Triethylamine.	25
5. Gas Chromatographic Retention Times of the Fluorotetrachlorobenzenes <u>9</u> , <u>10</u> , and <u>11</u> .	26
6. Negative Chemical Ionization Mass Spectral Results for Hexafluorobenzene and Hexachlorobenzene.	39
7. Negative Chemical Ionization Mass Spectral Results for the Polyfluorobenzene System.	44
8. Gas Chromatographic Retention Times of the Octafluorobiphenyls <u>50</u> - <u>55</u> .	62
9. Results Obtained for the Photolysis of Fluoropentachlorobenzene at 254 nm in Acetonitrile in the Presence of Triethylamine.	72
10. Results Obtained for the Photolysis of Fluoropentachlorobenzene at 254 nm in Hexane in the Presence of Triethylamine.	74

The Photochemistry of Some Polyhalobenzenes

INTRODUCTION

Reactions which are initiated by light are called photochemical reactions. The interaction of photons with molecules and the physical and chemical processes which follow the absorption of light are of great interest to the organic photochemist. Absorption of a photon of light by a molecule results in the excitation of an electron of a bond or a group. Since the energy levels of a molecule are quantized, the amount of energy required to raise an electron from a lower level to a higher one is a fixed quantity. Use of the proper frequency of light allows the excitation of a solute molecule in the presence of a large excess of a transparent solvent. Upon the absorption of ultraviolet light an excited molecule may cleave into two parts, since the energy of ultraviolet light is of the same order of magnitude as that of covalent bonds. Such a process is known as photolysis.

The electronic transitions for the absorption of a photon and subsequent loss of energy are depicted by the energy level diagram shown in Figure 1 on the next page. Radiative processes are shown by the straight lines and

radiationless processes by the wavy lines. The ground state is arbitrarily assigned a relative energy of zero.

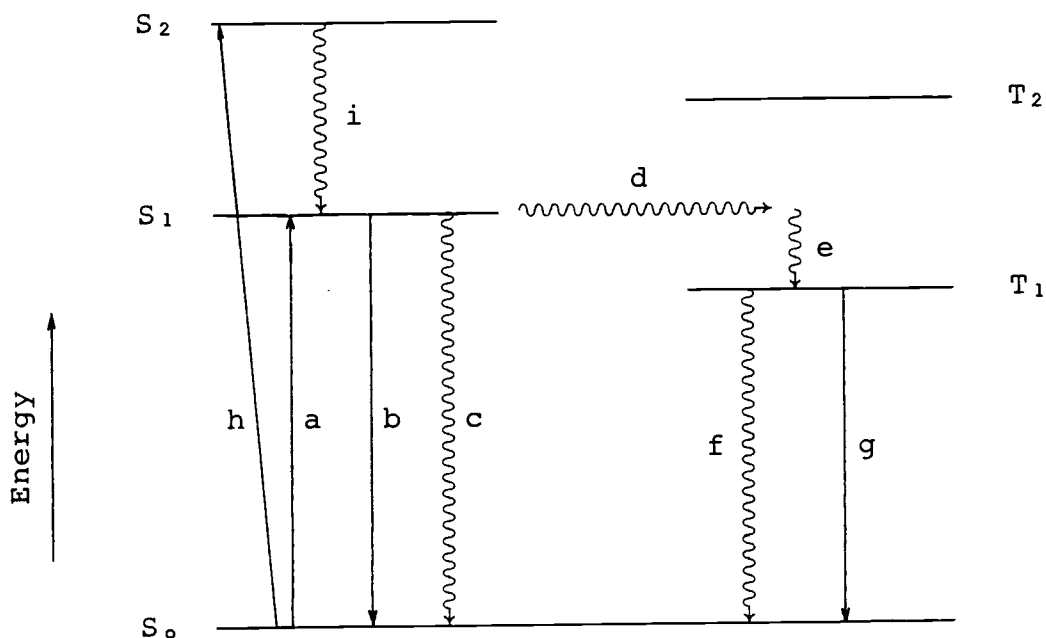


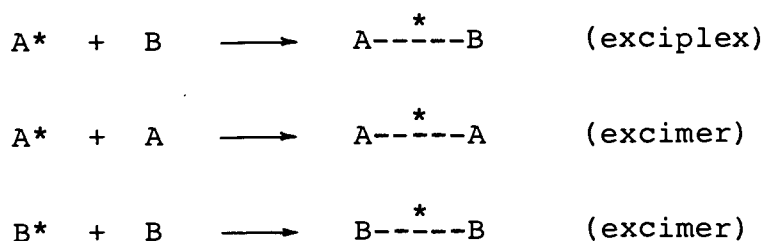
Figure 1. A concise energy level diagram showing transitions between excited states and the ground state.

When a molecule has been photochemically promoted to an excited state, it does not remain there for long. Most promotions are from the ground state S_0 to the first singlet excited state S_1 (a). Promotion from the ground state to the second excited state S_2 is represented by h . However, in liquids and solids this higher state usually drops very rapidly to the S_1 state by giving up its

energy to the environment through collisions with neighboring molecules (i). This radiationless process is called internal conversion. The first excited singlet S_1 or Triplet T_1 state may return to the ground state S_0 by emitting light: $S_1 \rightarrow S_0 + h\nu$ (b) or $T_1 \rightarrow S_0 + h\nu$ (g). In the former case, the process is referred to as fluorescence; whereas in the latter case the process is referred to as phosphorescence. A radiationless transition from the lowest vibrational level of S_1 to a vibrationally excited level of T_1 is called intersystem crossing (d). Cascade from an upper vibrational level of T_1 to the lowest one is depicted by e. Radiationless internal conversion from S_1 or T_1 to S_0 (c and f) is relatively slow compared to the rate of radiationless processes among excited states, because the separation of the energy levels is much larger in the former case.

All photochemical reactions involve an electronically excited state at some point. Each excited state has a definite energy, lifetime, and structure. These properties may all be somewhat different in going from one state to another. During the study of the photodefluorination of pentafluorobenzene, two kinds of electronically excited states were formed, the excimer and the exciplex.^{1,2,3} An electronically excited state, A^* , may react with any polar or polarizable ground state species, B, and generate a collision complex, A^*B , which

will be stabilized by some charge-transfer interaction. Usually, the observable properties of the new A^*B collision complex are different from those of A^* . Such a new electronically excited species is called an exciplex. When both A and B are the same species, then the collision complex, A^*A or B^*B , is called an excimer:



Use of the simple theory of molecular orbital (MO) interaction⁴ will enable us to rationalize the enhanced stabilization of the collision complex, excimer or exciplex, relative to the corresponding ground state collision pair. In the case of the ground state reaction between two molecules, the interaction of the two occupied orbitals will end up with no gain in energy during the collision, because the stabilization of two electrons will be cancelled out by the destabilization of two other electrons, as shown in Figure 2a on the next page. Although the interaction between occupied and unoccupied orbitals will lower the energy of the transition state, the energy separations are still so large that this kind

of interaction has only a second order effect. However, when the photochemically excited state of one molecule interacts with the ground state of another, which may or may not be the same species, the interaction will usually be strong, because the interacting orbitals are close in energy, as shown in Figure 2b.

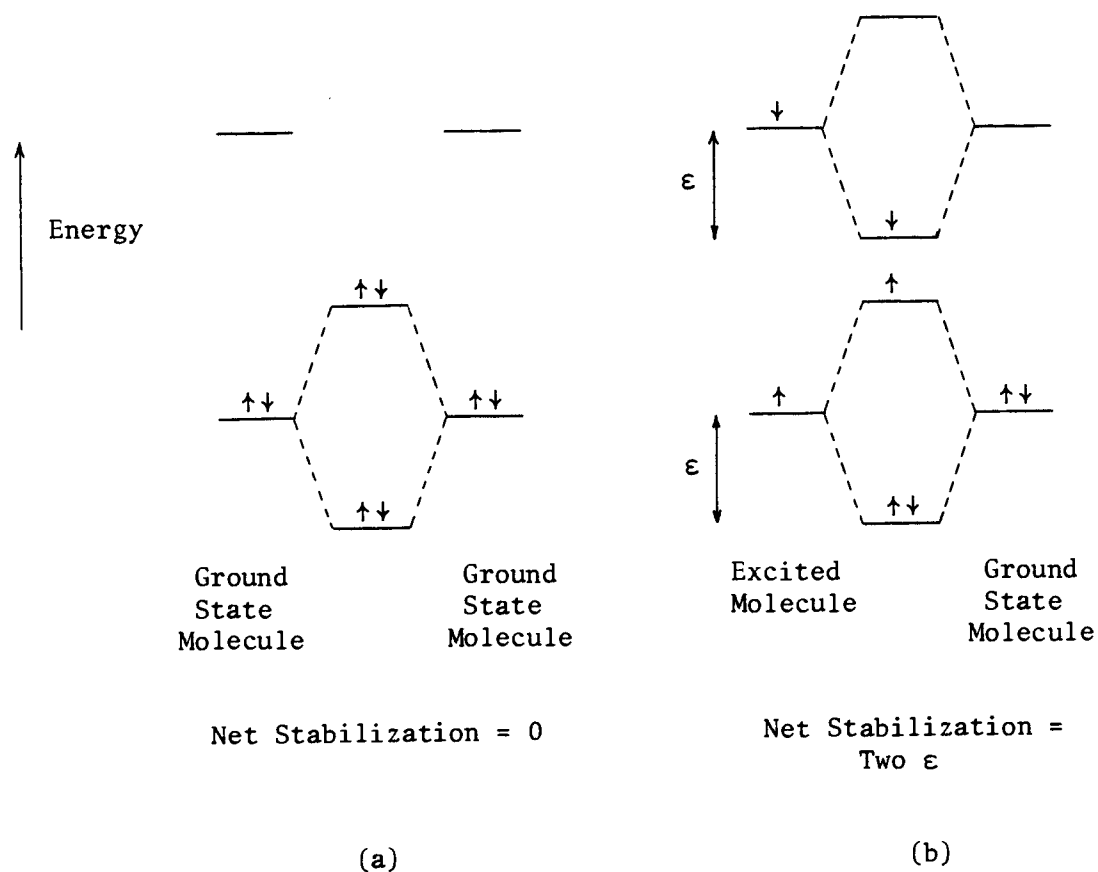
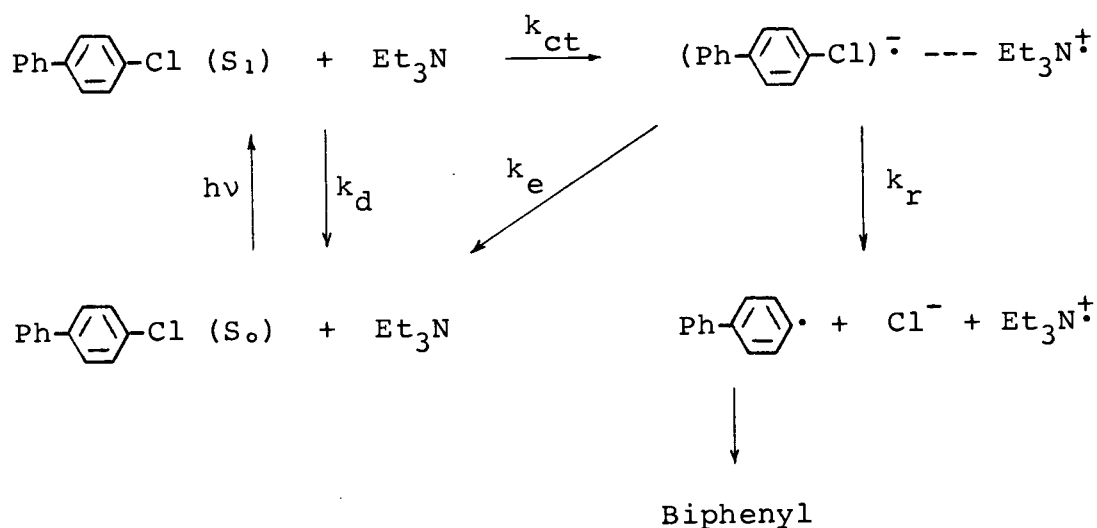


Figure 2. Orbital interactions of (a) AB collision pairs and (b) A*B collision complexes.

In this situation, three electrons are stabilized and only one electron is destabilized, as the electrons redistribute themselves from their original noninteracting orbitals to the new orbitals of the collision complex. Thus, the total energy of the excimer or exciplex is lower than that of the two noninteracting components.

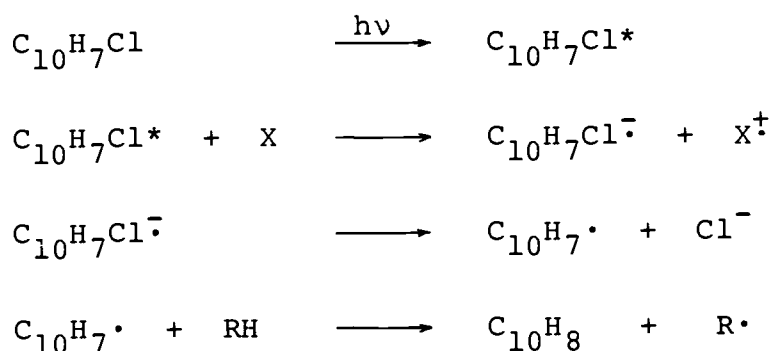
Application of photochemical theory to the study of the photodehalogenation of haloarenes will provide us with further understanding of the transition states and the reaction mechanisms.⁵ Ohashi et al. studied the photoinduced dechlorination of 4-chlorobiphenyl by triethylamine in acetonitrile.⁶ They observed that the triethylamine both quenched the fluorescence of the aryl chloride and also enhanced its photolability. They thus proposed the mechanism shown in Scheme I on the next page for the amine-assisted photodechlorination of 4-chlorobiphenyl. The singlet state may return to the ground state either by radiative or nonradiative decay (k_d) or undergo electron transfer with triethylamine to form a charge transfer complex (k_{ct}), which is the key intermediate of this reaction. The charge transfer complex thus generated can either undergo reverse electron transfer (k_e) or cleave to form products (k_r). It should be noted that a radical anion intermediate is the precursor undergoing fission to aryl radical and chloride ion.



Scheme I

Bunce et al. reported that the photoreduction of 1-chloronaphthalene to naphthalene was assisted by electron donors such as triethylamine (TEA) and 1,3-cyclohexadiene, and that the reaction proceeded via an excited charge-transfer complex.⁷ In the absence of such electron donors, 1-chloronaphthalene itself acted as a donor species, and the reaction quantum yield increased with increasing concentration of 1-chloronaphthalene, suggesting the involvement of an excimer in the reaction. Scheme II was proposed as the mechanism

for these photoreductions.



X = cyclohexadiene, TEA, or $\text{C}_{10}\text{H}_7\text{Cl}$

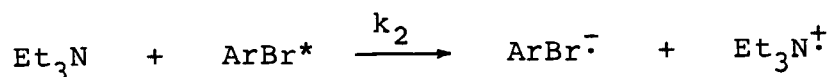
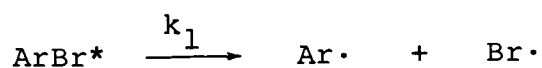
Scheme II

Bunce and his coworkers also reported that the use of a polar solvent such as an acetonitrile solution of an alkane, rather than a nonpolar solvent such as a pure alkane, was more effective in breaking up the radical cation - radical anion pair, thereby reducing the probability of back electron transfer, and thus accelerating both the direct and amine assisted reactions. This solvent effect supported the involvement of the exciplex or excimer intermediate.

Davidson and Goodin⁸ studied the photo-induced dehalogenation of various haloarenes by triethylamine using three solvents of widely differing polarity. Their

results, which are shown in Table 1, were consistent with those obtained for the study of the solvent effect on the dechlorination of 1-chloronaphthalene carried out by Bunce et al.⁷ The results in Table 1 show that the accelerating effect of TEA was more pronounced for chloro compounds than for bromo compounds in acetonitrile, and Davidson and Goodin⁸ used the following considerations to rationalize this observation:

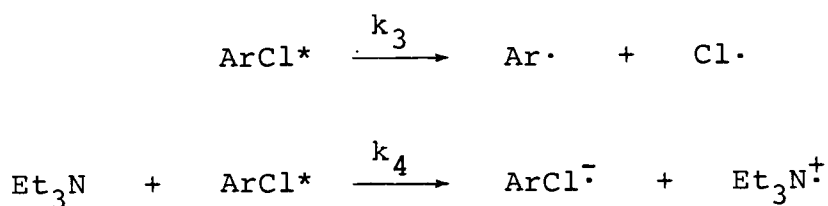
1. Due to the heavy atom effect, the lifetimes of the excited states of bromo compounds were shorter than those of the corresponding chloro compounds.
2. The homolysis of the C-Br bond competed effectively with the reaction with TEA; i.e., $k_1(\text{ArBr}^*) > k_2(\text{ArBr}^*)(\text{Et}_3\text{N})$.



On the other hand, the dehalogenation of chloro compounds was more energy demanding than that of the bromo compounds, which caused the reaction with TEA to be more competitive; i.e., $k_4(\text{ArCl}^*)(\text{Et}_3\text{N}) > k_3(\text{ArCl}^*)$.

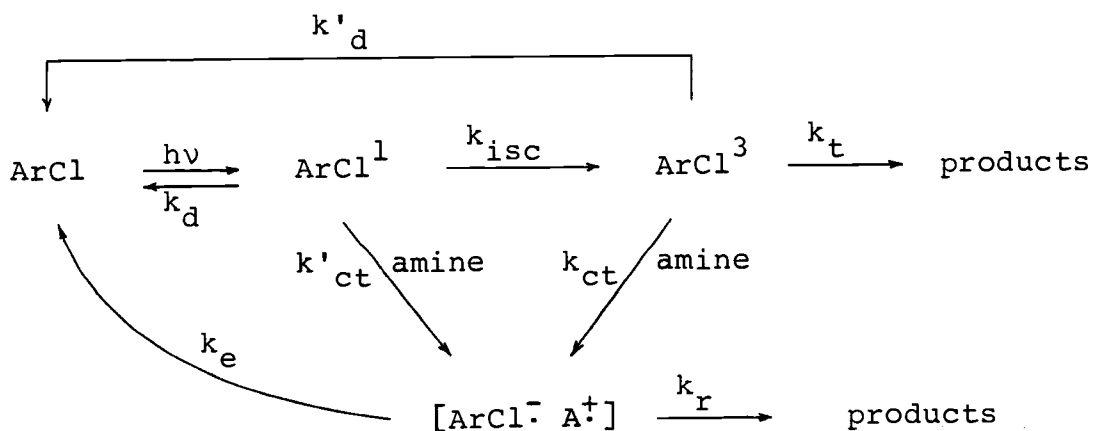
Table 1. Solvent Effects on the Rate of Product Formation in the Photolysis of Various Haloarenes in the Presence of Triethylamine.

Substrate	Product	Comparative Rate of Product Formation		
		Acetonitrile	Methanol	Cyclohexane
1-Chloronaphthalene	Naphthalene	34.5	4.1	1.0
1-Bromonaphthalene	Naphthalene	12.4	4.3	1.0
4-Chlorobiphenyl	Biphenyl	32.0	11.5	1.0
4-Bromobiphenyl	Biphenyl	6.9	4.6	1.0
4-Chloroanisole	Anisole	3.0	1.0	1.0
4-Bromoanisole	Anisole	1.9	1.4	1.0
4-Chlorobenzonitrile	Benzonitrile	11.7	2.8	1.0



It should be noted that these results indicated exciplex formation.

Bunce⁹ investigated the photodechlorination of aryl chlorides in the presence of aliphatic amines and proposed a mechanism in which the light absorption by the aryl halide was followed by the interactions of the amine with either the singlet or the triplet excited state of the halide, as shown in Scheme III.



SCHEME III

Bunce observed that the singlet state process led to fluorescence, while the triplet state interaction was mainly

responsible for the amine-assisted photodechlorination.

Freeman et al. studied the photochemistry of polychlorobenzenes and observed that the regiochemistry was very similar for the photodechlorination of trichlorobenzenes, tetrachlorobenzenes, and pentachlorobenzene in the presence of triethylamine, with and without acetophenone sensitizer (Tables 2 and 3).¹⁰ These results suggest that identical product determining intermediates are formed from both direct and sensitized irradiations in the presence of triethylamine, and that the dehalogenation of haloarenes does not solely involve the singlet excited state.

In the course of the photochemical reaction of haloarenes, both the excited state and the radical anion played important roles and were potential intermediates leading to product formation. In order to determine the relative importance of the excited state species and the related radical anion as product determining intermediates, Freeman et al. carried out the kinetic study of the photolysis of tri-, tetra-, and pentachlorobenzenes. Each polychloroarene was irradiated at 254 nm in acetonitrile in the presence of different concentrations of triethylamine. The kinetic results suggest the pathway shown in Scheme IV on p. 15, wherein a singlet state intermediate is assumed.

TABLE 2. Photolysis of Polychlorobenzenes^a in Acetonitrile with TEA^b Present.

Photoproducts:	YIELD (Mole %)				
	1,2,4-TCB	1,2,3-TCB	1,2,3,5-TCB	1,2,3,4-TCB	C ₆ HCl ₅
1,3-DCB	18.19±0.11	46.72±0.25	0.0	0.0	0.0
1,4-DCB	75.25±0.25	-	0.0	0.0	0.0
1,2-DCB	6.57±0.35	53.28±0.25	0.0	0.0	0.0
1,3,5-TCB	-	-	18.77±1.0	0.0	Trace
1,2,4-TCB	-	-	75.45±1.4	80.12±2.7	Trace
1,2,3-TCB	-	-	5.78±0.61	19.88±2.7	Trace
1,2,3,5-TCB	-	-	-	-	25.32±0.47
1,2,4,5-TCB	-	-	-	-	66.21±0.46
1,2,3,4-TCB	-	-	-	-	8.47±0.06

^a 0.05 M in each case.

^b 1.5 M.

^c Normalized and average of five runs with standard deviations.

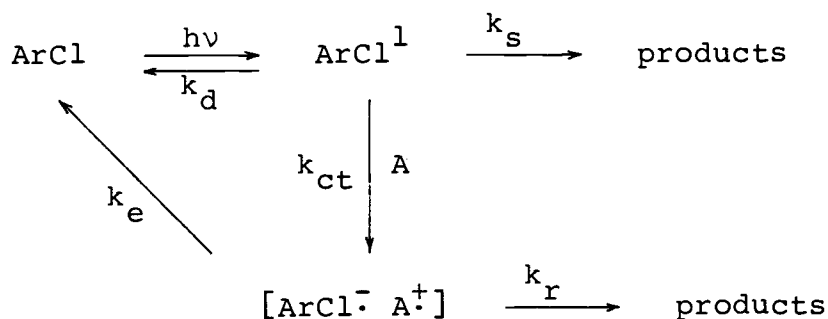
TABLE 3. Sensitized Photolysis of Polychlorobenzenes^a in Acetonitrile with TEA^b present.

Photoproducts:	YIELD (Mole %) ^c				
	1,2,4-TCB	1,2,3-TCB	1,2,3,5-TCB	1,2,3,4-TCB	C ₆ HCl ₅
1,3-DCB	21.11±0.37	42.90±1.94	0.0	0.0	0.0
1,4-DCB	72.91±0.40	-	0.0	0.0	0.0
1,2-DCB	5.98±0.27	57.10±1.94	0.0	0.0	0.0
1,3,5-TCB	-	-	22.21±0.71	0.0	Trace
1,2,4-TCB	-	-	72.94±0.78	83.38±0.79	Trace
1,2,3-TCB	-	-	4.85±0.47	16.62±0.79	Trace
1,2,3,5-TCB	-	-	-	-	24.33±0.23
1,2,4,5-TCB	-	-	-	-	69.43±0.33
1,2,3,4-TCB	-	-	-	-	6.24±0.44

^a 0.05 M in each case.

^b 1.5 M.

^c Normalized and average of five runs with standard deviations.



SCHEME IV

Using the steady state approximation, the expression shown in Equation 1 is obtained for the reciprocal of the quantum yield, $1/\Phi$, for product formation.

$$\frac{1}{\Phi} = \frac{k_s + k_d + k_{ct}[A]}{k_s + F \cdot k_{ct}[A]} \quad \text{where } F = \frac{k_r}{k_r + k_e} \quad (1)$$

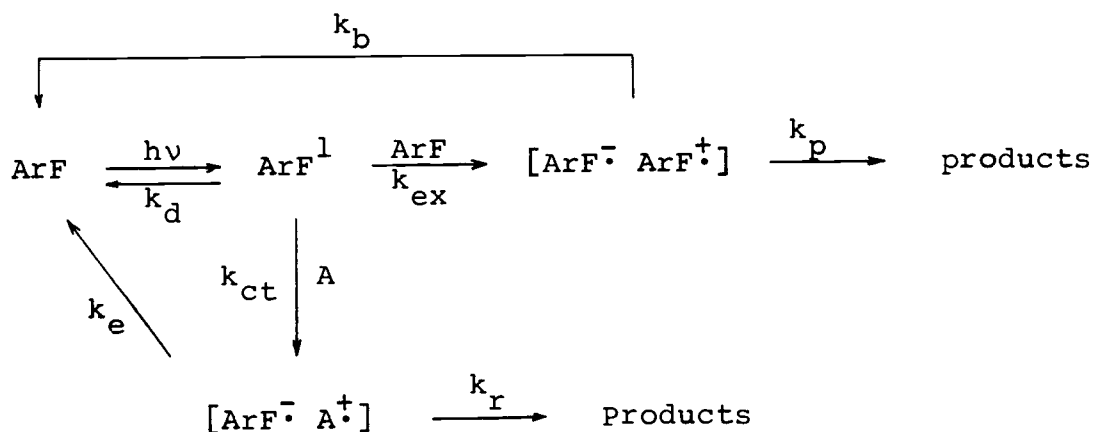
For higher concentrations of triethylamine, A, where $k_{ct}[A]$ and $F \cdot k_{ct}[A] \gg k_s$, Equation 1 reduces to Equation 2.

$$\frac{1}{\Phi} = \frac{1}{F} + \frac{k_d}{F \cdot k_{ct}[A]} \quad (2)$$

A plot of $1/\Phi$ vs. $1/[A]$ gives a straight line for higher concentrations of triethylamine, A (i.e., for lower values of $1/[A]$), as predicted by Equation 2, and thus suggests predominance of radical anion formation; whereas the plot flattens out for lower concentrations

of triethylamine, A (i.e., for higher values of $1/[A]$), in accordance with Equation 1, thus indicating the alternate route to products. The midpoint of the linear portion of the plot of $1/\phi$ vs. $1/[A]$ corresponds to the optimum concentration of triethylamine that would result in the predominance of the radical anion over the excited state as the product determining intermediate.

Freeman and Srinivasa¹¹ also studied the related aspects of the phototransformations of polyfluorobenzenes. A kinetic study of the photolysis of pentafluorobenzene was carried out in the presence and absence of triethylamine, and Scheme V was proposed as the mechanism. Products arise from two competing pathways, excimer formation and charge transfer complex formation between singlet pentafluorobenzene (ArF^1) and the electron donor reagent, triethylamine.



Scheme V

This proposed mechanism was supported by the following evidence:

1. The quantum yields for photolysis of pentafluorobenzene in the presence of different concentrations of triethylamine in acetonitrile and pentane were determined at 254 nm using cyclopentanone actinometry. The plot of $1/\phi$ versus $1/[A]$ for acetonitrile is presented in Figure 3, and the plot for pentane is similar. Application of the steady state assumption allows one to derive Equation 3.

$$\frac{1}{\phi} = \frac{k_{ct}[A] + k_{ex}[ArF] + k_d}{k_{ct}[A]F + k_{ex}[ArF]G} \quad \text{where } F = \frac{k_r}{k_r + k_e} \quad (3)$$

$$\text{and } G = \frac{k_p}{k_p + k_b}$$

For higher concentrations of triethylamine, Equation 3 is simplified to Equation 4.

$$\frac{1}{\phi} = \frac{1}{F} + \frac{k_{ex}[ArF] + k_d}{k_{ct}[A]F} \quad (4)$$

As can be seen in Figure 3, the plot of $1/\phi$ vs. $1/[A]$ is linear for higher concentrations of triethylamine (lower $1/[A]$), suggesting exciplex formation by electron transfer from triethylamine. However, the plot

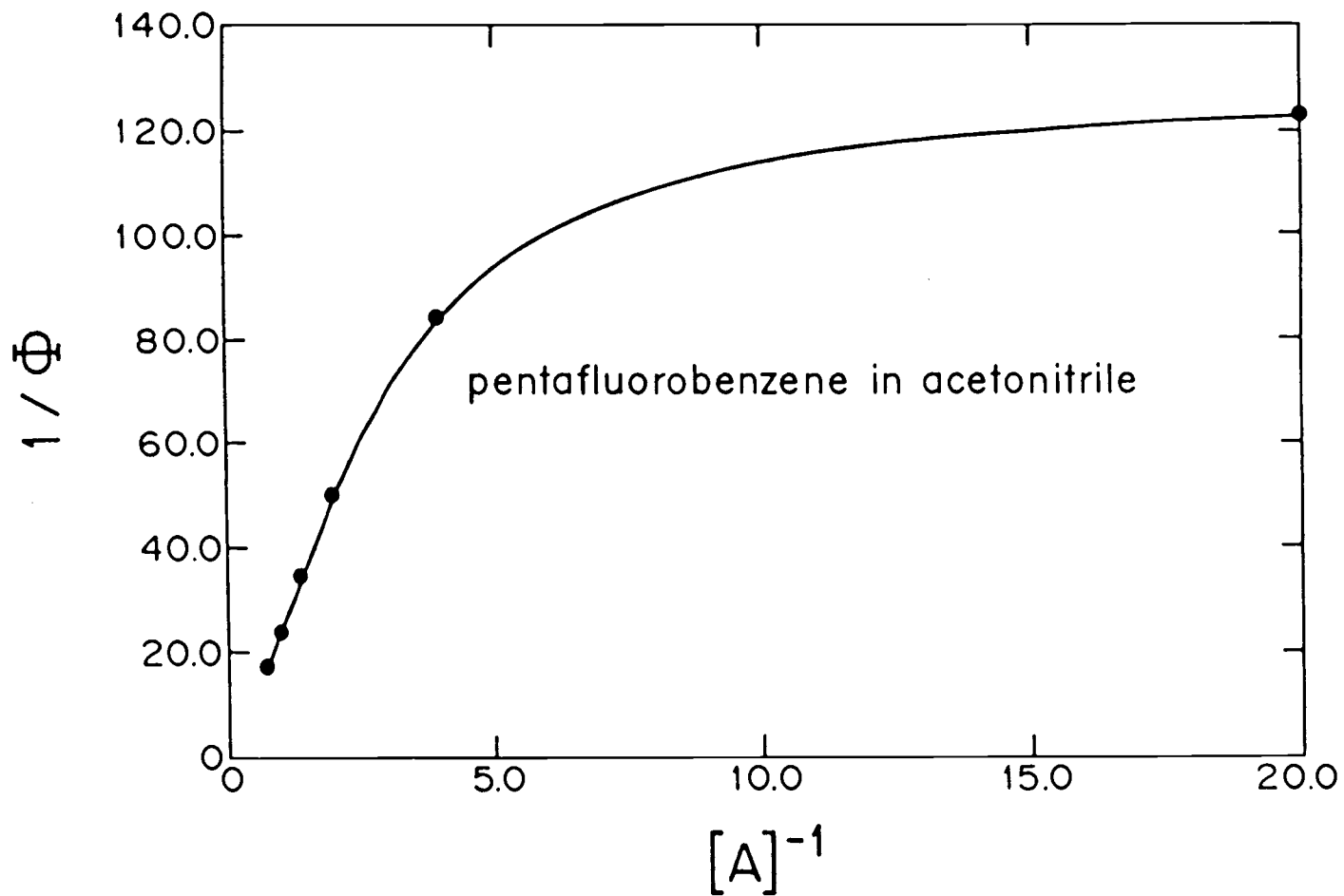
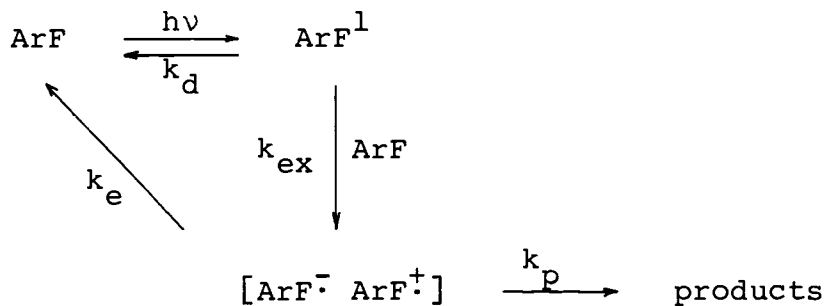


Figure 3. Plot of $1/\Phi$ versus the reciprocal of the triethylamine concentration for the photolysis of pentafluorobenzene in acetonitrile.

flattens out for lower concentrations of triethylamine, i.e., as $1/[A]$ increases, suggesting an alternate route to products in the absence of triethylamine.

2. The quantum yields for photolysis of different concentrations of pentafluorobenzene in acetonitrile at 254 nm were determined. Scheme VI was proposed as the mechanism.



Scheme VI

Using the steady state assumption, Equation 5 was derived.

where

$$\frac{1}{\phi} = \frac{1}{F} + \frac{k_d}{F \cdot k_{\text{ex}} [\text{ArF}]} \quad F = \frac{k_p}{k_p + k_e} \quad (5)$$

A plot of $1/\phi$ versus $1/[\text{ArF}]$ is linear, as shown in Figure 4 (correlation coefficient $r = 0.999$) This is a result which implies excimer formation.

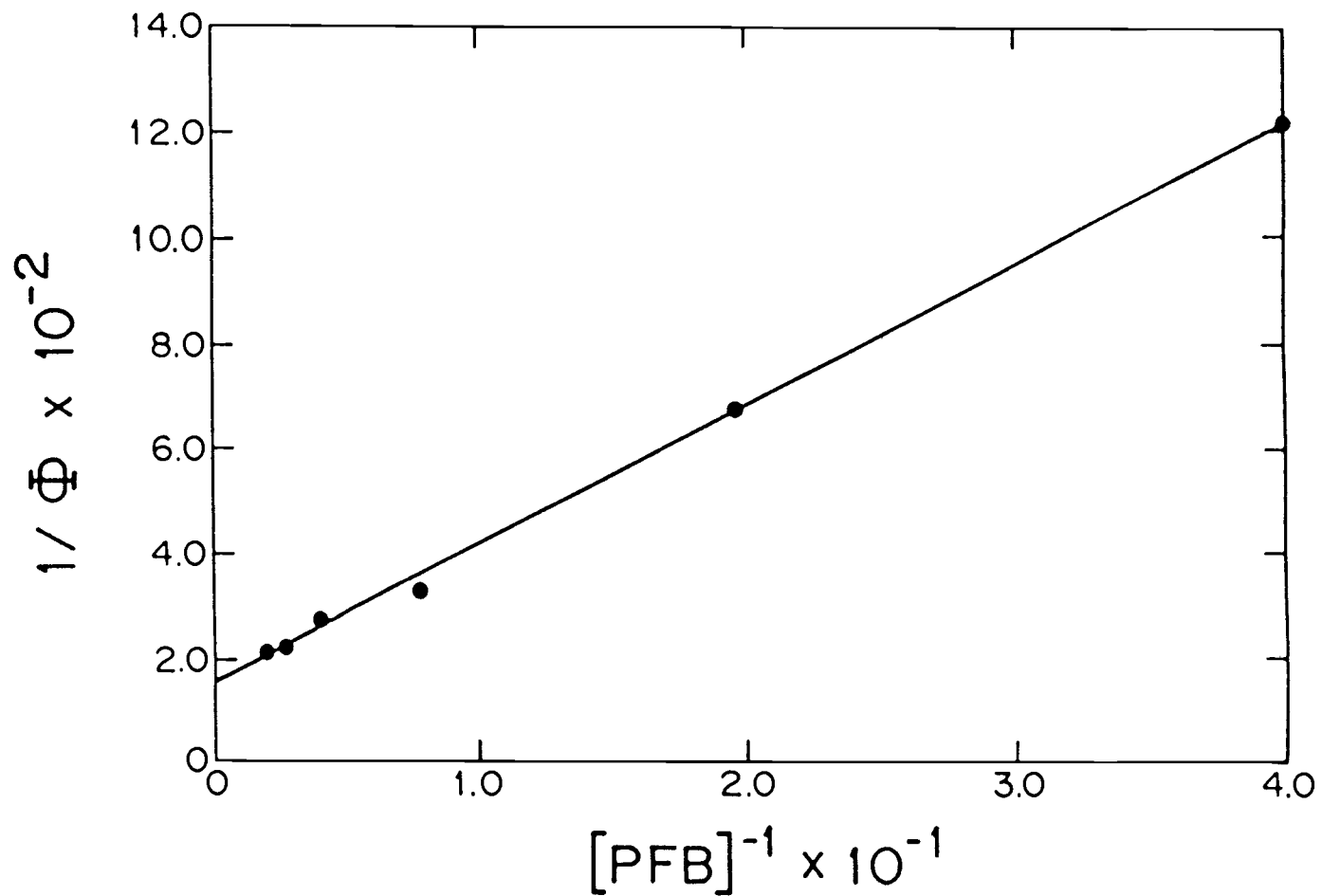
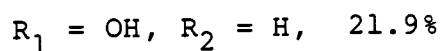
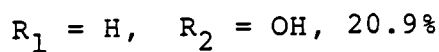
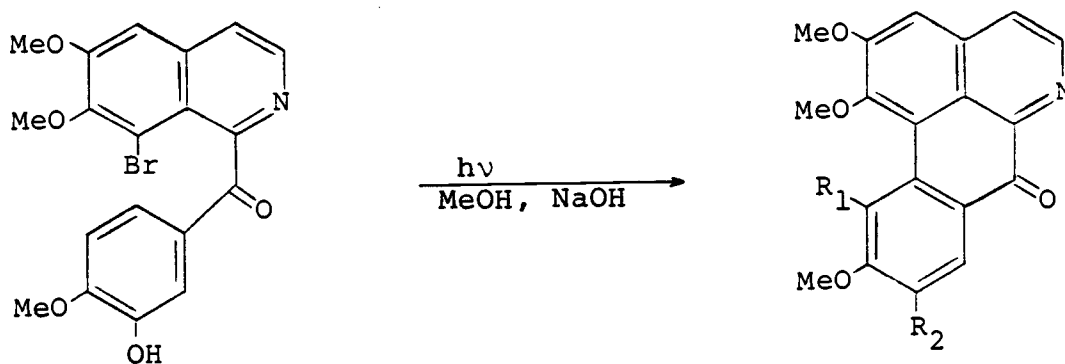
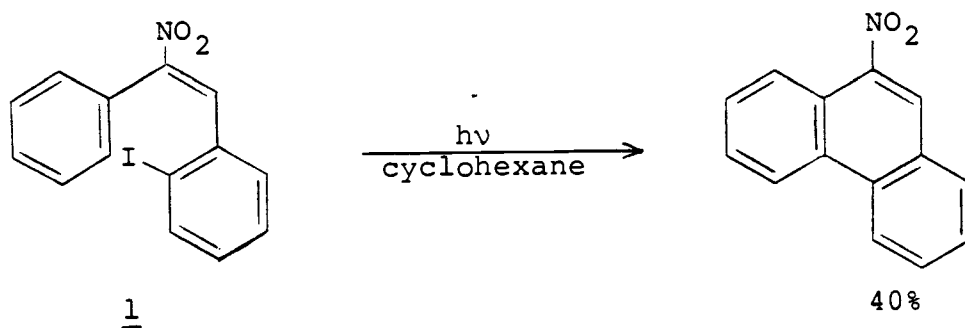
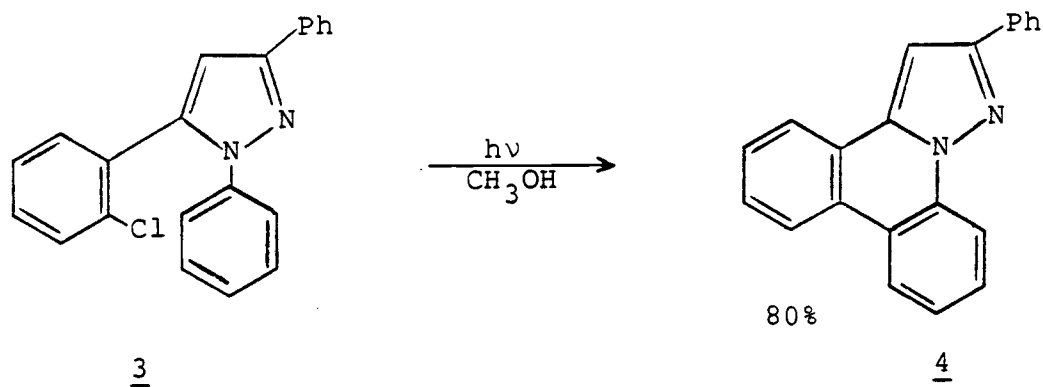


Figure 4. Plot of $1/\Phi$ versus the reciprocal of the pentafluorobenzene concentration for the photolysis of pentafluorobenzene in acetonitrile.

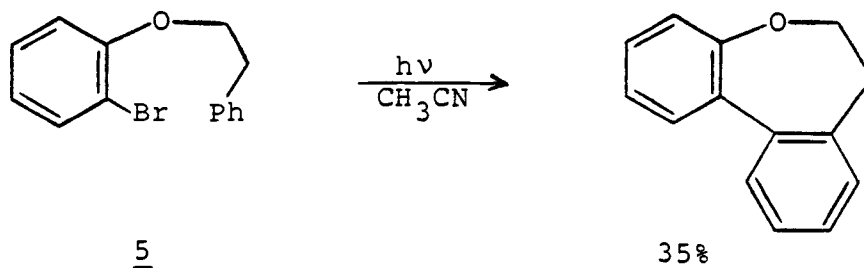
In addition to interest in mechanistic features of the photodehalogenation of haloarenes, the application of photodehalogenation to synthesis¹² has attracted the attention of synthetic organic chemists. A large number of ring-closure reactions can be carried out, which constitute an important step in the synthesis of many cyclic organic molecules. For instance, cyclization of 1 to 9-nitrophenanthrene was reported to proceed by C-I bond homolysis.¹³ and subsequent intramolecular arylation. Similarly, photolysis of 2 gave rise to two position isomers of athermaline.¹⁴



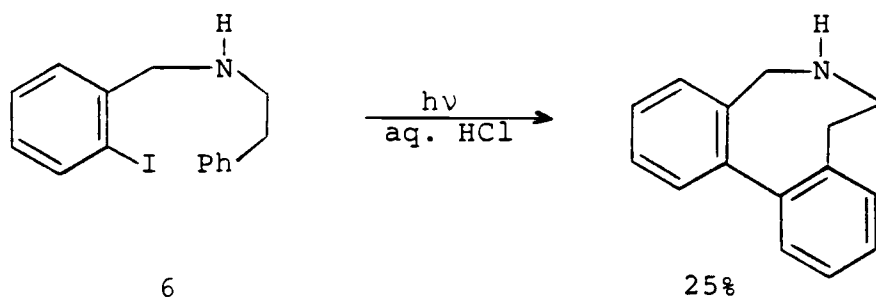
Another example¹⁵ is the photocyclization of 3 generating the pyrazole 4.



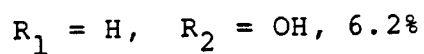
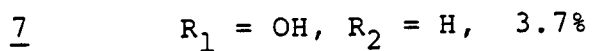
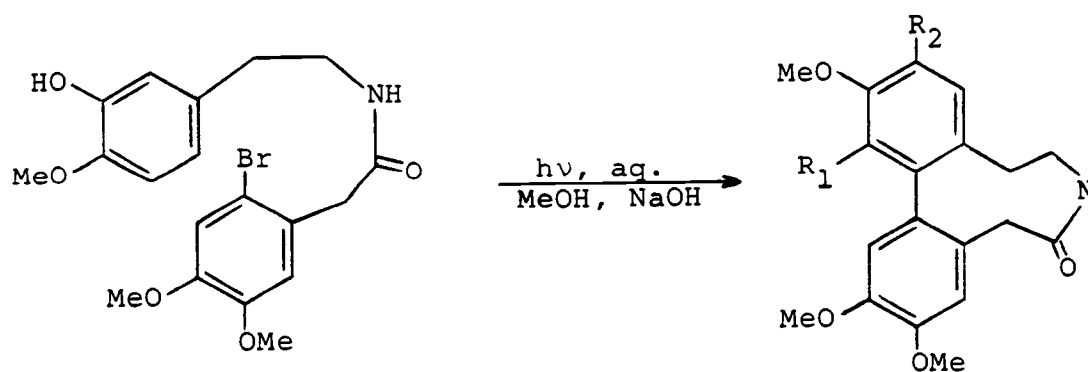
Some rings larger than six-membered have been successfully synthesized by photodehalogenation. One example is the formation of dihydrodibenzoxepin,¹⁶ a seven-membered ring, from 5.



Another example is the formation of 5,6,7,8-tetrahydrodibenz[*c,e*]azocine,¹⁷ an eight-membered ring, from 6.



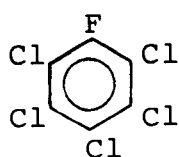
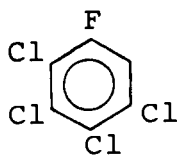
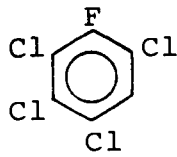
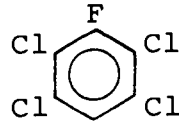
A third example is the generation of a nine-membered ring from 7, which is an intermediate for the synthesis of the alkaloid, erybidine.¹⁸



RESULTS AND DISCUSSION

The Regiochemistry of Photodechlorination of Fluoropentachlorobenzene

The results obtained previously by Freeman *et al.*^{10,11} on polychlorobenzene and polyfluorobenzene systems provide guidelines under which the photochemistry of heterohalobenzenes can be studied. It was anticipated that photolysis of a fluorochlorobenzene system would yield interesting results, which would provide a comparison of the effect of chlorine and fluorine substituents on product formation. Fluoropentachlorobenzene (8) was chosen for such a study. The irradiation of 8 at 254 nm in acetonitrile and in hexane in the presence of triethylamine gave 1-fluoro-2,3,4,5-, 1-fluoro-2,3,4,6-, and 1-fluoro-2,3,5,6-tetrachlorobenzene (9, 10, and 11, respectively). The mol percent yields are given in Table 4.

891011

Irradiation times were used which were just long enough to generate the primary products without other unexpected reactions taking place.

Table 4. Results Obtained for the Photolysis of Fluoropentachlorobenzene^a in the Presence of Triethylamine.

Photoproducts	Yield (mol %) ^b	
	Acetonitrile	Hexane
1-F-2,3,4,5-TCB	6.36 ± 0.23	8.91 ± 0.31
1-F-2,3,4,6-TCB	8.57 ± 0.09	12.31 ± 0.31
1-F-2,3,5,6-TCB	7.67 ± 0.09	5.20 ± 0.10

^a 0.025 M 8 and 0.75 M triethylamine in acetonitrile and hexane.

^b Average of five samples with standard deviation.

The fluorotetrachlorobenzenes 9 and 11 were identified by comparison of their GC retention times (Table 5) and EI mass spectra (Appendix I) with those of the corresponding synthesized compounds. Isomer 10 was not synthesized; however, GC-MS analysis indicates the presence of a third isomer of fluorotetrachlorobenzene in both the acetonitrile and hexane photolysis mixtures, and thus the formation of 1-fluoro-2,3,4,6-tetrachlorobenzene, since only three isomers are possible.

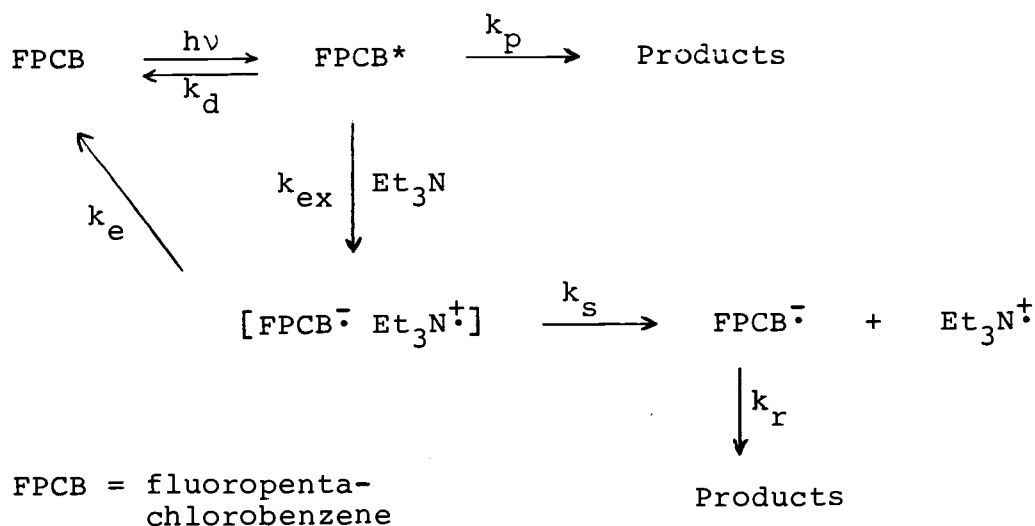
Table 5. Gas Chromatographic Retention Times of the Fluorotetrachlorobenzenes 9, 10, and 11.

	Gas Chromatographic Retention Times ^a (Seconds)		
	<u>11</u>	<u>10</u>	<u>9</u>
Fluorotetrachlorobenzene:			
Photolysis Product: ^b	6188	6296	6496
Synthetic Product:	6178	-	6507

^a Coinjection of 9 and 11 with the photolysis mixture was also used for the identification of the three isomers, 9, 10, and 11.

^b In acetonitrile.

To obtain similar yields of products (see Table 4), the irradiation time required when acetonitrile was used as the solvent was much shorter than when hexane was used; namely, 5 minutes in the former case and one hour in the latter case. This solvent effect implies the involvement of the exciplex intermediate. Thus the polar solvent, acetonitrile, was more effective than the nonpolar solvent, hexane, in breaking up the radical cation - radical anion pair, allowing the separated radical ions to diffuse into the bulk of the solution (k_s); see Scheme VII. This impeded back electron transfer from the fluoropentachlorobenzene radical anion to the triethyl amine radical cation (k_e) and speeded up the amine assisted reactions. This observation is in accordance with that of Bunce et al.⁷ and Davidson and Goodin.⁸



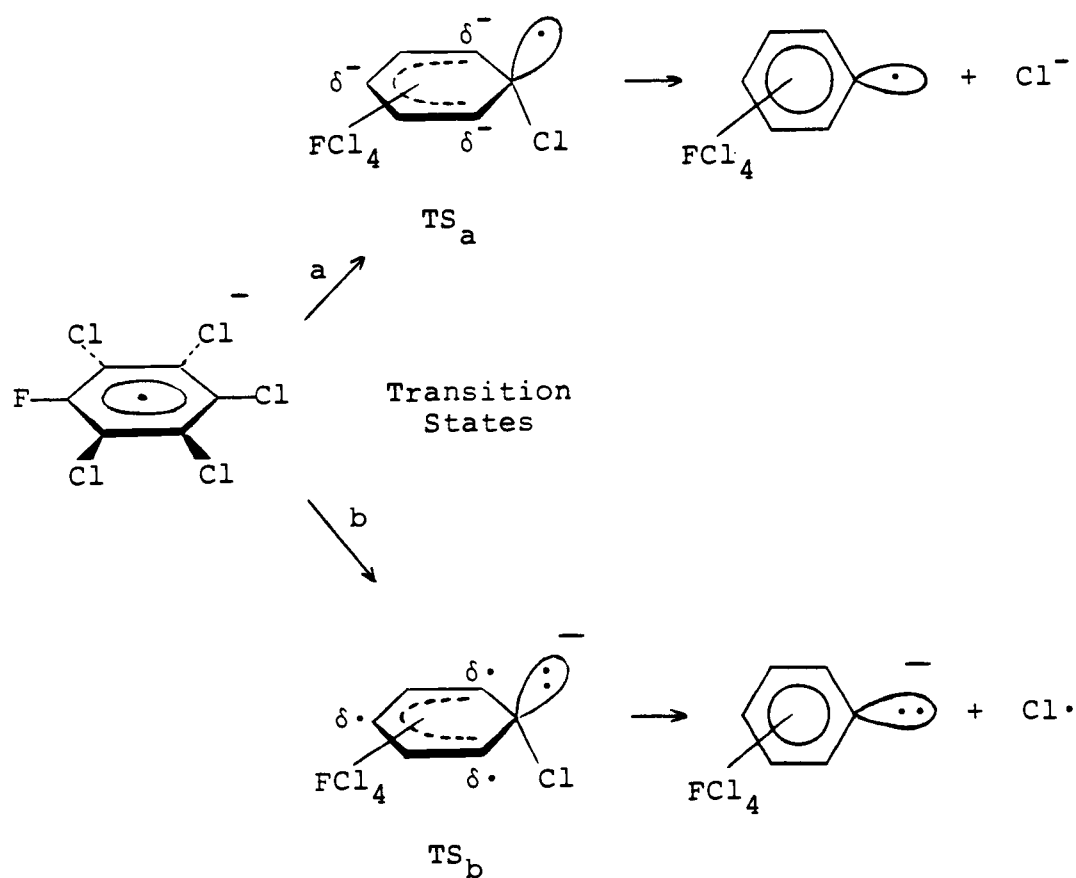
SCHEME VII

Use of the large excess (30-fold) of triethylamine should assure the predominance of the exciplex formed by electron transfer from triethylamine.¹⁰ Thus, under this condition the regiochemistry should characterize the radical anion intermediate.

In accordance with the negative chemical ionization mass spectrum of fluoropentachlorobenzene, two pathways, a and b, are proposed for the conversion of the radical anion intermediate into products, as shown in Scheme VIII on the next page in analogy to those proposed by Freeman et al. for polychlorobenzenes¹⁰ and polyfluorobenzenes¹¹ based on their negative chemical ionization mass spectra. These two pathways are based on the presence of the $(M - Cl)^-$ and Cl^- peaks in the mass spectrum of fluoropentachlorobenzene, whose intensities, relative to the parent radical anion base peak, are 0.0094 and 0.0075, respectively, yielding a ratio of $(M - Cl)^-/Cl^- = 1.3$.

The regiochemistries observed for the fluoropentachlorobenzene radical anion may be rationalized by considering the transition states, TS_a and TS_b , shown in Scheme VIII for the two competing pathways, a and b. In pathway a the parent radical anion undergoes fission to an aryl radical plus a chloride ion. Since the heterolytic fission of the C-Cl bond via a planar transition state would give rise to an excited state, the transition

state TS_a for pathway a would be expected to possess some of the character of a delocalized anion on the benzene ring with a bent localized radical center at which cleavage is taking place. Thus the negative charge should be dispersed in the transition state.



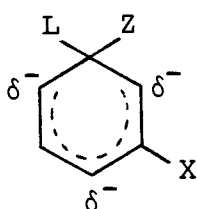
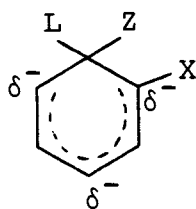
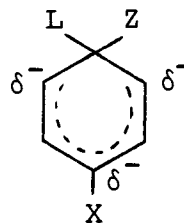
SCHEME VIII

In the case of pathway b, similar reasoning suggests the transition state TS_b , which possesses some of the character of a delocalized radical on the benzene ring with a bent localized carbanionic center. Thus the homolytic cleavage of the fluoropentachlorobenzene radical anion to form an aryl carbanion and a chlorine atom may involve concentration of negative charge.

Use of the nonpolar solvent, hexane, instead of the polar solvent, acetonitrile, should favor pathway a over pathway b, because in the proposed transition state TS_a , the negative charge is delocalized on the benzene ring, rather than localized on one carbon atom as in transition state TS_b . Since the proposed transition state TS_a for pathway a is remarkably similar to the delocalized intermediate formed in a nucleophilic aromatic substitution reaction, use of the I_π repulsion theory proposed by Burdon¹⁹ for nucleophilic aromatic substitution in polyhalobenzenes may help to explain the regiochemistry of C-Cl bond fission in the photodecomposition reactions of fluoropentachlorobenzene in hexane in the presence of the electron donor reagent, triethylamine.

It has been reported that the repulsion between the unshared pair of electrons on a halogen atom and a negative charge on the carbon atom to which it is attached increases in the order $I < Br < Cl < F$.²⁰ When the negative charge on the carbon in question is in a

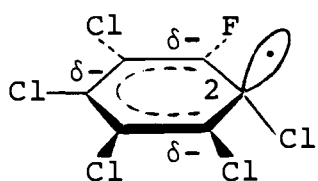
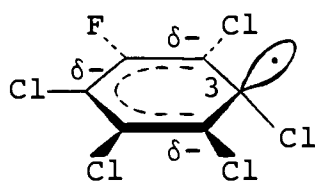
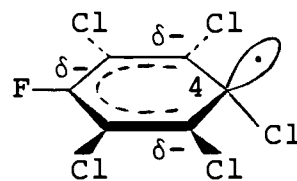
π -electron system, this electron-repulsion effect is called the I_{π} repulsion effect, and it also increases in the order $I < Br < Cl < F$.²⁰ The I_{π} repulsion theory has been applied successfully (with one exception)²¹ in rationalizing the orientation in aromatic nucleophilic substitution reactions by Burdon and his coworkers.^{19,22-24} They suggested that the order of stability for the Wheland intermediates formed in aromatic nucleophilic substitution would be 12 > 13 > 14, since there is no I_{π} repulsion effect in 12, and since the I_{π} repulsion effect in 14 is greater than in 13, because the para position has a greater partial negative charge than the ortho position.¹⁹

121314

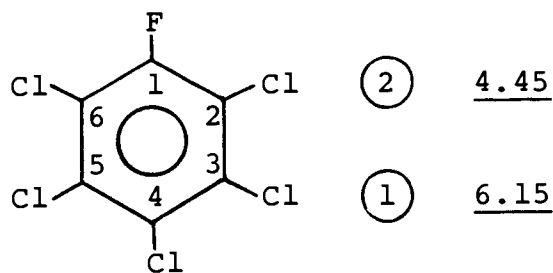
Z = Nucleophile
L = Leaving Group
X = Halogen

The generalized transition state TS_a of Scheme VIII (page 29) corresponds to the three possible transition

states 15, 16, and 17 for dechlorination at the 2, 3, and 4 positions of fluoropentachlorobenzene, respectively.

151617

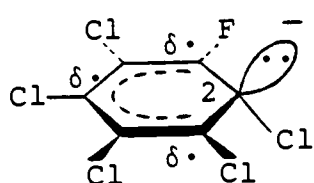
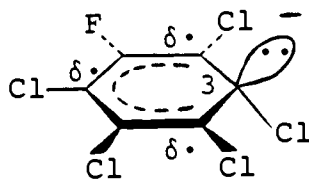
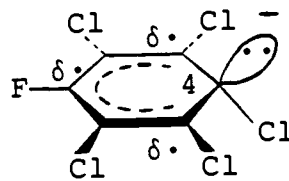
Application of the I_{π} repulsion theory to these three transition states, using the same reasoning as in the case of the Wheland intermediates and taking into account the greater I_{π} repulsion effect of fluorine as compared to chlorine, leads to the prediction that their stabilities should decrease in the order 16 > 15 > 17. Thus the predicted order for the rate of dechlorination at the three possible positions is 3 > 2 > 4, as indicated below by the circled numbers:



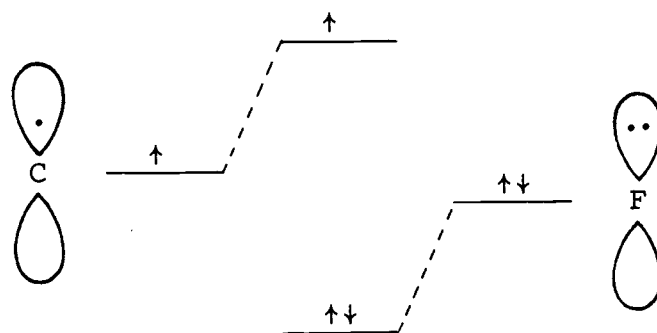
③ 5.20

The observed relative rates for dechlorination in hexane at the 2, 3, and 4 positions are 4.45, 6.15, and 5.20, respectively, and are indicated on the drawing on the previous page by the underlined numbers. These relative rates are based on the data in Table 4 and are corrected for statistical advantage. Thus, dechlorination is fastest at the 3 position, as predicted by the I_{π} repulsion theory; whereas dechlorination at the 4 position is faster than at the 2 position, which is the reverse of the predicted order. This reversal is likely a result of relief of steric hindrance which would be greater for dechlorination at the 4 position than at the 2 position, since the chlorine atom is larger than the fluorine atom.

Use of the polar solvent, acetonitrile, instead of the nonpolar solvent, hexane, should favor pathway b over pathway a (see Scheme VIII, page 29). The generalized transition state TS_D of Scheme VIII corresponds to the three possible transition states 18, 19, and 20 for dechlorination at the 2, 3, and 4 positions of fluoropentachlorobenzene, respectively.

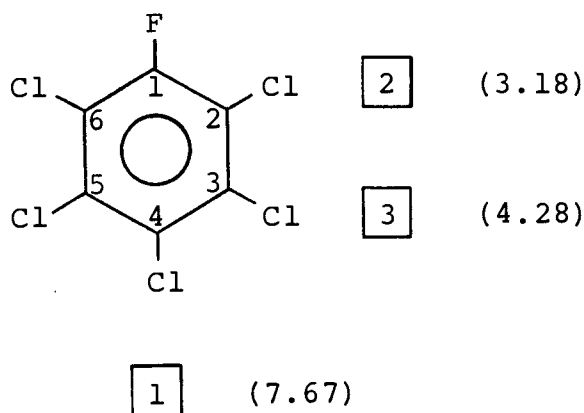
181920

In general, most substituents relative to hydrogen stabilize a radical,²⁵ since a p orbital of the substituent containing a lone pair of electrons can overlap with the p orbital of a radical center, as illustrated below for fluorine:



As a result of the overlap, two electrons go into the lower energy level and only one into the upper; thus, there is an overall drop in energy resulting in stabilization of the radical. Such stabilization by chlorine may be less than by fluorine, because a chlorine p orbital is much larger than a carbon p orbital; thus overlap between the p orbitals of carbon and chlorine is poorer than in the case of carbon and fluorine. Thus, the transition states 18 and 20 should be more stable than transition state 19, and dechlorination should take place faster at positions 2 and 4 than at position 3. Also, dechlorination may be expected to take place faster at position 4 than at position 2 because of the relief of steric congestion in the former case. Thus the

predicted order for the rate of dechlorination at the three possible positions is $4 > 2 > 3$, as indicated below by the numbers in the squares:



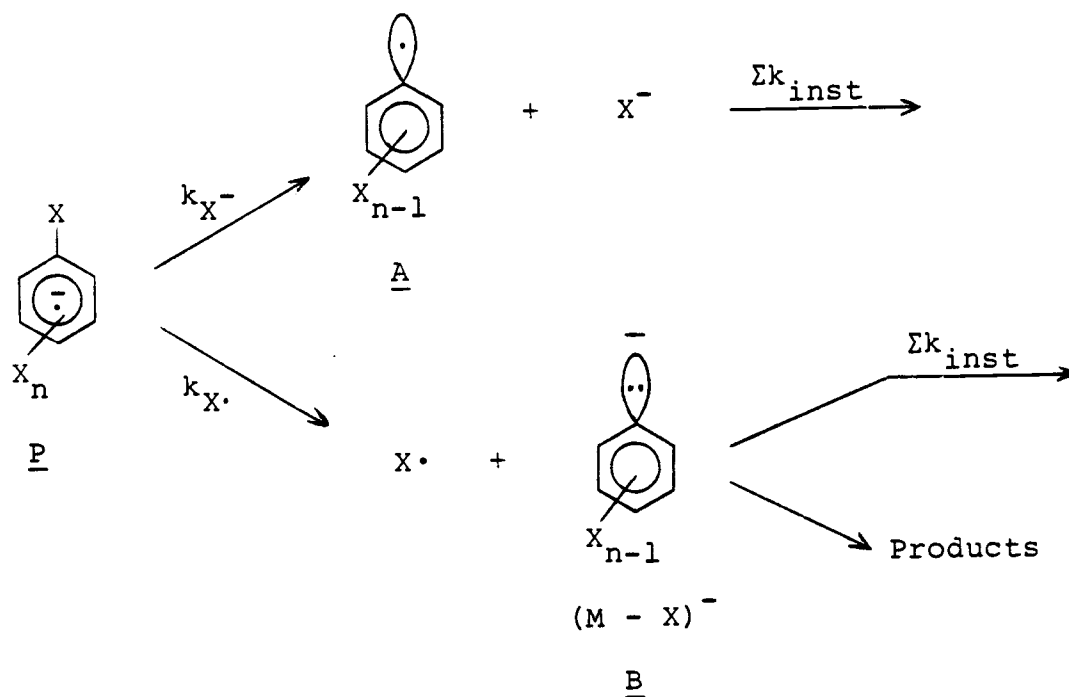
The observed relative rates for dechlorination in acetonitrile at the 2, 3, and 4 positions are 3.18, 4.28, and 7.67, respectively, and are indicated on the above drawing by the numbers in parentheses. The relative rates are based on the data in Table 4 and are corrected for statistical advantage. Thus dechlorination is fastest at the 4 position, as predicted; whereas dechlorination at the 3 position is faster than at the 2 position, which is the reverse of the predicted order. This reversal is likely a result of a greater relief of steric compression upon dechlorination at position 3 as compared to position 2. Another factor, which may account for the reversal, is that some products may form via the alternate pathway a of Scheme VIII (p. 29), which electrostatically favors

loss of chlorine from position 3 as compared to positions 2 and 4 (see p. 32).

Negative Chemical Ionization Mass Spectral Study of Bond Fission in Hexafluorobenzene and Hexachlorobenzene

As already discussed, the radical anion is viewed as the precursor to the formation of products in the photo-dehalogenation reactions in the presence of triethylamine. Thus, it was decided that it would be interesting to carry out further investigation of the mode of bond fission in polyhalobenzene radical anions using a different approach in order to obtain a better understanding of the mechanisms involved. One of the most direct methods of accomplishing this is the analysis of the negative chemical ionization mass spectra of polyhalobenzene substrates.

The decomposition of the radical anion P during the negative chemical ionization mass spectral process is depicted in Scheme IX on the next page. Loss of halide ion, X^- , leads to the formation of radical A; whereas loss of halogen atom, $X\cdot$, leads to formation of aryl anion B. Assuming that the aryl anion B does not decompose further by loss of halide ion (see p. 46), and assuming steady state concentrations of B and X^- , the kinetic relationships shown on the next page are obtained.^{26,27}



SCHEME IX

$$\frac{(X^-)}{(P)} = \frac{k_{X^-}}{\Sigma k_{inst}}$$

$$\frac{(B)}{(P)} = \frac{k_{X\cdot}}{\Sigma k_{inst}}$$

$$\frac{(B)/(P)}{(X^-)/(P)} = \frac{(B)}{(X^-)} = \frac{k_{X\cdot}}{k_{X^-}} = \frac{\text{rate}(X\cdot)}{\text{rate}(X^-)} \quad (6)$$

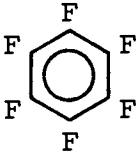
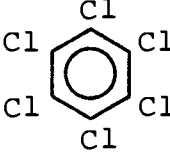
where Σk_{inst} = the sum of the rate terms for loss of X^- or aryl anion B due to instrumental parameters.

Thus, according to Equation 6, the ratio of the rates of $X\cdot$ and X^- loss, $\text{rate}(X\cdot)/\text{rate}(X^-)$, can be calculated from the intensities of the $(M - X)^-$ (aryl anion B) peak cluster and X^- peaks in the negative chemical ionization mass spectrum of the polyhalobenzene (relative to the intensity of the parent radical anion P peak cluster), and these intensities can also be related to the relative rate of $X\cdot$ loss, $\text{rate}(X\cdot)$, and relative rate of X^- loss, $\text{rate}(X^-)$.

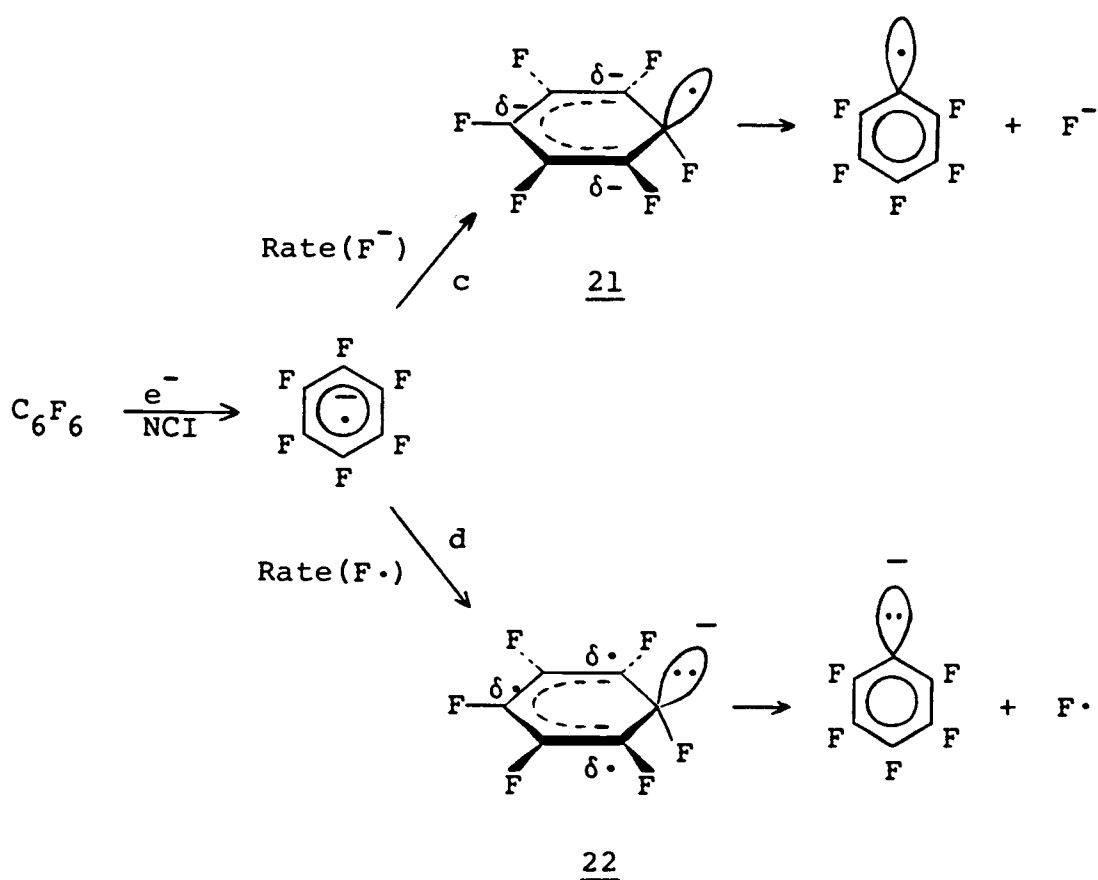
First of all, for the purpose of comparison, the negative chemical ionization mass spectra of hexafluorobenzene and hexachlorobenzene were obtained under the same instrumental conditions. The mass spectral results are presented in Table 6, and are rationalized qualitatively as follows.

1. Negative chemical ionization mass spectroscopy of hexafluorobenzene reveals that the parent radical anion undergoes fission by two pathways, c and d, and the result of $\text{rate}(F\cdot)/\text{rate}(F^-) = 57$ can be explained by considering the relative stabilities of the transition states 21 and 22 proposed in Scheme X on p. 40. According to the I_π repulsion theory, the fluorine destabilizes the negative charge on the π -system of transition state 21, thereby slowing down the rate of pathway c. On

Table 6. Negative Chemical Ionization Mass Spectral Results for Hexafluorobenzene and Hexachlorobenzene.

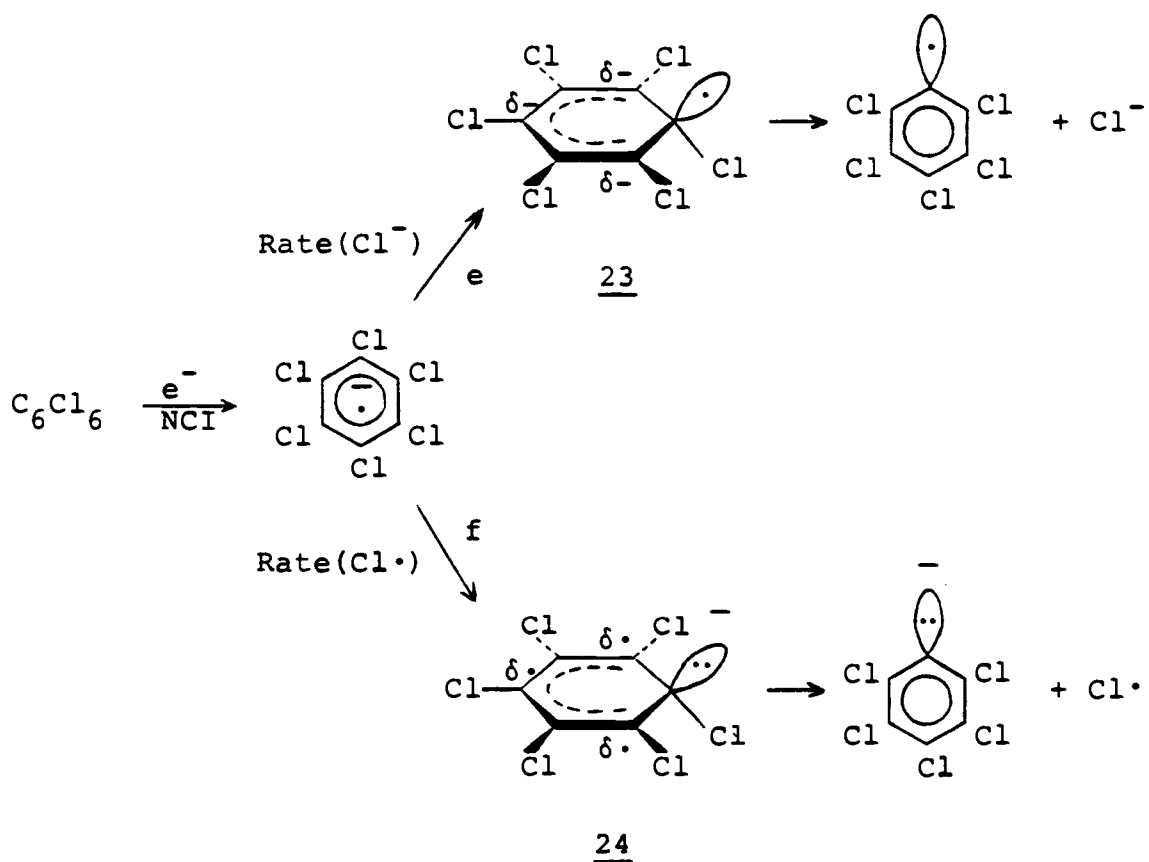
		
Relative rate of loss of F•	1.2	
Relative rate of loss of F ⁻	0.021	
Relative rate of loss of Cl•		0.75
Relative rate of loss of Cl ⁻		0.27
Rate(F•)/Rate(F ⁻)	57	
Rate(Cl•)/Rate(Cl ⁻)		2.8

the other hand, fluorine stabilizes the dispersed radical of transition state 22 by resonance and enhances the rate of pathway d. Consequently, pathway d is favored over pathway c.



SCHEME X

2. The same explanation can be offered for the result that pathway f undergoes bond fission faster than pathway e ($\text{rate}(\text{Cl}\cdot)/\text{rate}(\text{Cl}^-) = 2.8$) by considering the relative stabilities of transition states 23 and 24 shown in Scheme XI, which are analogous to transition states 21 and 22 of Scheme X.



SCHEME XI

3. The value of $\text{rate}(\text{Cl}\cdot)/\text{rate}(\text{Cl}^-) = 2.8$ is smaller than that of $\text{rate}(\text{F}\cdot)/\text{rate}(\text{F}^-) = 57$. This may be ascribed to a significantly smaller I_π repulsion effect in the case of chlorine as compared to fluorine ($\text{rate}(\text{Cl}^-) = 0.27$ vs. $\text{rate}(\text{F}^-) = 0.021$) and to a somewhat smaller resonance stabilization effect on the delocalized radical in the case of chlorine as compared to fluorine ($\text{rate}(\text{Cl}\cdot) = 0.75$ vs. $\text{rate}(\text{F}\cdot) = 1.2$).
4. The results, $\text{rate}(\text{Cl}^-) > \text{rate}(\text{F}^-)$ (0.27 vs. 0.021) and $\text{rate}(\text{F}\cdot) > \text{rate}(\text{Cl}\cdot)$ (1.2 vs. 0.75), are in agreement with the order predicted by the I_π repulsion theory in the former case, and with the order predicted by resonance stabilization theory in the latter case.

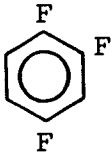
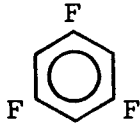
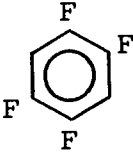
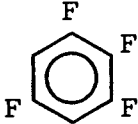
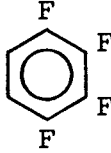
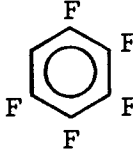
Negative Chemical Ionization Mass Spectral Study of Bond Fission in Polyfluorobenzenes

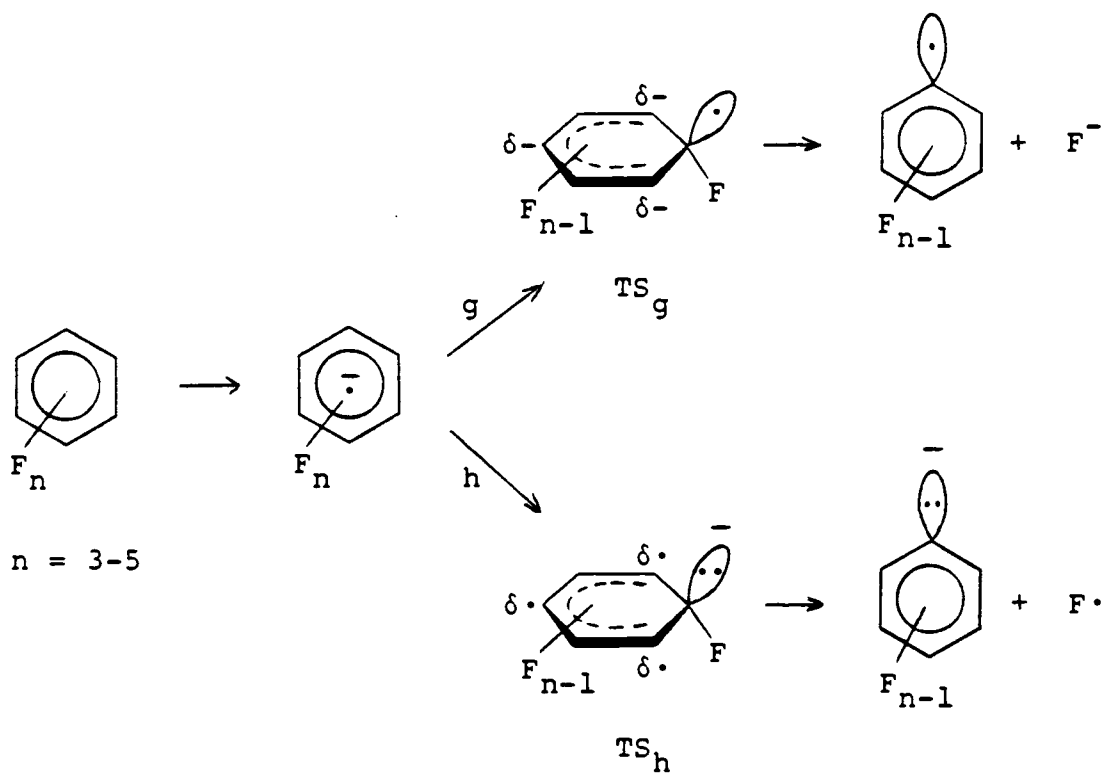
In order to investigate the mode of bond fission of polychlorobenzene radical anions generated in the course of photodechlorination, Freeman et al.¹⁰ studied the negative chemical ionization mass spectrometry of tri-, tetra-, penta-, and hexachlorobenzene(s). They found that in the case of tri-, tetra-, and pentachlorobenzene(s), chloride ion loss was favored over chlorine

atom loss; whereas in the case of hexachlorobenzene, chlorine atom loss was favored over chloride ion loss. In order to compare the mode of bond fission in the polychlorobenzene system with that of the polyfluorobenzene system, tri-, tetra-, and pentafluorobenzene(s) were investigated by negative chemical ionization mass spectrometry, in addition to hexafluorobenzene. The results are presented in Table 7 and show that fluorine atom loss is favored over fluoride ion loss in the fission of the C-F bond of polyfluorobenzene radical anions. In other words, polyfluorobenzene radical anions prefer undergoing homolytic rather than heterolytic bond cleavage in the gas phase. This behavior is quite different from that of the polychlorobenzene system.

The results for the polyfluorobenzene system can be explained by considering the relative stabilities of the transition states TS_g and TS_h proposed in Scheme XII on p. 45. According to the reasoning applied to transition states 21 and 22 shown in Scheme X on p. 40. for hexafluorobenzene, transition state TS_h is more stable than TS_g for all the polyfluorobenzenes investigated, and thus bond fission leading to fluorine atom loss (pathway h) is favored over bond fission leading to fluoride ion loss (pathway g).

Table 7. Negative Chemical Ionization Mass Spectral Results for the Polyfluorobenzene System.

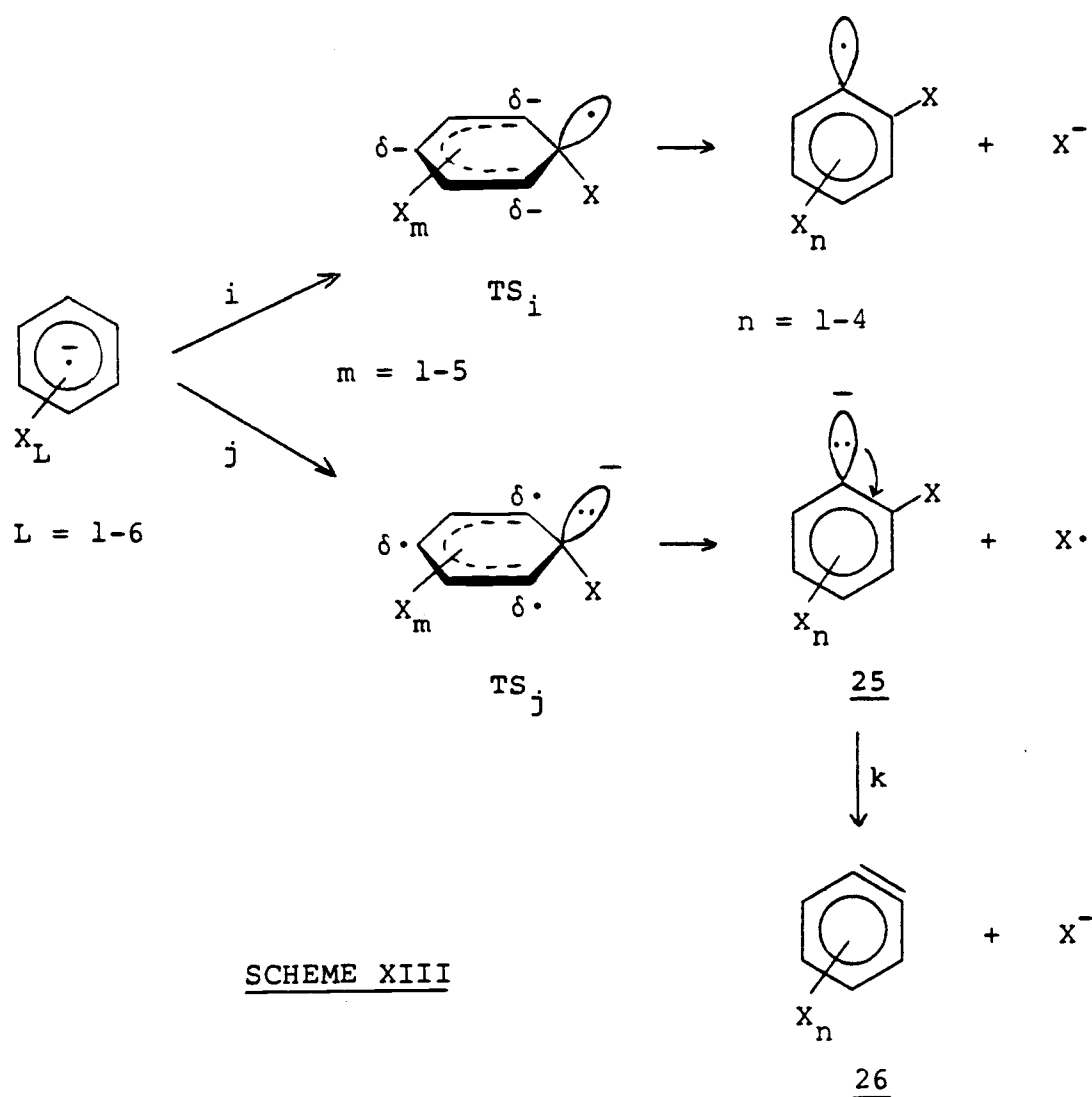
						
loss of F•	yes	yes	yes	yes	yes	yes
loss of F ⁻	no	no	no	no	no	no



SCHEME XII

The Detection of Further Decomposition of the Aryl Anion

During the study of the mode of bond fission of polyhalobenzene radical anions, the question arose of whether further decomposition of the aryl anion 25 was taking place (pathway k of Scheme XIII) generating benzyne (26) and halide ion.



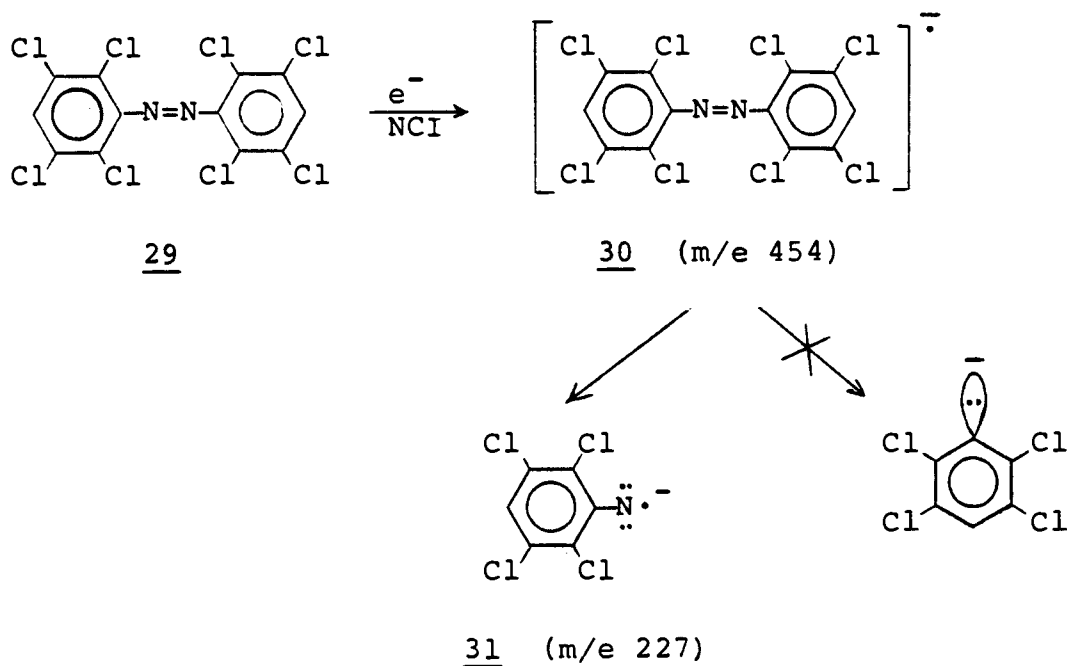
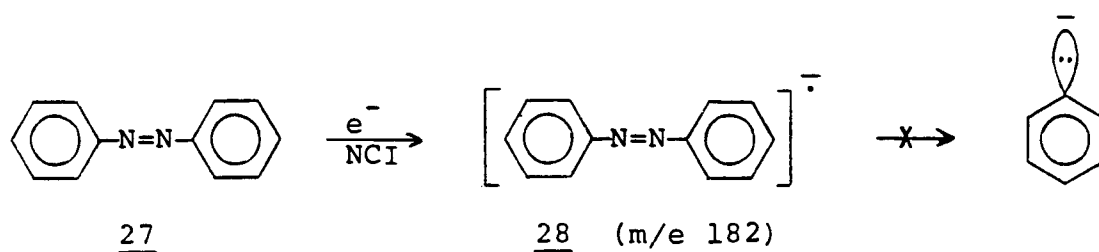
If this further decomposition took place, then the measurement of the amount of X^- formed based on the analysis of the negative chemical ionization mass spectrum would be greater than the amount of X^- formed only by pathway i. This further decomposition of the aryl anion 25 would thus affect the measurement of the ratio for the loss of halogen atom $X\cdot$ versus the loss of halide ion X^- , and would thereby complicate the correlation of the regiochemistry of the photodehalogenation with the relative stabilities of the transition states TS_i and TS_j . In order to check the stability of aryl anions of general structure 25 which are generated from the bond fission of their parent radical anions, six compounds, 27, 29, 32, 35, 38, and 41, (see Schemes XIV, XV, and XVII on pp. 49, 50, and 56, respectively) were investigated using negative chemical ionization mass spectrometry. For the chlorine containing compounds, 29, 32, 35, and 41, three possibilities may be considered:

1. The possibility of detecting the aryl anion of general structure 25 without detecting any chloride ion: this would indicate that the aryl anion is stable during the time of flight from ion source to detector.
2. The possibility of detecting both the aryl anion of general structure 25 and the chloride ion: this case

would be complicated, because the chloride ion loss could be due to the further decomposition of the aryl anion, or could be due to bond fission of its parent radical anion.

3. The possibility of detecting the chloride ion without detecting the aryl anion of general structure 25: this would indicate that the chloride ion arises from the bond fission of its parent radical anion, which in turn would mean that the negative chemical ionization mass spectrometric experiments for studying the stability of aryl anions were not successful.

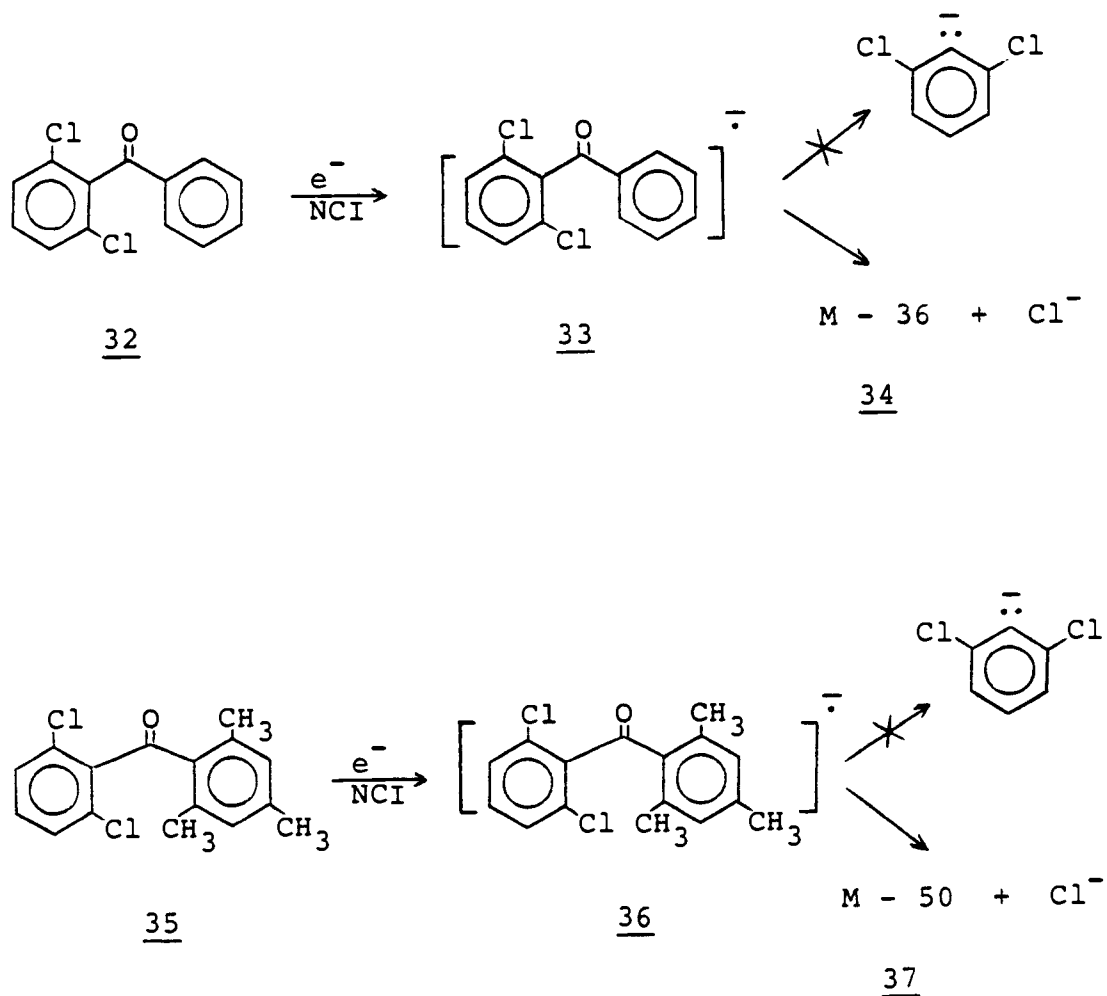
The results for azobenzene (27) and 2,2',3,3',5,5',6,6'-octachloroazobenzene (29) are illustrated in Scheme XIV on the next page. No aryl anion was formed by the bond fission of the radical anions 28 and 30 during the negative chemical ionization process. In the case of the radical anion 30, N=N bond cleavage occurred generating 31. However, such N=N bond cleavage was not detected for radical anion 28. This difference in the results is probably due to the stabilization of the negative charge of 31 by the electron withdrawing effect of the chlorine atoms, which would be lacking in the case of N=N bond cleavage of 28.



SCHEME XIV

The results for 2,6-dichlorobenzophenone (32) and 2,6-dichloro-2',4',6'-trimethylbenzophenone (35) are shown in Scheme XV on the next page, and their mass spectra are given in Figures 5 and 6, respectively. No aryl anion was formed by the bond fission of the radical

anions 33 and 36. Instead, 32 gives a base peak at $M - 36$, which results from loss of HCl and corresponds to 34, and a weak chloride ion peak; whereas 35 gives a chloride ion base peak and a moderately intense peak based at $M - 50$, which results from the loss of CH_3Cl and corresponds to 37.



SCHEME XV

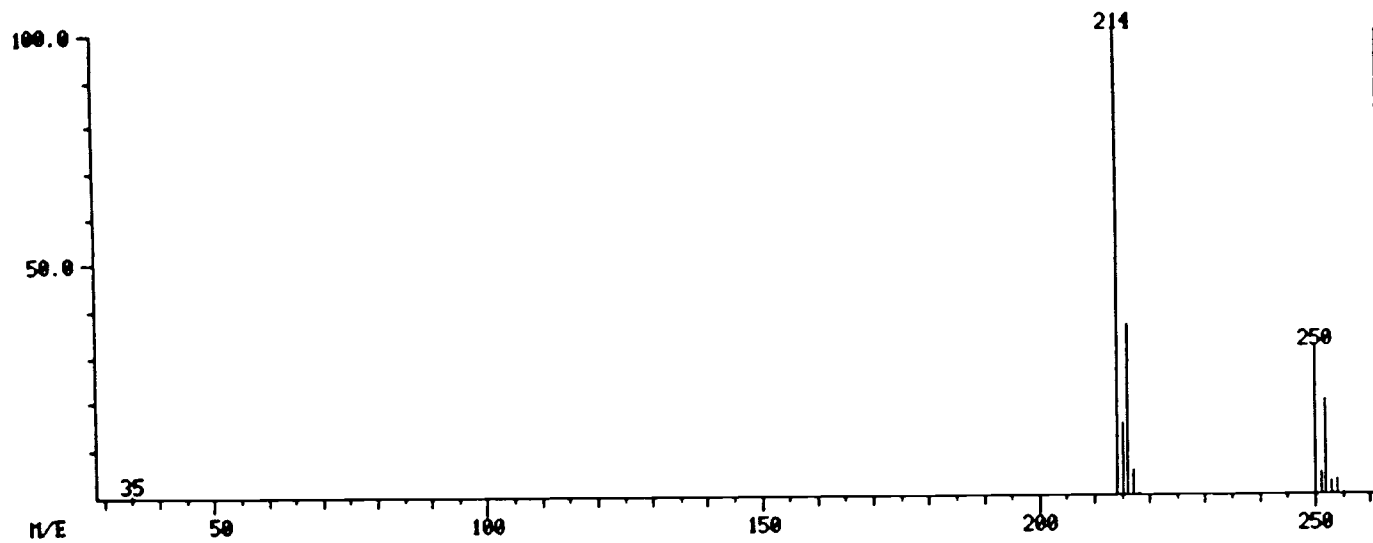


Figure 5. The negative chemical ionization mass spectrum of 2,6-dichlorobenzophenone (32).

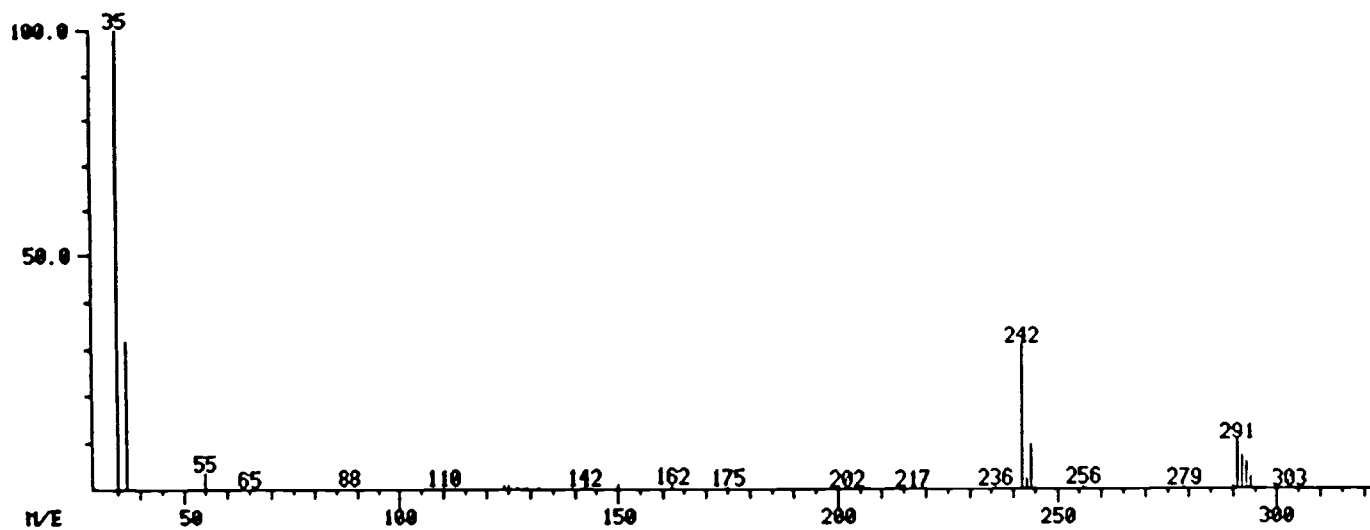
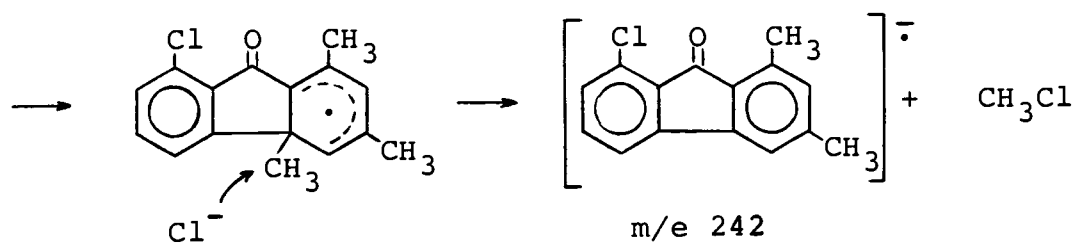
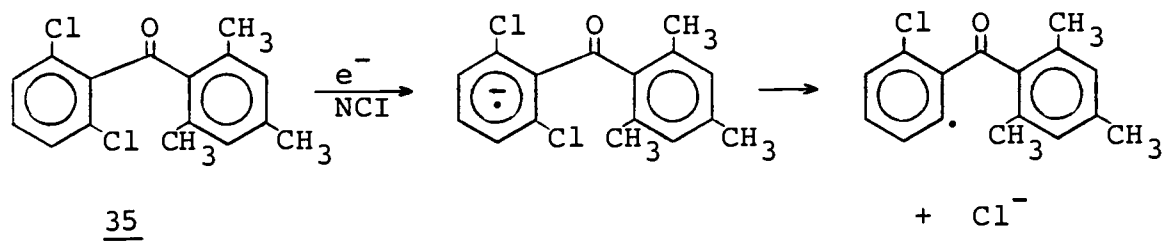
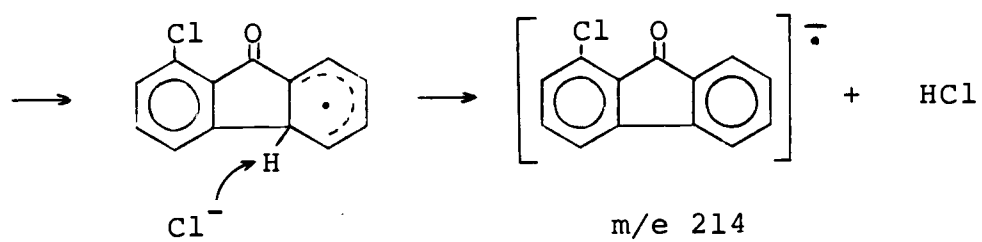
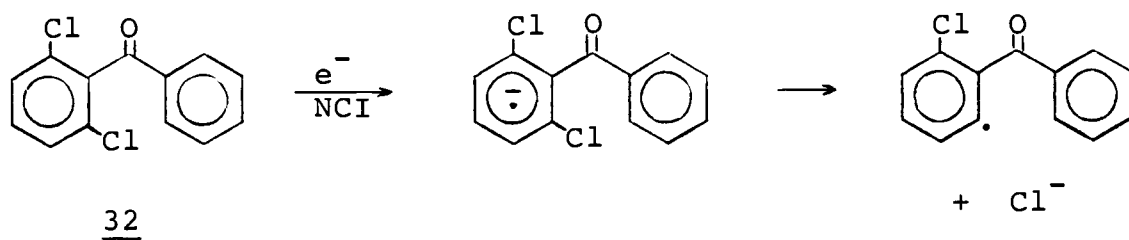


Figure 6. The negative chemical ionization mass spectrum of 2,6-dichloro-2',4',6'-trimethylbenzophenone (35).

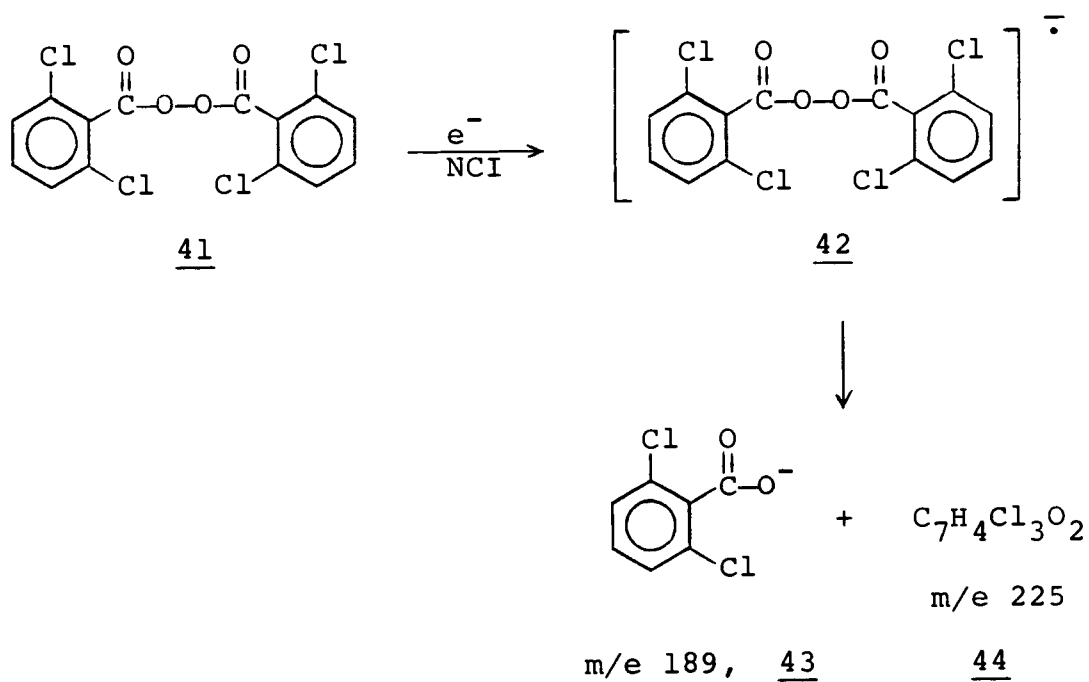
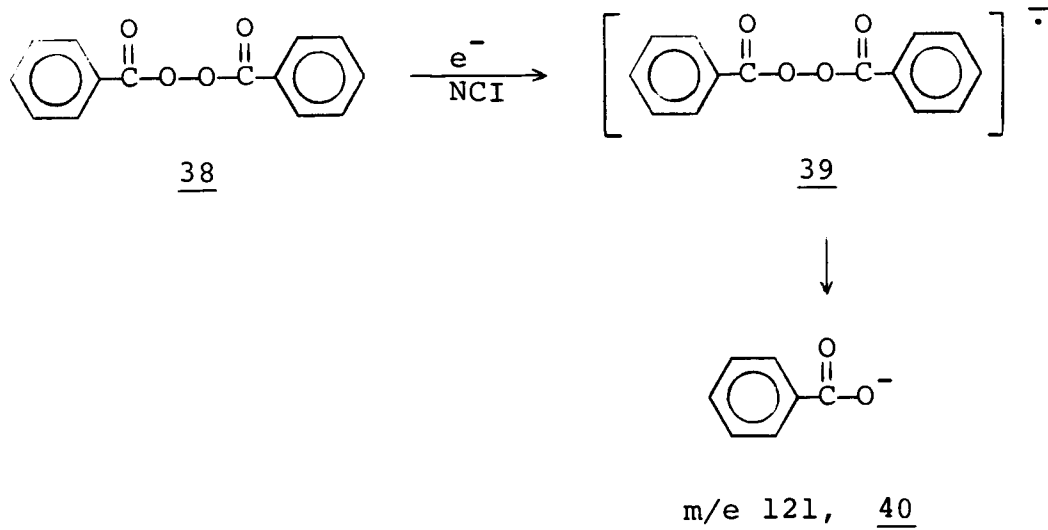
In order to elucidate these two negative chemical ionization mass spectra, a possible mechanism is proposed for each case (Scheme XVI on the next page). After capture of an electron in the negative chemical ionization process, the negative charge is expected to develop on the benzene ring bearing the chlorine atoms, because it will be stabilized by the electron withdrawing effect of the chlorines. Upon loss of chloride ion, followed by intramolecular free radical cyclization, the radical anions 34 and 37 are formed. Considering the relative stabilities of 34 and 37, 34 should be more favored than 37, because the electron donating effect of the methyl groups on 37 will destabilize the developed negative charge. Indeed, the observed peak intensities indicate that the formation of 34 occurs more readily than that of 37 (i.e., the more intense base peak of fragment 34 observed in the mass spectrum of 32 as compared to the less intense peak of fragment 37 observed in the mass spectrum of 35, and the less intense accompanying chloride ion peak observed in the former case as compared to the more intense chloride ion base peak observed in the latter case, in each case comparing intensities which are relative to the intensity of the parent radical anion peak cluster). Thus during the formation of 34 and 37, more chloride ions were consumed in forming HCl in the former case than in forming CH₃Cl in the latter case.



SCHEME XVI

The results for benzoyl peroxide (38) and 2,2',6,6'-tetrachlorobenzoyl peroxide (41) are shown in Scheme XVII on the next page. No aryl anion was formed from the bond fission of the radical anions 38 and 41 during the negative chemical ionization process. In the case of 38, O-O bond cleavage occurred and generated the benzoate anion (40). In the case of 41, a peak cluster based at m/e 189 was obtained, indicating the formation of the dichlorobenzoate anion 43 as a result of O-O bond cleavage. Also, a moderately intense chloride ion peak and a moderately intense peak cluster based at m/e 225 were obtained, which remain a structural puzzle.

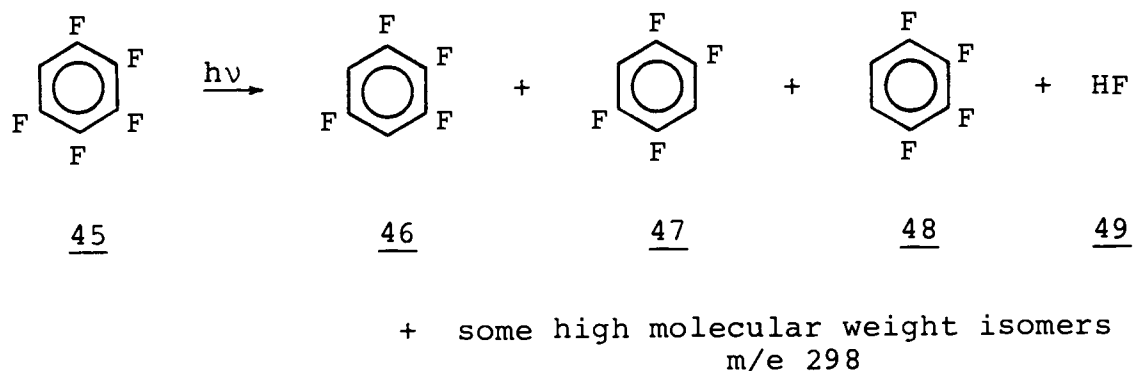
Thus, in the mass spectra of compounds 29, 32, 35, and 41, only the chloride ion was detected, without the formation of the aryl anion. Therefore, the negative ionization mass spectrometric experiment for studying the stability of the aryl anion of general structure 25 (see Scheme XIII, p. 46) was not successful.



SCHEME XVII

Identification of the Octafluorobiphenyls Formed in the
Photolysis of Pentafluorobenzene

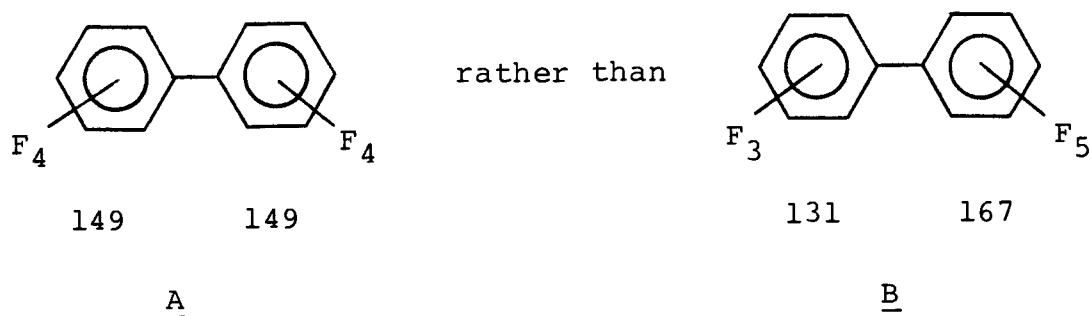
Freeman and Srinivasa¹¹ studied the photolysis of pentafluorobenzene (45) at 254 nm in acetonitrile in the absence of triethylamine. They observed the formation of the following products: 1,2,3,5-, 1,2,4,5-, and 1,2,3,4-tetrafluorobenzene (46 (0.11%), 47 (1.09%), and 48 (0.09%), respectively), HF (49), and at least four high molecular weight isomers with m/e 298 (0.91, 0.85, 0.26, and 0.08%), which were not identified.



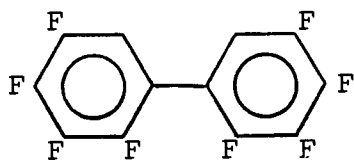
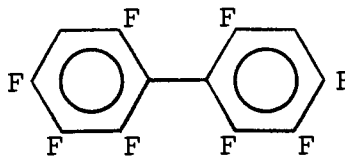
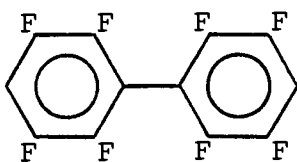
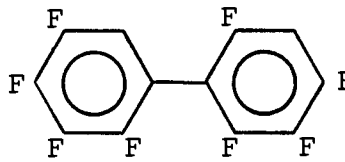
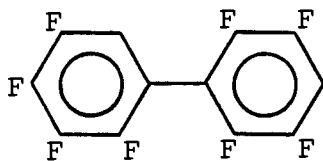
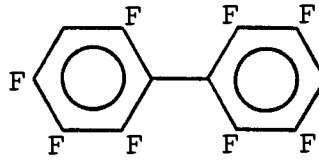
Thus, in order to identify the high molecular weight isomers, the photolysis of pentafluorobenzene was repeated, using the same general procedure as before. Particular attention was given to the identification of the previously unidentified isomers. The GC peaks obtained in GC-MS analyses using a 60 M carbowax capillary column included 6 peaks whose mass spectra showed m/e 298. The four major peaks corresponded to the high molecular weight

isomers obtained in the previous investigation by Freeman and Srinivasa;¹¹ whereas the other two peaks were very small.

The m/e 298 peak cluster appearing in the mass spectrum of each of the six isomers suggests that the isomers could be octafluorobiphenyls with formula $C_{12}H_2F_8$. However, 12 isomers are possible for octafluorobiphenyl. The mass spectra of each of the six isomeric photolysis products with m/e 298 show a characteristic peak at m/e 149, which arises from the cleavage of the C-C bond between the two benzene rings, and implies that four fluorines are attached to each benzene ring (A), rather than three fluorines being present on one ring, and five on the other (B).

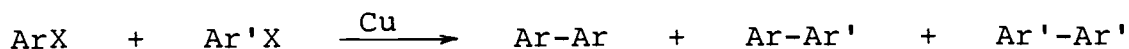
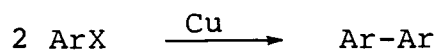


Thus, the six isomers corresponding to B can be ruled out; whereas the six isomers corresponding to A (50 - 55) are assigned to the products which were formed during the photolysis of pentafluorobenzene (45).

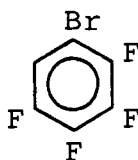
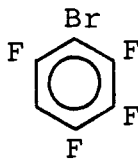
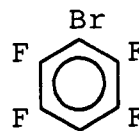
505152535455

In order to identify the six isomers, 50 - 55, they were synthesized using the Ullmann reaction,²⁸⁻²⁹ whereby a biaryl is formed by the condensation of two aromatic halide molecules in the presence of finely divided copper powder. Both symmetric and asymmetric biaryls can be

synthesized by this reaction:



For the preparation of 50 - 55, three starting materials were used: 1-bromo-2,3,4,5-tetrafluorobenzene (56), 1-bromo-2,3,4,6-tetrafluorobenzene (57), and 1-bromo-2,3,5,6-tetrafluorobenzene (58).

565758

Subjecting 56, 57, and 58 to the Ullmann reaction lead to the formation of 2,2',3,3',4,4',5,5'-octafluorobiphenyl (50), 2,2',3,3',4,4',6,6'-octafluorobiphenyl (51), and 2,2',3,3',5,5',6,6'-octafluorobiphenyl (52), respectively. Using a mixture of 56 and 57, 56 and 58, and 57 and 58 as the starting materials gave rise to 2,2',3,3',4,4',5,6'-octafluorobiphenyl (53), 2,2',3,3',4,5,5',6'-octafluorobiphenyl (54), and 2,2',3,3',4,5',6,6'-octafluorobiphenyl (55) as the major products, respectively. In

each case the product was separated and purified by preparative gas chromatography using an OV-101 or Carbowax column. The molecular structures of 50 - 55 were identified by ^1H -NMR, ^{13}C -NMR (Appendix II), ^{19}F -NMR (Appendix III), and mass spectrometry.

After obtaining the six desired synthetic products 50 - 55 by the Ullmann reaction, the identification of the corresponding six isomers of octafluorobiphenyl generated by the photolysis of pentafluorobenzene was carried out by comparing their gas chromatographic retention times with those of the synthesized compounds and by mass spectrometry. The experiment was carried out on a Finnigan 4023 mass spectrometer equipped with a Finnigan 9610 gas chromatograph, using a 60 M DX-4 Carbowax capillary column.

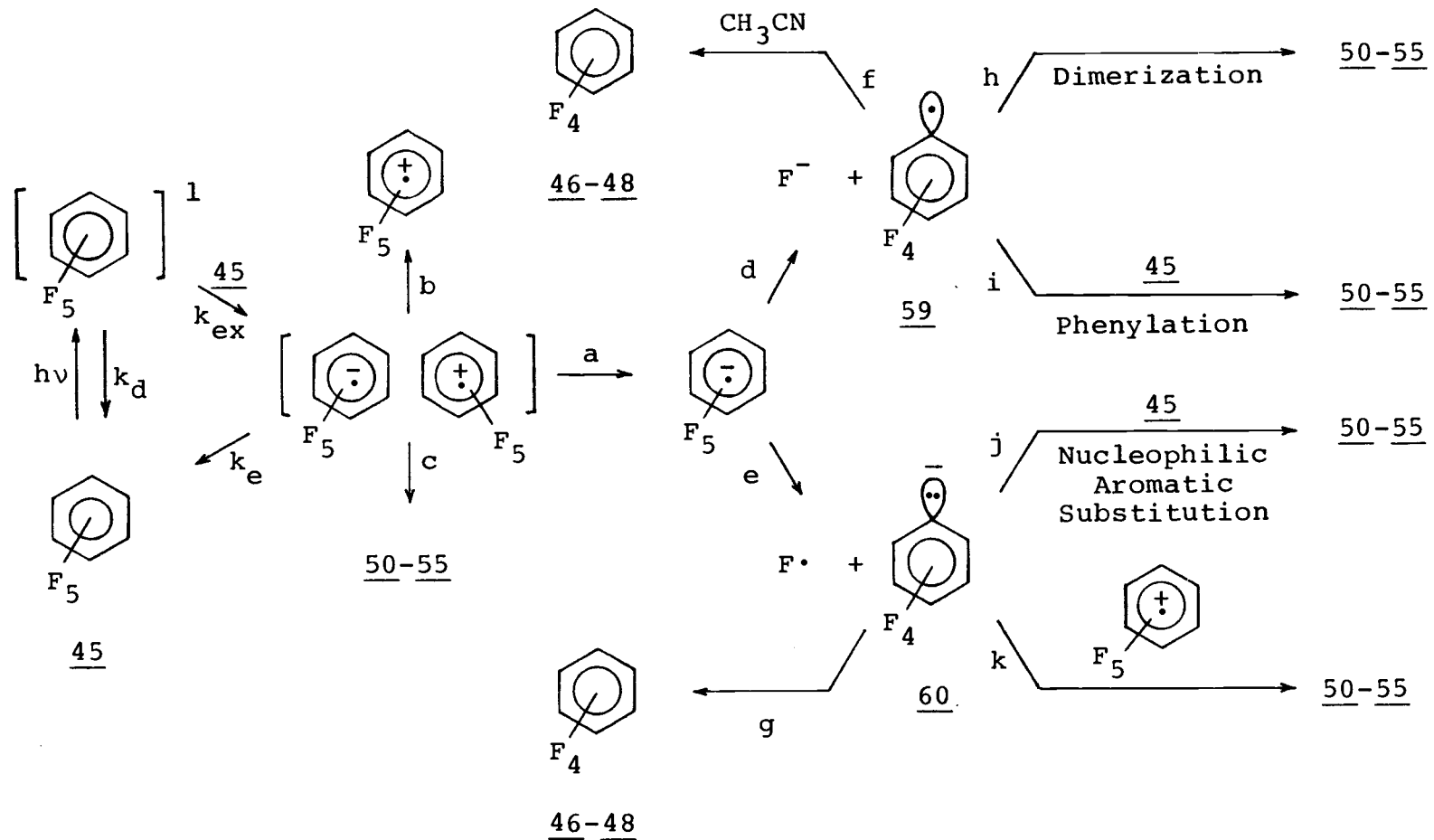
The gas chromatographic retention times of the six octafluorobiphenyl isomers obtained both by the Ullmann reaction and by photolysis of pentafluorobenzene are presented in Table 8 on the next page. These retention times, as well as the corresponding mass spectra, demonstrate that the octafluorobiphenyls 50, 52, 53, and 54 correspond to the photolysis products obtained by Freeman and Srinivasa¹¹ with the product compositions of 0.91, 0.85, 0.26, and 0.08%, respectively. The product compositions of the other two octafluorobiphenyl isomers, 51 and 55, which Freeman and Srinivasa¹¹ did not detect,

are estimated to be smaller than 0.01% in both cases (the GC peaks of 51 and 55 are too small to be integrated accurately).

Table 8. Gas Chromatographic Retention Times of the Octafluorobiphenyls 50 - 55.

	Gas Chromatographic Retention Times (Seconds)					
	<u>51</u>	<u>55</u>	<u>53</u>	<u>52</u>	<u>54</u>	<u>50</u>
Octafluorobiphenyl:						
Photolysis Product:	1213	1262	1282	1308	1333	1377
Synthetic Product:	1209	1259	1280	1306	1331	1376

Rationalization of the product compositions of the six octafluorobiphenyl isomers generated by the photolysis of pentafluorobenzene at 254 nm in acetonitrile in the absence of triethylamine is very complicated because of the significant number of possible pathways presented in Scheme XVIII on the next page, leading to the formation of the octafluorobiphenyls 50 - 55.



SCHEME XVIII

According to the mechanism proposed by Freeman and Srinivasa,¹¹ the products are formed by a pathway involving excimer formation--see Scheme VI on page 19. Use of the polar solvent, acetonitrile, will break up the radical cation - radical anion components of the excimer complex and allow the separated radical anion (pathway a) and radical cation (pathway b) to diffuse into the bulk of the solution. In the excimer complex, the radical cation and radical anion may couple with each other followed by the loss of fluorine to generate the six octafluorobiphenyl isomers 50 - 55.

Two reaction pathways are possible for the radical anion. In the first reaction pathway, the radical anion undergoes bond fission to generate fluoride ion and the tetrafluorobenzene radical 59 (pathway d; see also Scheme XII on page 45), which may pick up a hydrogen atom from the solvent, acetonitrile, to form the tetrafluorobenzenes 46 - 48 (pathway f). The radical 59 may also undergo dimerization (pathway h) or phenylation with 45 (pathway i), forming 50 - 55 in both cases.

In the second reaction pathway, the radical anion undergoes bond fission to generate fluorine atom and the tetrafluorobenzene anion 60 (pathway e; see also Scheme XII on page 45), which may react with 45 by nucleophilic aromatic substitution to form 50 - 55. The anion 60 may also react with the pentafluoro radical

cation followed by the loss of fluorine to form 50 - 55.

Thus, the six octafluorobiphenyl isomers 50 - 55 may be formed by a number of different pathways, and this complicates the determination of the relative reaction rate for each pathway. Therefore, any attempt to rationalize the product composition of the six octafluorobiphenyl isomers formed by the photolysis of pentafluorobenzene in acetonitrile would be very complicated and challenging.

EXPERIMENTAL

General

Melting points were obtained using either a Mel-Temp device or a Büchi melting point apparatus and are uncorrected. Infrared spectra (IR) were obtained with a Perkin-Elmer Model 735B spectrophotometer. Ultraviolet spectra (UV) were obtained using a Cary 118 spectrophotometer. Nuclear magnetic resonance spectra (NMR) were recorded with a Bruker AM 400 (^1H at 400.14 MHz, ^{13}C at 100.62 MHz, and ^{19}F at 376.50 MHz) or with a Varian FT 80 spectrometer (^1H at 79.54 MHz). Gas chromatographic (GC) analyses were carried out using a Varian 3700 gas chromatograph equipped with a flame ionization detector. Product ratios and percentage yields calculated from chromatographic data are based on the relative peak areas measured by a Hewlett-Packard 3373B integrator. Dodecane was used as the internal standard. Preparative gas chromatography was performed using a Varian 3700 gas chromatograph equipped with a thermal conductivity detector. All of the columns used with the Varian 3700 gas chromatograph were made in the lab. Direct mass spectra (MS) and GC-MS data were obtained on a Finnigan 4023 mass spectrometer equipped with a Finnigan 9610 gas chromatograph. Exact mass determinations were performed on a

Bruker MS 50. Elemental analyses were performed by Mic Anal, Tucson, Arizona.

Preparation of Fluoropentachlorobenzene (8)

The procedure of Silberrad³⁰ was used. A mixture of 10 mL (0.106 mol) of fluorobenzene, 100 mL (0.982 mol) of sulphuryl chloride, 2 mL (0.025 mol) of sulphur monochloride, and 2 g (0.015 mol) of anhydrous aluminum chloride was refluxed at 70 - 80°C for 12 hours using an oil bath. The reaction mixture was cooled to room temperature and then partitioned between 200 mL of benzene and 100 mL of water. The benzene layer was washed with 100 mL portions of an aqueous solution of 20% KOH until the aqueous layer remained basic. After the benzene layer had been dried over anhydrous MgSO₄, the solvent was removed using a rotary evaporator, and the solid residue was filtered and recrystallized twice from 95% ethanol, yielding 15.5 g (54.5%) of crude 8 as white crystals. A small part of the crude product was purified by sublimation and pure 8 was obtained: mp 148 - 149°C; UV: λ_{\max} (CH₃CN) 254 nm (sh, ϵ 2460), λ_{\max} (cyclohexane) 254 nm (sh, ϵ 3020); IR(KBr): 1400 - 1300 cm⁻¹ (C-F), 775 - 730 cm⁻¹ (C-Cl); ¹³C-NMR (100.62 MHz, CDCl₃): δ 120.95 (C-2 and C-6, d, $J_{\text{CCF}} = 20.12$ Hz), δ 128.80 (C-4), δ 131.58 (C-3 and C-5), δ 153.18 (C-1, d, $J_{\text{CF}} =$

252.52 Hz); GC-MS (negative CI): M^- parent peak cluster m/e (with relative intensity) = 266 (59.98), 268 (100), 270 (65.17), 272 (9.66), 274 (1.70), 276 (0.02).

Preparation of 1-Fluoro-2,3,4,5-tetrachlorobenzene (9)

The procedure of Finger and Reed³¹ was used. A mixture of 1.0 g (0.004 mol) of 2,3,4,5-tetrachloroaniline and 15 mL of concentrated hydrochloric acid was cooled to -5°C while being stirred well. The resulting mixture was diazotized by the addition of a solution of 0.29 g (0.004 mol) of sodium nitrite in 3 mL of water, while the temperature and stirring efficiency were constantly monitored. After the diazotization was complete, a solution of 1.4 g (0.013 mol) of sodium tetrafluoroborate was added rapidly. The slurry was stirred for 30 min at about -10°C , filtered and washed with water, and the diazonium fluoroborate was dried in the desiccator overnight. The dry diazonium fluoroborate salt was placed in a sublimation apparatus and heated gently using a Bunsen burner until decomposition began, after which the reaction occurred spontaneously. A white vapor was generated, which condensed as a solid on the cooled central tube (cold finger) of the sublimation apparatus. Heating was continued cautiously from time to time as needed to keep the reaction going. After thermal decomposition was

completed, the condensed solid was recrystallized from 95% ethanol, yielding 0.4 g (39.6%) of nearly pure 9: mp 177 - 180 °C; IR (KBr): 1400 - 1340 cm^{-1} (C-F), 770 - 720 cm^{-1} (C-Cl); $^1\text{H-NMR}$ (400.14 MHz, CDCl_3): δ 7.30 (d, 1 H $J_{\text{HF}} = 8.15$ Hz); $^{13}\text{C-NMR}$ (100.62 MHz, CDCl_3): δ 116.37 (C-6, d, $J_{\text{CCF}} = 25.66$ Hz), δ 121.11 (C-2, d, $J_{\text{CCF}} = 20.45$ Hz), δ 128.71 (C-4, d, $J_{\text{CCCCF}} = 4.14$ Hz), δ 132.34 (C-5, d, $J_{\text{CCCCF}} = 10.23$ Hz), δ 134.29 (C-3), δ 156.49 (C-1, d, $J_{\text{CF}} = 253.08$ Hz); GC-MS (EI): M^+ parent peak cluster m/e (with relative intensity) = 232 (78.25), 234 (100), 236 (49.16), 238 (8.46), 240 (0.32).

Preparation of 1-Fluoro-2,3,5,6-tetrachlorobenzene (11)

Compound 11 was prepared in the same manner as 9, using 1.0 g (0.004 mol) of 2,3,5,6-tetrachloroaniline, 15 mL of concentrated hydrochloric acid, 0.29 g (0.004 mol) of sodium nitrite, and 1.4 g (0.013 mol) of sodium tetrafluoroborate. The crude product, which was obtained by carrying out thermal decomposition of the diazonium fluoroborate in the manner described for 9, was recrystallized from 95% ethanol, yielding 0.31 g (30.7%) of nearly pure 11: mp 70 - 72 °C; IR (KBr): 1350 - 1300 cm^{-1} (C-F), 730 - 700 cm^{-1} (C-Cl); $^1\text{H-NMR}$ (400.14 MHz, CDCl_3): δ 7.56 (d, 1 H, $J_{\text{HF}} = 2.85$ Hz); $^{13}\text{C-NMR}$ (100.62 MHz, CDCl_3): δ 120.71 (C-2 and C-6, d, $J_{\text{CCF}} = 20.13$ Hz),

δ 126.01 (C-4, d, $J_{\text{CCCCF}} = 2.97$ Hz), δ 132.24 (C-3 and C-5), δ 155.33 (C-1, d, $J_{\text{CF}} = 253.74$ Hz); GC-MS (EI): M^+ parent peak cluster m/e (with relative intensity) = 232 (78.50), 234 (100), 236 (49.25), 238 (9.00), 240 (0.31).

Photolysis of Fluoropentachlorobenzene (8) in Acetonitrile in the Presence of Triethylamine and Product Analysis

Reagent grade acetonitrile (Baker Chemical Company) was freshly distilled from phosphorus pentoxide, and its purity was found to be $\gg 99\%$ by GC analysis. Dodecane (Aldrich, 99%) and triethylamine (Aldrich, 99%) were used as obtained. A 25.0 mL solution of 8 (0.169 g, 6.3×10^{-4} mol, 0.025 M), dodecane (100 μL , 0.0749 g, 4.4×10^{-4} mol), and triethylamine (1.90 g, 0.019 mol, 0.75 M) in acetonitrile was prepared. Three mL portions of the photolysis solution were placed in five quartz tubes (Ace Glass, 170 mm X 15 mm) equipped with pyrex glass sliding stoppers and were degassed through three or four freeze-pump-thaw cycles. The tubes were sealed under vacuum and then irradiated for 5 minutes in a Rayonet merry-go-round reactor (the Southern New England Co.) equipped with eight 2537 A° Rull lamps. The temperature of the reactor was maintained at 40°C by passing a stream of air through the apparatus during the period of irradiation.

The photolysis mixtures were analyzed by gas chromatography using a Varian 3700 gas chromatograph equipped with a flame ionization detector. First, the following columns were tried: a 20 ft. X 1/8 in. column containing 7% OV 17 supported on Chromosorb W, AW/DMCS (80/100 mesh), a 10 ft. X 1/8 in. column containing 10% Carbowax (20 M) supported on Chromosorb P, AW/DMCS (60/80 mesh), a 6 ft. X 1/8 in. column containing 7% OV 101 supported on Chromosorb W, AW/DMCS (60/80 mesh), and a 10 ft. X 1/8 in. column containing 10% Carbowax and 10% SF 96 supported on Chromosorb P, AW/DMCS (60/80 mesh). Although many different temperature programs were used, the peaks for the three isomers of fluorotetrachlorobenzene could not be resolved. Finally, the following combined column system was used successfully in resolving the three isomers: a 10 ft. X 1/8 in. column containing 10% SE 30 supported on Chromosorb P, AW/DMCS (60/80 mesh) connected to a 10 ft. X 1/8 in. column containing 20% Carbowax (20 M) supported on Chromosorb P, AW/DMCS (80/100 mesh). The temperature of the combined columns was programmed to be held at 35°C for 30 min, and then to increase from 35° to 180°C at 5°C/min, and an injector temperature of 200°C and detector temperature of 230°C were used. Helium was used as the carrier gas at a flow rate of about 30 mL/min. The photoproducts were identified by comparing their retention times with those of known compounds and by mass

spectrometry. The mass spectral analyses were carried out on a Finnigan 4023 mass spectrometer equipped with a Finnigan 9610 gas chromatograph using the combined column system described above. The results for each sample are listed in Table 9. The average of the results obtained for the five samples with standard deviations are listed in Table 4 in the Results and Discussion Section.

Table 9. Results Obtained for the Photolysis of Fluoropentachlorobenzene at 254 nm in Acetonitrile in the Presence of Triethylamine.

Photo-products	Yield (mol %) ^a				
	Sample 1	Sample 2	Sample 3	Sample 4	Sample 5
9	6.01	6.23	6.58	6.64	6.34
10	8.62	8.70	8.54	8.57	8.42
11	7.70	7.84	7.64	7.61	7.58

^a The mol % yields are based on the number of moles of fluoropentachlorobenzene used (6.3×10^{-4} mol).

Photolysis of Fluoropentachlorobenzene (8) in Hexane in the Presence of Triethylamine and Product Analysis

Reagent grade hexane (EM Science) was freshly distilled from calcium hydride, and its purity was found to be >> 99% by GC analysis. Dodecane (Aldrich, 99%) and triethylamine (Aldrich, 99%) were used as obtained. The same photolysis procedure was used as for 8 in acetonitrile. A 25.0 mL solution of 8 (0.169 g, 6.3×10^{-4} mol, 0.025 M), dodecane (100 μ L, 0.0749 g, 4.4×10^{-4} mol), and triethylamine (1.92 g, 0.019 mol, 0.75 M) in hexane was prepared. Five 3 mL samples of the photolysis solution were irradiated for one hour.

The five photolysis samples were analyzed in the same manner as the acetonitrile photolysis samples of 8. The results for each sample are listed in Table 10 on the next page. The average of the results obtained for the five samples with standard deviations are listed in Table 4 in the Results and Discussion Section.

Table 10. Results Obtained for the Photolysis of Fluoropentachlorobenzene at 254 nm in Hexane in the Presence of Triethylamine.

Photo-products	Yield (mol %) ^a				
	Sample 1	Sample 2	Sample 3	Sample 4	Sample 5
<u>9</u>	8.76	9.00	9.11	8.89	8.79
<u>10</u>	11.73	12.53	12.62	12.38	12.27
<u>11</u>	5.03	5.26	5.31	5.22	5.18

^a The mol % yields are based on the number of moles of fluoropentachlorobenzene used (6.3×10^{-4} mol).

Negative Chemical Ionization Mass Spectrometric Study of Fluoropentachlorobenzene (8)

The mass spectrometric study was conducted on a Finnigan 4023 instrument equipped with a Finnigan 9610 gas chromatograph. A 4500 source modification was used. Methane (Matheson, ultra high purity, 99.97%) was used as the reagent gas in this investigation, and the gauge pressure was approximately 0.5 torr. The source temperature and electron energy of the mass spectrometer were

150°C and 80 eV, respectively. A 10 ft. X 2 mm, 7% OV 101 glass column (Supelcoport) was used. The temperature of the GC column was programmed from 60° to 300°C at a rate of 10°C/min.

Negative Chemical Ionization Mass Spectrometric Study of Hexafluorobenzene and Hexachlorobenzene

Both hexafluorobenzene (Aldrich) and hexachlorobenzene (Aldrich) were used as obtained. The mass spectrometric study was carried out in the same manner as for fluoropentachlorobenzene, using the same conditions. The experimental results are presented in Table 6 in the Results and Discussion Section.

Negative Chemical Ionization Mass Spectrometric Study of Polyfluorobenzenes

The following compounds were used as obtained: 1,2,4-trifluorobenzene (Columbia Organic Chemicals Co.), 1,3,5-trifluorobenzene (Aldrich), 1,2,4,5-tetrafluorobenzene (Aldrich), 1,2,3,5-tetrafluorobenzene (Aldrich), 1,2,3,4-tetrafluorobenzene (Chemicals Procurement Lab, Inc.), and pentafluorobenzene (Aldrich).

The mass spectrometric study was performed on the same instrument as in the case of fluoropentachlorobenzene. Methane (Matheson, ultra high purity, 99.97%) was

was used as the reagent gas, and the gauge pressure was approximately 0.4 torr. The source temperature and electron energy of the mass spectrometer were 190°C and 80 eV, respectively. A 10 ft. X 2 mm glass column containing 5% OV 101 on Chromosorb 750 (100/120 mesh) was used. The temperature of the GC column was maintained at 60°C isothermally. The results are presented in Table 7 in the Results and Discussion Section.

Detection of Further Decomposition of the Aryl Anion Using Negative Chemical Ionization Mass Spectrometry

Azobenzene (Aldrich) was used as obtained. Benzoyl peroxide was provided by Prof. G. J. Gleicher, Oregon State University. The following compounds were synthesized as described in the sections which follow:

2,2',3,3',5,5',6,6'-octafluoroazobenzene (29), 2,6-dichlorobenzophenone (32), 2,6-dichloro-2',4',6'-trimethylbenzophenone (35), and 2,2',6,6'-tetrachlorobenzoyl peroxide (41).

The mass spectrometric study was performed on the same instrument as in the case of fluoropentachlorobenzene. Methane (Matheson, ultra high purity, 99.97%) was used as the reagent gas.

In the case of azobenzene and 2,2',3,3',5,5',6,6'-octachloroazobenzene, the gauge pressure of methane was

approximately 0.8 torr. The source temperature and electron energy of the mass spectrometer were 190°C and 55 eV, respectively. Sample introduction was achieved by using a probe.

In the case of 2,6-dichloro-2',4',6'-trimethylbenzophenone and 2,6-dichlorobenzophenone, the gauge pressure of methane was approximately 0.4 torr. The source temperature and electron energy of the mass spectrometer were 190°C and 70 eV, respectively. A 10 ft., 5% OV 101 glass column was used. The GC column temperature was programmed from 150° to 275°C at a rate of 10°C/min.

In the case of benzoyl peroxide and 2,2',6,6'-tetrachlorobenzoyl peroxide, the gauge pressure of methane was approximately 0.4 torr. The source temperature and electron energy were 120°C and 70 eV, respectively. Sample introduction was achieved by using a probe.

Preparation of 2,2',3,3',5,5',6,6'-Octafluoroazobenzene (29)

The procedure of McBee, et al.³² was used. To a magnetically stirred slurry of 2 g (0.0087 mol) of 2,3,5,6-tetrachloroaniline in 40 mL of 95% ethanol, 160 mL of an aqueous solution of 5.25% sodium hypochlorite (bleach, Master Chemical Co.) was added, and the reaction mixture turned pink immediately. After 15 minutes of

stirring at room temperature, the reaction mixture turned red. Stirring was continued for another 10 hours. Then the reaction mixture was filtered, and the red solid was washed with plenty of water and recrystallized from toluene, yielding 0.32 g (16%) of 29: mp 247 - 250°C; IR (KBr): 1400 cm^{-1} (N=N), 870 cm^{-1} (C-N); $^1\text{H-NMR}$ (79.54 MHz, CDCl_3): δ 7.65 (s, 2 H, aromatic); GC-MS (EI) m/e (with relative intensity): M^+ parent peak cluster: 454 (5.9), 456 (14.1), 458 (18.6), 460 (10.0), 462 (4.0), 464 (1.1); also: 213 (77.9), 215 (100), 217 (48.6), 219 (10.3), 221 (0.8).

Preparation of 2,6-Dichlorobenzophenone (32)

A mixture of 1.0 g (0.0052 mol) of 2,6-dichlorobenzoic acid and 1.0 mL (1.631 g, 0.014 mol) of thionyl chloride was placed in a dry 25 mL three-necked round bottomed flask which was equipped with a reflux condenser capped with a drying tube containing calcium chloride. The two unused necks of the flask were stoppered. The mixture was heated gently using an oil bath until the evolution of gases stopped (about 30 min). The mixture was warmed at about 90°C for 10 min while mechanically stirred in order to remove the excess thionyl chloride. The acid chloride thus obtained was a yellow liquid which needed no further purification. While the contents of

of the flask were still warm, 6 mL (0.067 mol) of benzene was added. After the solution was stirred thoroughly and cooled in an ice bath, 0.70 g (0.0052 mol) of aluminum chloride was added rapidly to the flask in one lot, and the reflux condenser was immediately reconnected. After a few minutes the rapid evolution of hydrogen chloride ceased, and the reaction mixture was refluxed for 3.5 hours. Then the reaction mixture was cooled, poured into a mixture of 1 mL of concentrated hydrochloric acid and 10 g of ice, and stirred thoroughly for 5 min. The organic layer was separated and saved, while the aqueous layer was extracted with 15 mL of ethyl ether and then added to the organic layer. The combined organic layer was washed twice with 10 mL portions of an aqueous solution of 20% sodium hydroxide. After the organic layer had been dried over anhydrous MgSO_4 , the solvent was removed using a rotary evaporator, and the solid residue was filtered and recrystallized twice from absolute alcohol, yielding 0.95 g (73%) of pure 32 as white crystals: mp 82 - 83°C; IR (KBr): 1670 cm^{-1} (C=O); $^1\text{H-NMR}$ (79.54 MHz, CDCl_3): δ 7.1 - 7.8 (m, 8 H); $^{13}\text{C-NMR}$ (100.62 MHz, CDCl_3): δ 128.11, 128.95, 129.60, 130.73, 131.90, 134.29, 135.42, 137.73, 192.57; GC-MS (EI) m/e (with relative intensity): M^+ parent peak cluster: 250 (28.74), 252 (18.55), 254 (3.05); other peaks: 173 (24.62), 175 (15.69); 105 (100); 77 (30.03).

Preparation of 2,6-Dichloro-2',4',6'-trimethylbenzophenone (35)

Compound 35 was prepared in the same manner as 32, using 1.0 g (0.0052 mol) of 2,6-dichlorobenzoic acid, 1.0 mL (1.631 g, 0.014 mol) of thionyl chloride, 1.0 mL (8.64 g, 0.072 mol) of 1,3,5-trimethylbenzene, and 0.7 g (0.0052 mol) of aluminum chloride. The crude product was recrystallized from absolute alcohol, yielding 0.47 g (30.5%) of pure 35 as white crystals: mp 146 - 149°C; IR (KBr): 3000 - 2800 cm^{-1} (aliphatic C-H stretch), 1670 cm^{-1} (C=O); $^1\text{H-NMR}$ (79.54 MHz, CDCl_3): δ 2.22 (s, 6 H, two CH_3 's) δ 2.27 (s, 3 H, one CH_3), δ 6.82 (d, 2 H, J = about 0 - 1 Hz, aromatic), δ 7.20 - 7.30 (m, 3 H, aromatic); $^{13}\text{C-NMR}$ (100.62 MHz, CDCl_3): δ 20.92, 21.22, 128.91, 130.04, 130.91, 133.06, 135.82, 137.99, 139.52, 141.22, 195.45; GC-MS (EI) m/e (with relative intensity): M^+ parent peak cluster: 292 (1.46), 294 (0.88), 296 (0.14); other peaks: 257 (100), 259 (32.51); 242 (23.30), 244 (7.49); 222 (72.00); 173 (17.33); 145 (16.26), 147 (45.97); 119 (43.97).

Preparation of 2,2',6,6'-Tetrachlorobenzoyl Peroxide (41)

The procedure of Price and Krebs³³ was used. First the acid chloride of 2,6-dichlorobenzoic acid was prepared in the same manner as had been done in the

synthesis of 2,6-dichlorobenzophenone (32), using the same amounts of the starting materials (1.0 g, 0.0052 mol of 2,6-dichlorobenzoic acid and 1.0 mL, 1.631 g, 0.0014 mol of thionyl chloride). The acid chloride thus obtained was a yellow liquid which needed no further purification. After it was cooled down to room temperature, 10 mL of toluene was added. The toluene solution was added dropwise over a period of about 20 min to a solution which had been prepared by adding 0.28 g (0.0036 mol) of sodium peroxide to cold water, whose temperature had been brought down to 0 - 5°C before adding the sodium peroxide. The temperature was maintained at 0°C by using an ice-water-salt bath. After the mixture had been stirred for an additional 3 hours, the precipitate was filtered and washed with 100 mL of cold water as rapidly as possible. A white solid was collected, yielding 0.62 g (62.7%) of 41, which turned liquid at room temperature. IR (film): 1790 cm^{-1} (C=O), 1200 - 1000 cm^{-1} (C-O), 1000 - 800 cm^{-1} (O-O); $^1\text{H-NMR}$ (79.54 MHz, CDCl_3): δ 7.25 - 7.37 (m, 6 H, aromatic); GC-MS (negative CI) m/e (with relative intensity): $(\text{M} + 1)^-$ parent peak cluster: 379 (40.41), 381 (56.74), 383 (31.97), 385 (8.61), 387 (0.55); other peaks: 225 (56.02), 227 (56.74), 229 (22.11), 231 (3.27); 189 (100), 191 (87.48), 193 (12.28); 35 (30.82), 37 (10.04).

Preparation of 2,2',3,3',4,4',5,5'-Octafluorobiphenyl (50)

A mixture of 0.5 g of 1-bromo-2,3,4,5-tetrafluorobenzene and 0.5 g of finely divided copper was sealed in an evacuated pyrex glass tube (approximate size = 7 cm X 11 mm) and heated in an oil bath at 210 - 220°C for 55 hours. The product was extracted with ether, the copper residue was filtered off, and the ether was evaporated. The crude product was purified by preparative gas chromatography, using a column containing 7% OV 101 on Chromosorb W (60/80 mesh); 101 mg (31%) of 50 was obtained as white crystals, mp 75 - 77°C. $^1\text{H-NMR}$ (400.14 MHz, CDCl_3): δ 6.98 - 7.05 (m, 2 H, aromatic); $^{13}\text{C-NMR}$ (100.62 MHz, CDCl_3): see Appendix II; $^{19}\text{F-NMR}$ (376.50 MHz, CDCl_3): see Appendix III; GC-MS (EI) m/e (relative intensity): 298 (M^+ , 100), 149 (12.37); exact mass m/e: 298.00378 (calcd. for $\text{C}_{12}\text{H}_2\text{F}_8$: 298.00286).

Preparation of 2,2',3,3',4,4',6,6'-Octafluorobiphenyl (51)

A mixture of 0.5 g of 1-bromo-2,3,4,6-tetrafluorobenzene and 0.5 g of finely divided copper was sealed in an evacuated pyrex glass tube (approximate size = 7 cm X 11 mm) and heated in an oil bath at 210 - 220°C for 55 hours. The product was extracted with ether, the copper residue was filtered off, and the ether was evaporated.

The crude product was purified by preparative gas chromatography, using a column containing 7% OV 101 on Chromosorb W (60/80 mesh); 137 mg (42%) of 51 was obtained as a white solid, mp 61 - 63°C. $^1\text{H-NMR}$ (400.14 MHz, CDCl_3): δ 6.90 - 6.97 (m, 2 H, aromatic); $^{13}\text{C-NMR}$ (100.62 MHz, CDCl_3): see Appendix II; $^{19}\text{F-NMR}$ (376.50 MHz, CDCl_3): see Appendix III; GC-MS (EI) m/e (relative intensity): 298 (M^+ , 100), 149 (11.34); exact mass m/e: 298.00378 (calcd. for $\text{C}_{12}\text{H}_2\text{F}_8$: 298.00286).

Preparation of 2,2',3,3',4,4',5,6'-Octafluorobiphenyl (53)

A mixture of 0.5 g of 1-bromo-2,3,4,5-tetrafluorobenzene, 0.5 g of 1-bromo-2,3,4,6-tetrafluorobenzene, and 1.0 g of finely divided copper was sealed in an evacuated pyrex glass tube (approximate size = 7 cm X 11 mm) and heated in an oil bath at 210 - 220°C for 55 hours. The product was extracted with ether, the copper residue was filtered off, and the ether was evaporated. The isomeric octafluorobiphenyls were separated by preparative gas chromatography using a column containing 7% OV 101 on Chromosorb W (60/80 mesh). The column temperature was programmed from 120° (10 min hold) to 190°C at a rate of 5°C/min, and an injector port temperature of 210°C and detector temperature of 230°C were used. Three octafluorobiphenyl isomers were obtained as white crystals:

68 mg (10.5%) of 2,2',3,3',4,4',5,5'-octafluorobiphenyl (50), 77 mg (11.8%) of 2,2',3,3',4,4',6,6'-octafluorobiphenyl (51), and 119 mg (18.3%) of 2,2',3,3',4,4',5,6'-octafluorobiphenyl (53); GC peak area ratios = approximately 1:1:2 for 50:51:53; mp of 53: 38 - 40°C; $^1\text{H-NMR}$ (400.14 MHz, CDCl_3): δ 6.90 - 6.99 (m, 1 H, aromatic), δ 7.00 - 7.05 (m, 1 H, aromatic); $^{13}\text{C-NMR}$ (100.62 MHz, CDCl_3): see Appendix II; $^{19}\text{F-NMR}$ (376.50 MHz, CDCl_3): see Appendix III; GC-MS (EI) m/e (relative intensity): 298 (M^+ , 100), 149 (17.01); exact mass m/e: 298.00378 (calcd. for $\text{C}_{12}\text{H}_2\text{F}_8$: 298.00286). Elem. anal. calcd. for $\text{C}_{12}\text{H}_2\text{F}_8$: C, 48.34; H, 0.68. Found: C, 47.93; H, 0.50.

Preparation of 2,2',3,3',4,5,5',6'-Octafluorobiphenyl (54)

A mixture of 0.5 g of 1-bromo-2,3,4,5-tetrafluorobenzene, 0.5 g of 1-bromo-2,3,5,6-tetrafluorobenzene, and 1.0 g of finely divided copper was sealed in an evacuated pyrex glass tube (approximate size = 7 cm X 11 mm) and heated in an oil bath at 220 - 225°C for 60 hours. The product was extracted with ether, the copper residue was filtered off, and the ether was evaporated. The isomeric octafluorobiphenyls were separated by preparative gas chromatography using a column containing 7% OV 101 on Chromosorb W (60/80 mesh). The column temperature was

programmed from 120° (10 min hold) to 190°C at a rate of 5°C/min, and an injector port temperature of 210°C and detector temperature of 230°C were used. Three octafluorobiphenyl isomers were obtained as white crystals: 52 mg (8.0%) of 2,2',3,3',5,5',6,6'-octafluorobiphenyl (52), 70 mg (10.8%) of 2,2',3,3',4,4',5,5'-octafluorobiphenyl (50), and 121 mg (18.6%) of 2,2',3,3',4,5,5',6'-octafluorobiphenyl (54); GC peak area ratios = approximately 1:1:2 for 50:52:54; mp of 54: 51 - 53°C; ¹H-NMR (400.14 MHz, CDCl₃): δ 7.02 - 7.08 (m, 1 H, aromatic), δ 7.17 - 7.26 (m, 1 H, aromatic); ¹³C-NMR (100.62 MHz, CDCl₃): see Appendix II; ¹⁹F-NMR (376.50 MHz, CDCl₃): see Appendix III; GC-MS (EI) m/e (relative intensity): 298 (M⁺, 100), 149 (12.98); exact mass m/e: 298.00378 (calcd. for C₁₂H₂F₈: 298.00286).

Preparation of 2,2',3,3',4,5',6,6'-Octafluorobiphenyl (55)

A mixture of 0.5 g of 1-bromo-2,3,4,6-tetrafluorobenzene, 0.5 g of 1-bromo-2,3,5,6-tetrafluorobenzene, and 1.0 g of finely divided copper was sealed in an evacuated pyrex glass tube (approximate size = 7 cm X 11 mm) and heated in an oil bath at 220 - 225°C for 60 hours. The product was extracted with ether, the copper residue was filtered off, and the ether was evaporated. The isomeric octafluorobiphenyls were separated by preparative gas

chromatography using a column containing 16% Carbowax 20 M on Chromosorb W, AW/DMCS (60/80 mesh). Three octafluorobiphenyl isomers were obtained as white crystals: 79 mg (12.2%) of 2,2',3,3',5,5',6,6'-octafluorobiphenyl (52), 90 mg (13.8%) of 2,2',3,3',4,4',6,6'-octafluorobiphenyl (51), and 165 mg (25.3%) of 2,2',3,3',4,5',6,6'-octafluorobiphenyl (55); GC peak area ratios = approximately 1:1:2 for 51:52:55; mp of 55: 53 - 56°C; $^1\text{H-NMR}$ (400.14 MHz, CDCl_3): δ 6.93 - 7.00 (m, 1 H, aromatic), δ 7.19 - 7.27 (m, 1 H, aromatic); $^{13}\text{C-NMR}$ (100.62 MHz, CDCl_3): see Appendix II; $^{19}\text{F-NMR}$ (376.50 MHz, CDCl_3): see Appendix III; GC-MS (EI) m/e (relative intensity): 298 (M^+ , 100), 149 (11.97); exact mass m/e: 298.00328 (calcd. for $\text{C}_{12}\text{H}_2\text{F}_8$: 298.00286).

Preparation of 2,2',3,3',5,5',6,6'-Octafluorobiphenyl (52)

The octachlorobiphenyl isomer 52 was generated during the preparations of 54 and 55, yielding 52 mg and 79 mg, respectively, mp 83 - 85°C. $^1\text{H-NMR}$ (400.14 MHz, CDCl_3): δ 7.22 - 7.30 (m, 2 H, aromatic); $^{13}\text{C-NMR}$ (100.62 MHz, CDCl_3): see Appendix II; $^{19}\text{F-NMR}$ (376.50 MHz, CDCl_3): see Appendix III; GC-MS (EI) m/e (relative intensity): 298 (M^+ , 100), 149 (14.69); exact mass m/e: 298.00378 (calcd. for $\text{C}_{12}\text{H}_2\text{F}_8$: 298.00286).

Photolysis of Pentafluorobenzene (45) in Acetonitrile in the Absence of Triethylamine

The photolysis of 45 was repeated, using the same general procedure of Freeman and Srinivasa.¹¹ A 25.0 mL solution in acetonitrile of 45 (1.04 g, 0.247 M) was prepared. Exactly 10.0 mL of this solution was pipetted into a quartz tube with a side arm (25.0 mL) fitted with a nitrogen inlet adapter (19/14) containing a long stem whose tip almost touched the bottom of the tube. The side arm was connected to an absorption unit containing 200 mL of an aqueous solution of 30% NaOH. The quartz tube was placed inside the merry-go-round reactor chamber and irradiated with the eight 254 nm lamps surrounding the tube for a period of 30 min, while nitrogen gas was passed through the reaction mixture in a slow stream (one to two bubbles per second for one hour). Cold air was passed through the chamber during the photolysis in order to maintain the temperature constant at 40°C. The hydrogen fluoride gas, which was evolving during the reaction, was swept out by the nitrogen stream into the absorption unit and was converted to NaF.

The six isomers of octafluorobiphenyl generated by the photolysis of pentafluorobenzene were identified by comparing their gas chromatographic retention times and mass spectra with those of the synthetic products 50 - 55 prepared by the Ullmann reaction. The experiment was

carried out on a Finnigan 4023 mass spectrometer equipped with a Finnigan 9610 gas chromatograph, using a 60 M DX-4 Carbowax capillary column. The temperature was programmed to be held at 50°C for 5 min, and then to increase from 50° to 180°C at a rate of 5°C/min. A GC injector temperature of 190°C and MS source temperature of 150°C were used. Helium was used as the carrier gas at a flow rate of about 2 mL/min.

BIBLIOGRAPHY

1. Förster, T. Angew. Chem. Int. Ed. Eng. 1969, 8, 333.
2. Turro, N. J.; "Modern Molecular Photochemistry"; Benjamin/Cumming Publishing Co., Inc., Menlo Park, Calif., 1978; p 137.
3. Barltrop, J. A.; Coyle, J. D.; "Excited States in Organic Chemistry"; Wiley: New York, 1975; p 103.
4. Fleming, I.; "Frontier Orbitals and Organic Chemical Reactions"; Wiley: New Nork, 1980; p 208.
5. Davidson, R. S.; Goodin, J. W.; Kemp, G.; In "Advances in Physical Organic Chemistry"; Gold. V., Bethell, D., Eds.; Academic Press: London, 1984; Vol. 20, p. 191.
6. Ohashi, M.; Tsujimoto, K.; Seki, K. J. Chem. Soc., Chem. Commun. 1973, 384.
7. Bunce, N. J.; Pilon, P.; Ruzo, L. O.; Sturch, D. J. J. Org. Chem. 1976, 41, 3023.
8. Davidson, R. S.; Goodin, J. W. Tetrahedron Lett. 1981, 22, 163.
9. Bunce, N. J. J. Org. Chem. 1982, 47, 1948.
10. Freeman, P. K.; Srinivasa, R.; Campbell, J. A.; Deinzer, M. L. J. Am. Chem. Soc., Submitted.
11. Freeman, P. K.; Srinivasa, R., Unpublished.
12. Grimshaw, J.; deSilva, A. P. Chem. Soc. Rev. 1981, 10, 181.
13. Kupchan, S. M.; Wormser, H. C. J. Org. Chem. 1965, 30, 3792.
14. Kametani, T.; Nitadori, R.; Terasawa, H.; Takahashi, K. Tetrahedron 1977, 33, 1069.
15. Grimshaw, J.; deSilva, A. P. Can. J. Chem. 1980, 58, 1880.

16. Brightwell, N. E.; Griffin, G. W. J. Chem. Soc., Chem. Commun. 1973, 37.
17. Jeffs, P. W.; Hansen, J. F.; Brine, G. A. J. Org. Chem. 1975, 40, 2883.
18. Ito, K.; Tanaka, H. Chem. Pharm. Bull. Japan. 1974, 22, 2108.
19. Burdon, J. Tetrahedron 1965, 21, 3373.
20. Clark, D. T.; Murrell, J. N.; Tedder, J. M. J. Chem. Soc. 1963, 1250.
21. Burdon, J.; Childs, A. C.; Parsons, I. W.; Tatlow, J. C. J. Chem. Soc., Chem. Commun. 1982, 534.
22. Burdon, J.; Gill, H. S.; Parsons, I. W.; Tatlow, J. C. J. Chem. Soc., Perkin Trans. 1. 1980, 1726
23. Burdon, J.; Parsons, I. W.; Gill, H. S. J. Chem. Soc., Perkin Trans. 1. 1979, 1351.
24. Burdon, J.; Parsons, I. W. J. Am. Chem. Soc. 1977, 99, 7445.
25. Chamber, R. D.; "Fluorine In Organic Chemistry"; Wiley: New York, 1973; p 7.
26. Bursey, M. M.; McLafferty, F. W. J. Am. Chem. Soc. 1966, 88, 529.
27. Bursey, M. M.; McLafferty, F. W. J. Am. Chem. Soc. 1967, 89, 1.
28. Fanta, P. E. Chem. Rev. 1964, 64, 613.
29. Nield, E.; Stephens, R.; Tatlow, J. C. J. Chem. Soc. 1959, 166.
30. Silberrad, O. J. Chem. Soc. 1922, 1015.
31. Finger, G. C.; Reed, F. H. J. Am. Chem. Soc. 1944, 66, 1972.
32. McBee, E. T.; Calundann, G. W.; Morton, C. J.; Hodgins, T.; Wesseler, E. P. J. Org. Chem. 1972, 37, 3140.
33. Price, C. C.; Krebs, E. Org. Synth. III 1955, 649.

APPENDICES

Appendix I

GC-MS^a Data for Photoproducts of Fluoropentachlorobenzene

Photoproducts:	<u>9</u>	<u>10</u>	<u>11</u>
m/e	% Relative Intensity		
92	22.15	25.61	24.16
116	12.50	13.09	12.64
117	14.74	14.90	14.67
127	21.24	21.50	21.05
162	25.83	25.38	25.16
164	16.52	15.79	16.53
197	30.78	30.03	28.91
199	30.47	26.97	27.91
232	78.45	78.76	78.79
234	100.00	100.00	100.00
236	47.62	49.06	49.28

^a EI, 70 eV.^b Only values with ten percent or greater have been included.

Appendix II

 ^{13}C -NMR Spectra of the Octafluorobiphenyls 50 - 55

The ^{13}C -NMR spectra appear in Figures 7 - 12, and the chemical shifts and intensities are listed for each spectrum on the page which immediately follows it. The spectra were taken at 100.62 MHz using CDCl_3 as the solvent and TMS as the internal standard.

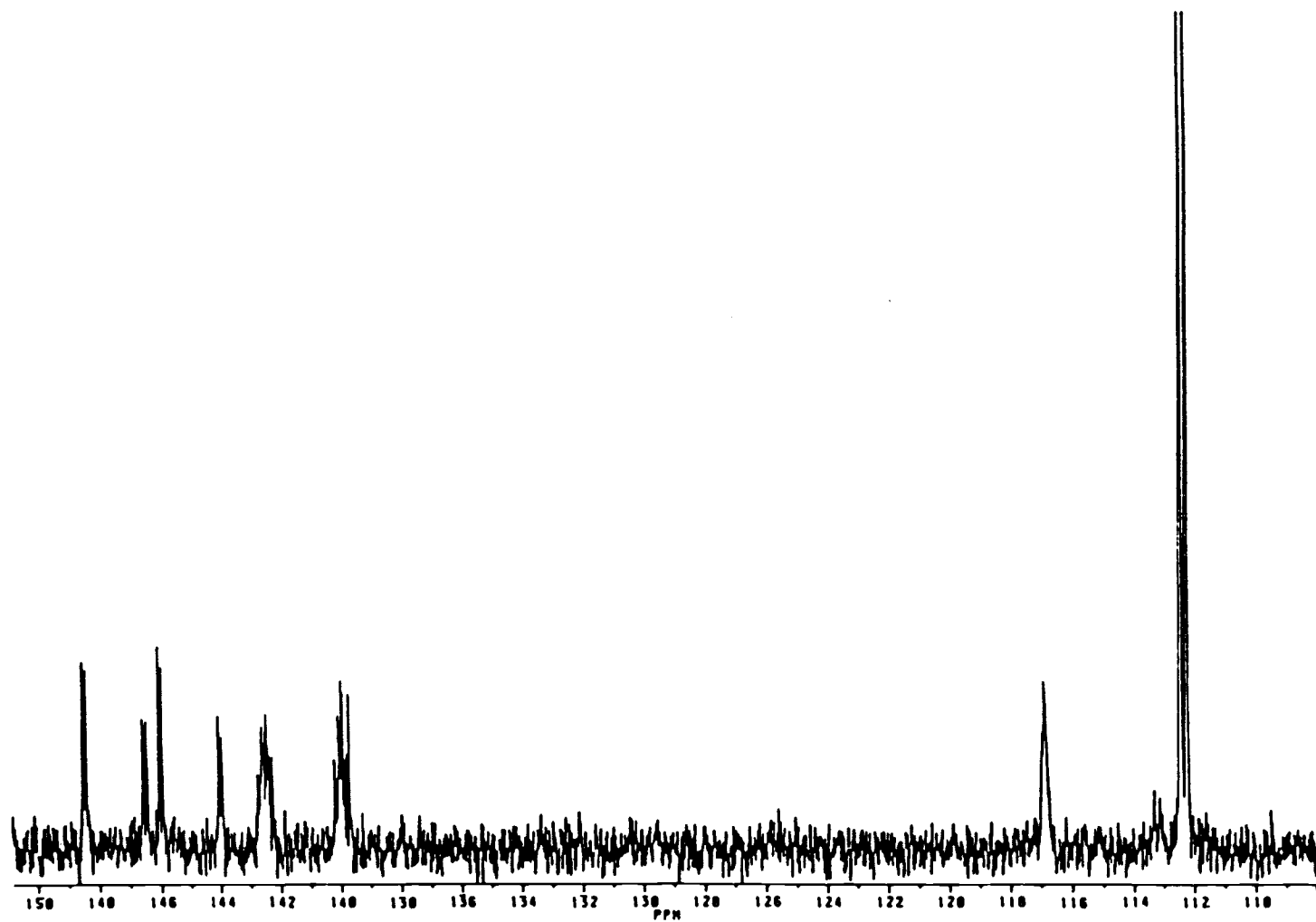


Figure 7. ^{13}C -NMR spectrum of 2,2',3,3',4,4',5,5'-octafluorobiphenyl (50).

List of chemical shifts (ppm from TMS) and relative intensities for the ^{13}C -NMR spectrum of 50 (Fig. 7)

#	PPM	INTENSITY
1	148.4917	9.800
2	148.3860	9.404
3	146.5482	6.772
4	146.4040	6.635
5	146.0225	10.518
6	145.9192	9.341
7	144.0155	6.879
8	143.9146	5.878
9	142.5713	6.516
10	142.4169	6.964
11	142.2208	4.994
12	140.2216	4.838
13	139.9522	8.634
14	139.8963	8.073
15	139.7863	5.111
16	139.6993	7.960
17	116.8940	8.556
18	112.4302	49.287
19	112.2465	47.747

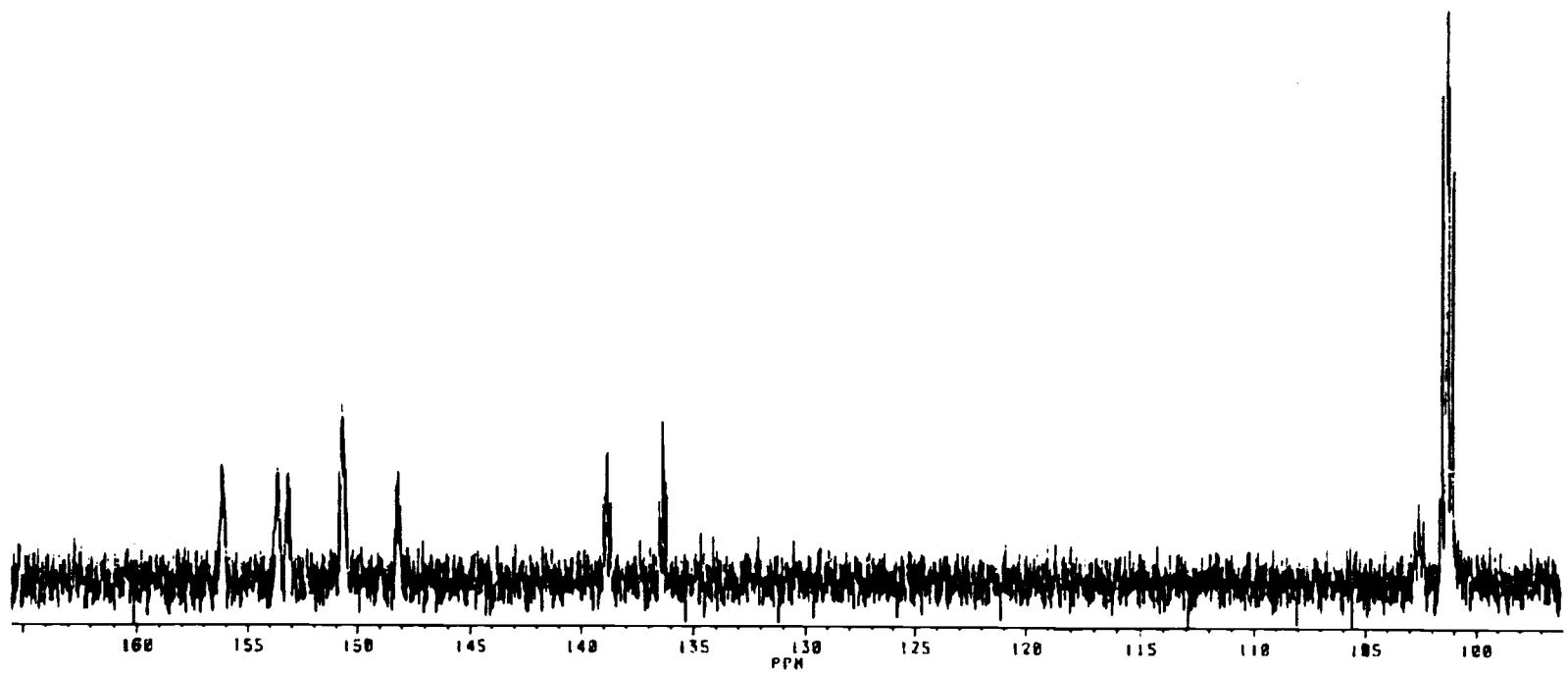


Figure 8. ^{13}C -NMR spectrum of 2,2',3,3',4,4',6,6'-octafluorobiphenyl (51).

List of chemical shifts (ppm from TMS) and relative intensities for the ^{13}C -NMR spectrum of 51 (Fig. 8)

#	PPM	INTENSITY
1	156.1667	4.864
2	153.5957	4.711
3	153.1642	4.530
4	153.1193	4.588
5	153.0228	3.823
6	150.8329	3.984
7	150.7007	7.411
8	150.6334	6.846
9	150.4970	4.635
10	150.4432	2.805
11	148.2570	3.895
12	148.1555	4.585
13	138.9584	3.557
14	138.8533	5.204
15	138.8068	5.418
16	138.6599	3.311
17	136.5237	3.422
18	136.3719	6.876
19	136.3202	5.642
20	136.2154	4.105
21	136.1692	3.526
22	102.6153	3.362
23	102.4123	2.679
24	101.6026	21.081
25	101.3876	24.174
26	101.3315	20.604
27	101.2979	21.097
28	101.1131	16.759
29	101.0818	17.880

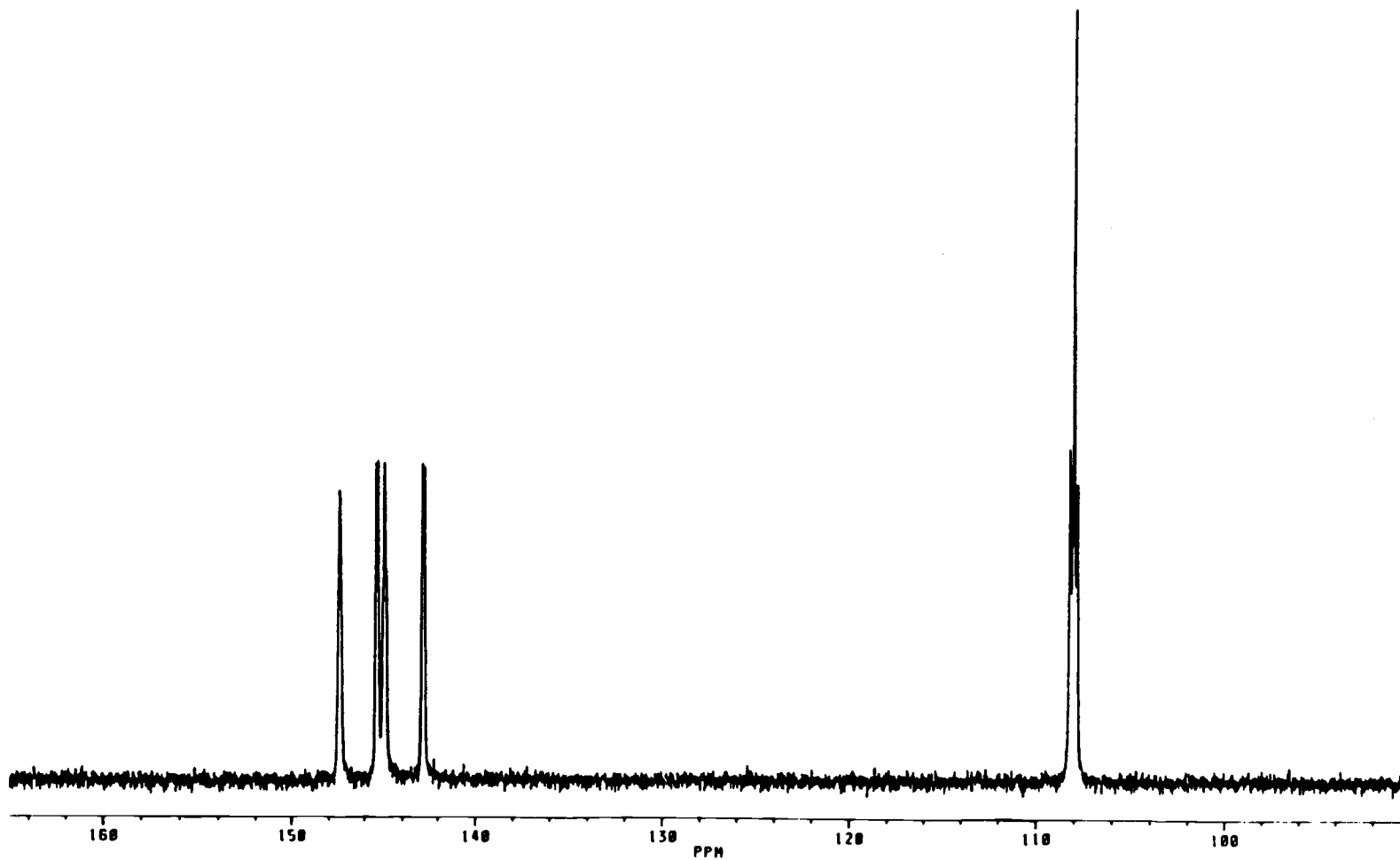


Figure 9. ^{13}C -NMR spectrum of 2,2',3,3',5,5',6,6'-octafluorobiphenyl (52).

List of chemical shifts (ppm from TMS) and relative intensities for the ^{13}C -NMR spectrum of 52 (Fig. 9)

#	PPM	INTENSITY
1	147.3702	10.130
2	145.3809	11.242
3	145.2603	11.082
4	144.9082	10.903
5	144.8089	7.030
6	142.8847	11.044
7	142.7617	10.683
8	108.2372	11.353
9	108.0225	27.181
10	107.8055	10.505

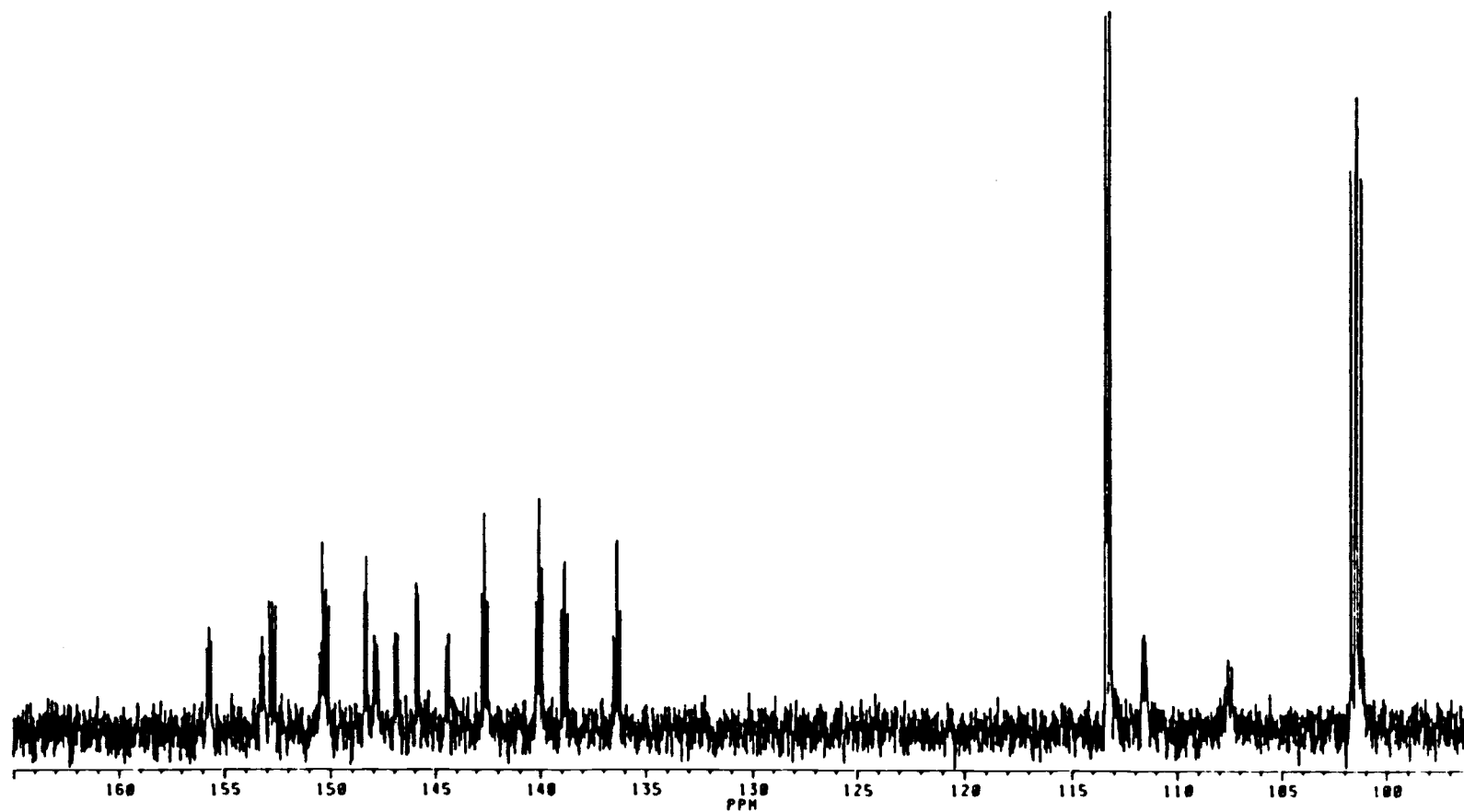


Figure 10. ^{13}C -NMR spectrum of 2,2',3,3',4,4',5,6'-octafluorobiphenyl (53).

List of chemical shifts (ppm from TMS) and relative intensities for the ^{13}C -NMR spectrum of 53 (Fig. 10)

#	PPM	INTENSITY	#	PPM	INTENSITY
1	155.8115	1.842	51	138.9781	2.711
2	155.6985	2.305	52	138.8759	3.867
3	155.5779	1.980	53	138.8207	3.816
4	153.2601	1.773	54	138.7204	2.424
5	153.2064	2.135	55	138.6676	2.608
6	153.1690	1.782	56	136.5433	2.126
7	152.8859	2.890	57	136.4892	2.086
8	152.8314	2.486	58	136.3864	4.236
9	152.7775	2.446	59	136.3323	4.217
10	152.7398	2.932	60	136.2341	2.325
11	152.6870	2.256	61	136.1798	2.678
12	152.6294	2.112	62	113.3434	16.076
13	152.5739	2.786	63	113.1389	16.244
14	150.5210	1.758	64	111.6500	2.041
15	150.3589	4.254	65	111.5632	2.260
16	150.3074	3.012	66	111.4815	2.008
17	150.2475	2.881	67	107.5634	1.577
18	150.1938	3.142	68	101.7150	12.701
19	150.1571	2.468	69	101.6764	12.549
20	150.1024	2.506	70	101.4991	13.033
21	150.0491	2.776	71	101.4600	14.335
22	148.4408	2.682	72	101.4363	14.230
23	148.4055	3.124	73	101.3971	13.550
24	148.3782	2.451	74	101.2203	13.031
25	148.3359	2.781	75	101.1815	13.050
26	148.3123	3.861			
27	148.2750	2.841			
28	148.0046	1.813			
29	147.9490	2.103			
30	147.8629	1.935			
31	146.9463	2.170			
32	146.8487	2.118			
33	145.9699	2.895			
34	145.9465	2.830			
35	145.9321	3.290			
36	145.9093	3.175			
37	145.8690	2.660			
38	145.8408	3.017			
39	145.8039	2.420			
40	144.4866	1.919			
41	144.3414	2.176			
42	142.7937	2.098			
43	142.7587	3.334			
44	142.7258	2.317			
45	142.6712	2.551			
46	142.6270	4.877			
47	142.5972	4.190			
48	142.5039	2.515			
49	142.4721	2.959			
50	140.2611	2.289			
51	140.2076	2.891			
52	140.1764	2.729			
53	140.1390	2.423			
54	140.0921	4.456			
55	140.0523	5.448			
56	140.0102	2.760			
57	139.9722	2.608			
58	139.3246	3.644			
59	139.3881	2.993			
60	139.0309	2.606			

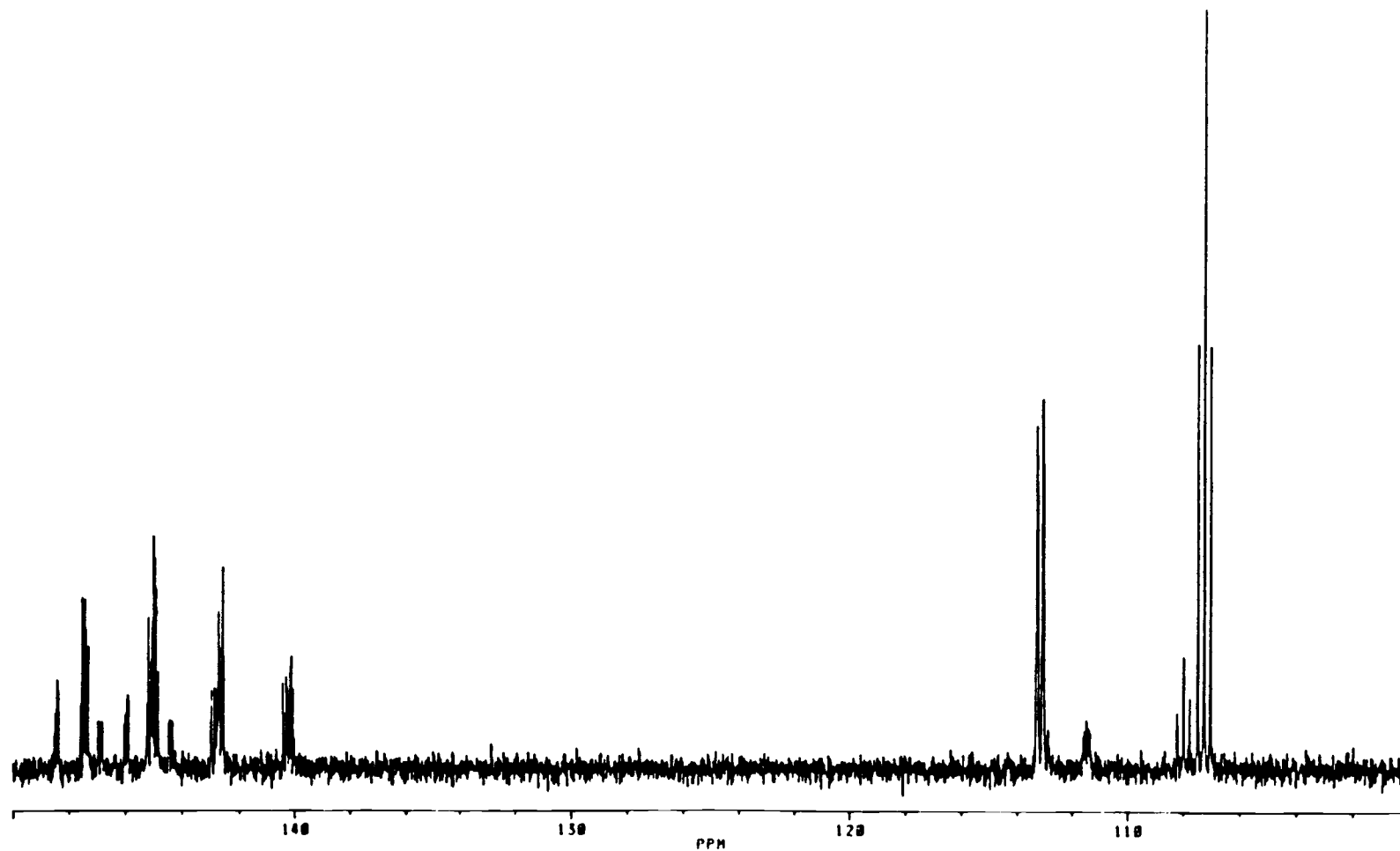


Figure 11. ^{13}C -NMR spectrum of 2,2',3,3',4,5,5',6'-octafluorobiphenyl (54).

List of chemical shifts (ppm from TMS) and relative intensities for the ^{13}C -NMR spectrum of 54 (Fig. 11)

#	PPM	INTENSITY			
1	148.5084	.913	61	108.1909	1.376
2	148.4783	1.355	62	107.9672	2.733
3	148.4432	1.277	63	107.7448	1.508
4	148.4031	1.547	64	107.4567	9.534
5	148.3666	1.440	65	107.2342	18.328
6	147.5891	1.974	66	107.0093	9.627
7	147.5467	2.869			
8	147.4864	2.788			
9	147.4442	4.096			
10	147.4034	2.684			
11	147.3484	2.322			
12	147.3039	2.449			
13	146.9554	1.202			
14	146.8161	1.213			
15	146.0357	1.100			
16	146.0052	1.383			
17	145.9716	1.192			
18	145.9308	1.320			
19	145.9089	1.444			
20	145.8944	1.398			
21	145.8714	1.213			
22	145.2320	1.657			
23	145.1898	3.335			
24	145.1500	1.725			
25	145.1046	2.590			
26	145.0468	3.588			
27	145.0065	4.495			
28	144.9677	4.291			
29	144.9237	3.219			
30	144.8629	2.791			
31	144.8224	2.389			
32	144.4095	1.110			
33	144.3153	1.096			
34	142.9759	1.072			
35	142.9443	1.442			
36	142.8508	2.020			
37	142.8139	2.138			
38	142.7785	1.643			
39	142.7002	3.689			
40	142.6603	2.802			
41	142.5978	1.735			
42	142.5578	4.097			
43	142.5180	2.589			
44	140.4195	1.414			
45	140.3871	1.174			
46	140.2978	1.664			
47	140.2646	1.826			
48	140.2220	1.357			
49	140.1912	1.294			
50	140.1462	2.162			
51	140.1022	2.296			
52	140.0249	1.333			
53	139.9846	.816			
54	113.2564	8.322			
55	113.2416	8.072			
56	113.0523	8.789			
57	113.0362	9.125			
58	112.8476	.939			
59	111.4539	1.114			
60	111.4279	1.055			

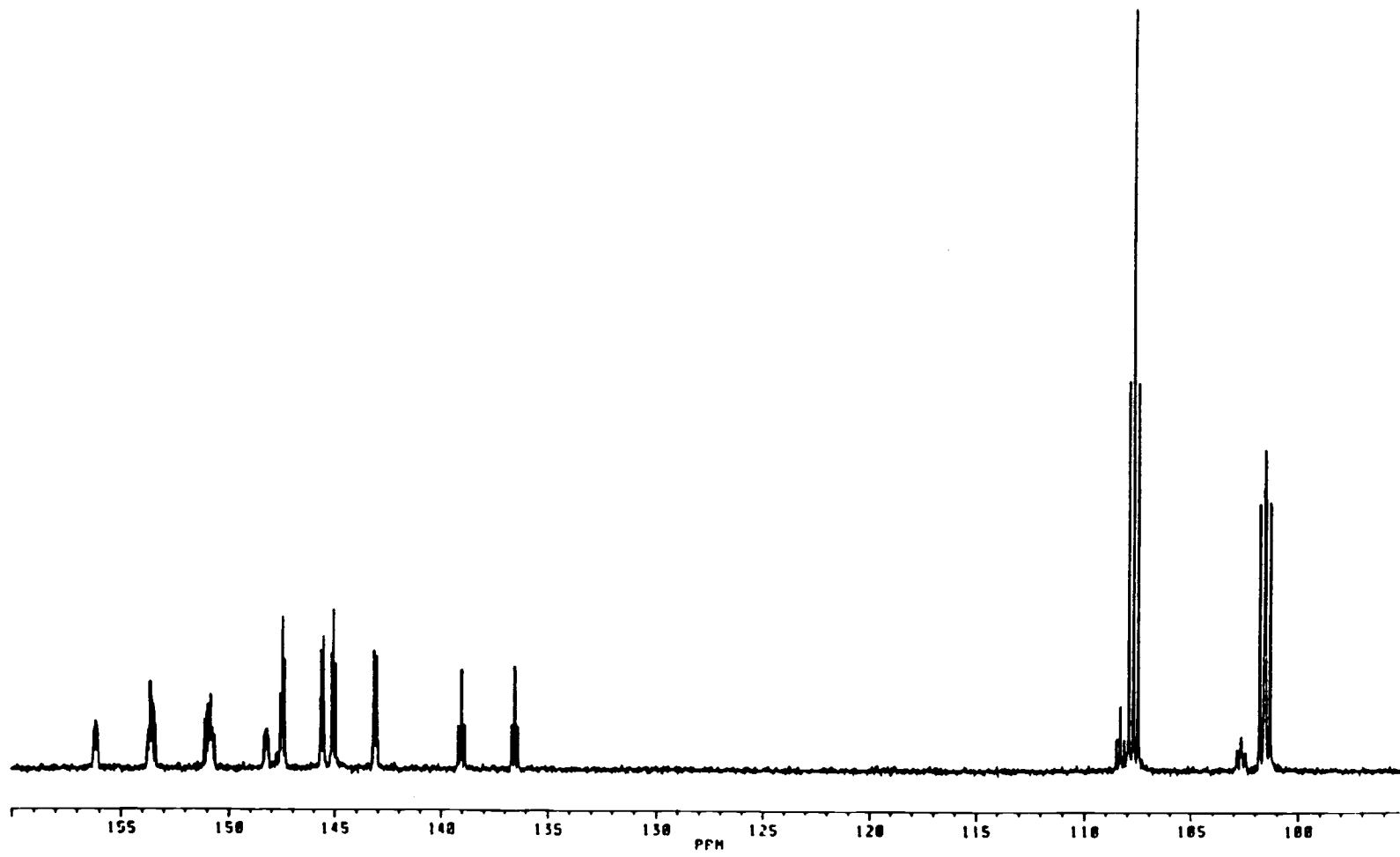


Figure 12. ^{13}C -NMR spectrum of 2,2',3,3',4,5',6,6'-octafluorobiphenyl (55).

List of chemical shifts (ppm from TMS) and relative intensities for the ^{13}C -NMR spectrum of 55 (Fig. 12)

#	PPM	INTENSITY			
1	156.2451	.890			
2	156.2094	.966			
3	156.1756	.998			
4	156.1358	1.157			
5	156.0839	.999			
6	156.0490	1.023			
7	156.0124	.898			
8	153.7531	.839			
9	153.7174	.950			
10	153.6812	1.035			
11	153.6486	2.142			
12	153.5923	2.117			
13	153.5380	1.728			
14	153.5012	1.577			
15	153.4852	1.565			
16	153.4470	1.490			
17	153.3925	1.386			
18	153.3383	1.080			
19	151.1175	1.198			
20	151.0628	1.232			
21	151.0053	1.327			
22	150.9680	1.416			
23	150.9523	1.554			
24	150.9144	1.426			
25	150.8864	1.025			
26	150.8603	1.542			
27	150.8310	1.098			
28	150.8047	1.860			
29	150.7701	.989			
30	150.7439	.957			
31	150.7172	.982			
32	150.6828	.850			
33	148.2984	.837			
34	148.2665	.923			
35	148.2390	.883			
36	148.2129	.957			
37	148.1853	.946			
38	147.5866	1.829			
39	147.5385	1.103			
40	147.5246	1.293			
41	147.4794	3.280			
42	147.4474	3.620			
43	147.3734	2.248			
44	147.3430	2.616			
45	145.6696	1.760			
46	145.6280	2.831			
47	145.5897	1.882			
48	145.5364	1.817			
49	145.4982	3.180			
50	145.4597	1.642			
51	145.1510	2.736			
52	145.1002	1.982			
53	145.0505	3.824			
54	144.9318	2.519			
55	143.1915	1.641			
56	143.1514	2.869			
57	143.1120	1.636			
58	143.0591	1.567			
59	143.0226	2.748			
60	142.9838	1.374			
61	139.1848	1.062			
62	139.1314	.971			
63	139.0318	2.352			
64	138.9785	2.366			
65	138.8792	1.065			
66	138.8265	1.040			
67	138.6969	1.075			
68	138.6433	1.056			
69	138.5443	2.455			
70	138.4912	2.361			
71	138.3917	1.058			
72	138.3385	.998			
73	108.3168	1.577			
74	107.9267	9.222			
75	107.7045	18.261			
76	107.4800	9.193			
77	102.6372	.854			
78	101.8133	6.412			
79	101.7755	6.369			
80	101.5957	6.713			
81	101.5560	7.647			
82	101.5393	7.448			
83	101.4990	6.647			
84	101.3197	6.538			
85	101.2822	6.394			

Appendix III

 ^{19}F -NMR Spectra of the Octafluorobiphenyls 50 - 55

The ^{19}F -NMR spectra appear in Figures 13 - 18, and the chemical shifts and intensities are listed for each spectrum on the page which immediately follows it. The spectra were taken at 376.50 MHz using CDCl_3 as the solvent and hexafluorobenzene as the internal standard (chemical shift = -163 ppm relative to the chemical shift of trichlorofluoromethane of 0 ppm).

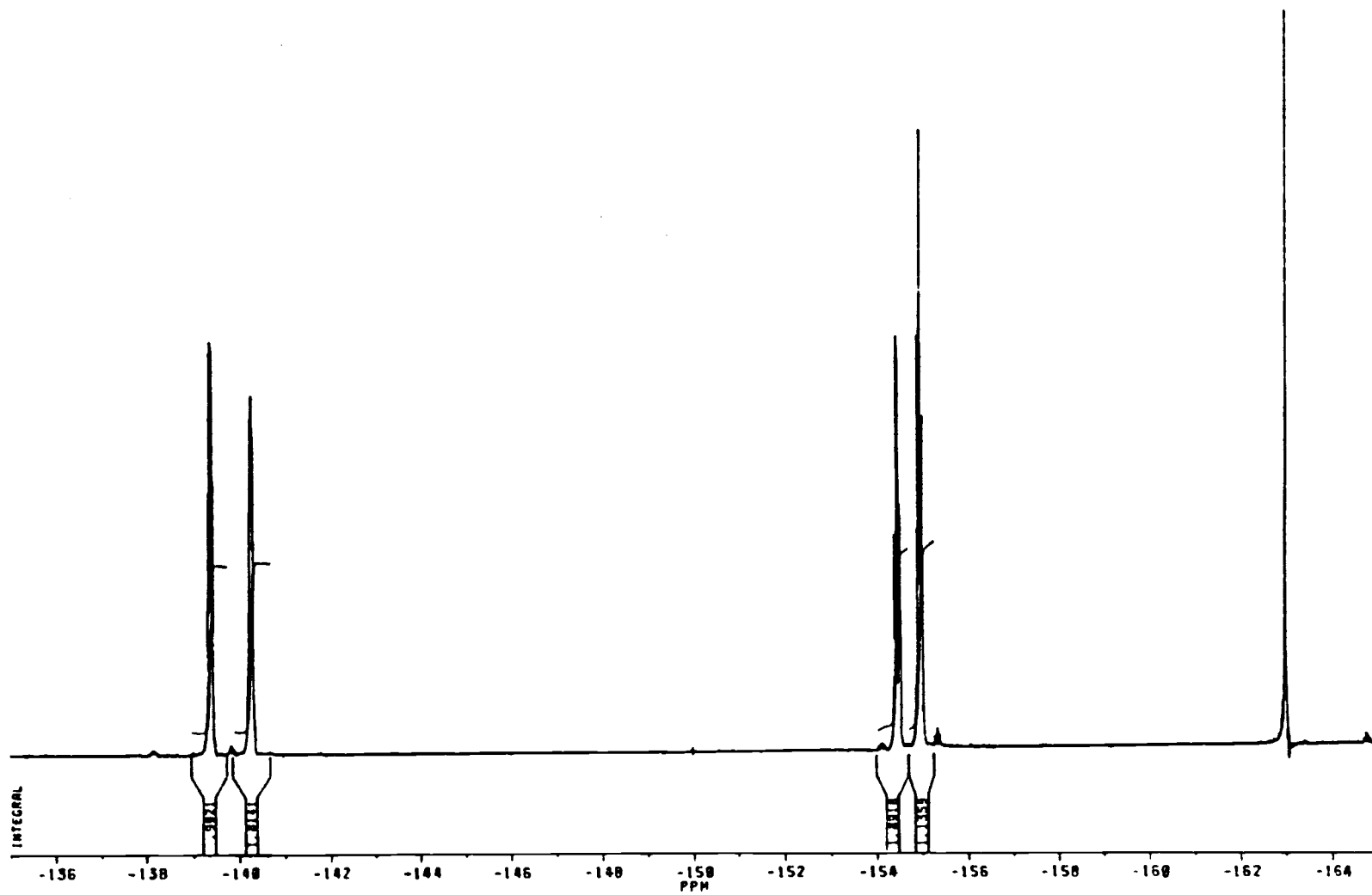


Figure 13. ^{19}F -NMR spectrum of 2,2',3,3',4,4',5,5'-octafluorobiphenyl (50).

List of chemical shifts (ppm from CFCl_3) and relative intensities for the ^{19}F -NMR spectrum of 50 (Fig. 13)

#	PPM	INTENSITY
1	-139.3091	5.416
2	-139.3174	6.394
3	-139.3358	8.228
4	-139.3415	9.952
5	-139.3492	8.304
6	-139.3666	10.026
7	-139.3739	9.471
8	-139.3917	7.875
9	-139.3983	9.803
10	-139.4045	7.572
11	-139.4233	6.605
12	-139.4316	4.748
13	-140.1739	1.376
14	-140.1873	1.854
15	-140.2166	5.816
16	-140.2303	8.109
17	-140.2450	8.088
18	-140.2578	8.690
19	-140.2705	7.899
20	-140.2853	7.648
21	-140.2990	5.094
22	-154.3860	4.880
23	-154.3989	5.325
24	-154.4068	5.258
25	-154.4192	4.929
26	-154.4418	9.551
27	-154.4522	10.059
28	-154.4612	9.765
29	-154.4720	9.574
30	-154.4948	6.028
31	-154.5071	5.988
32	-154.5153	6.031
33	-154.5277	5.736
34	-154.8790	1.586
35	-154.8960	5.411
36	-154.9033	10.086
37	-154.9104	8.147
38	-154.9503	10.341
39	-154.9570	15.446
40	-154.9643	10.099
41	-154.9815	3.572
42	-155.0032	6.237
43	-155.0104	8.245
44	-155.0179	4.819
45	-162.9997	115.416
46	-163.0120	2.376

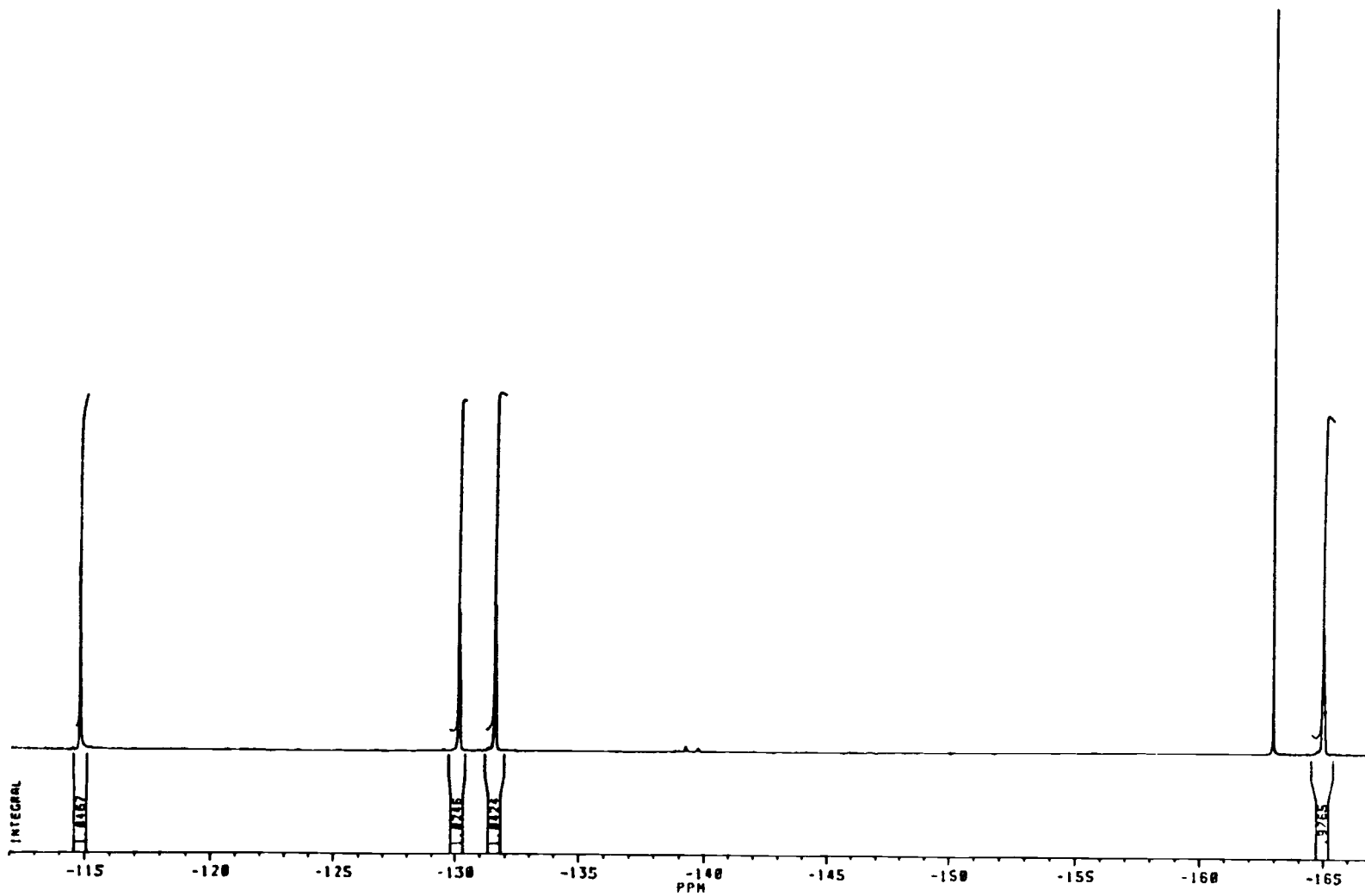


Figure 14. ^{19}F -NMR spectrum of 2,2',3,3',4,4',6,6'-octafluorobiphenyl (51).

List of chemical shifts (ppm from CFCl_3) and relative intensities for the ^{19}F -NMR spectrum of 51 (Fig. 14)

#	PPM	INTENSITY
1	-114.8057	2.687
2	-114.8244	4.449
3	-114.8349	4.485
4	-114.8534	2.856
5	-130.1161	2.433
6	-130.1351	3.492
7	-130.1550	2.634
8	-130.1641	2.843
9	-130.1729	2.543
10	-130.1927	3.340
11	-130.2117	2.175
12	-131.5602	2.722
13	-131.5669	2.793
14	-131.5791	3.568
15	-131.5997	2.542
16	-131.6048	2.555
17	-131.6253	3.491
18	-131.6437	2.360
19	-162.9999	18.006
20	-164.9545	1.322
21	-164.9731	1.631
22	-164.9794	1.658
23	-164.9961	1.838
24	-165.0102	2.601
25	-165.0266	2.940
26	-165.0358	2.856
27	-165.0521	2.443
28	-165.0661	1.694
29	-165.0829	1.487
30	-165.1078	1.063

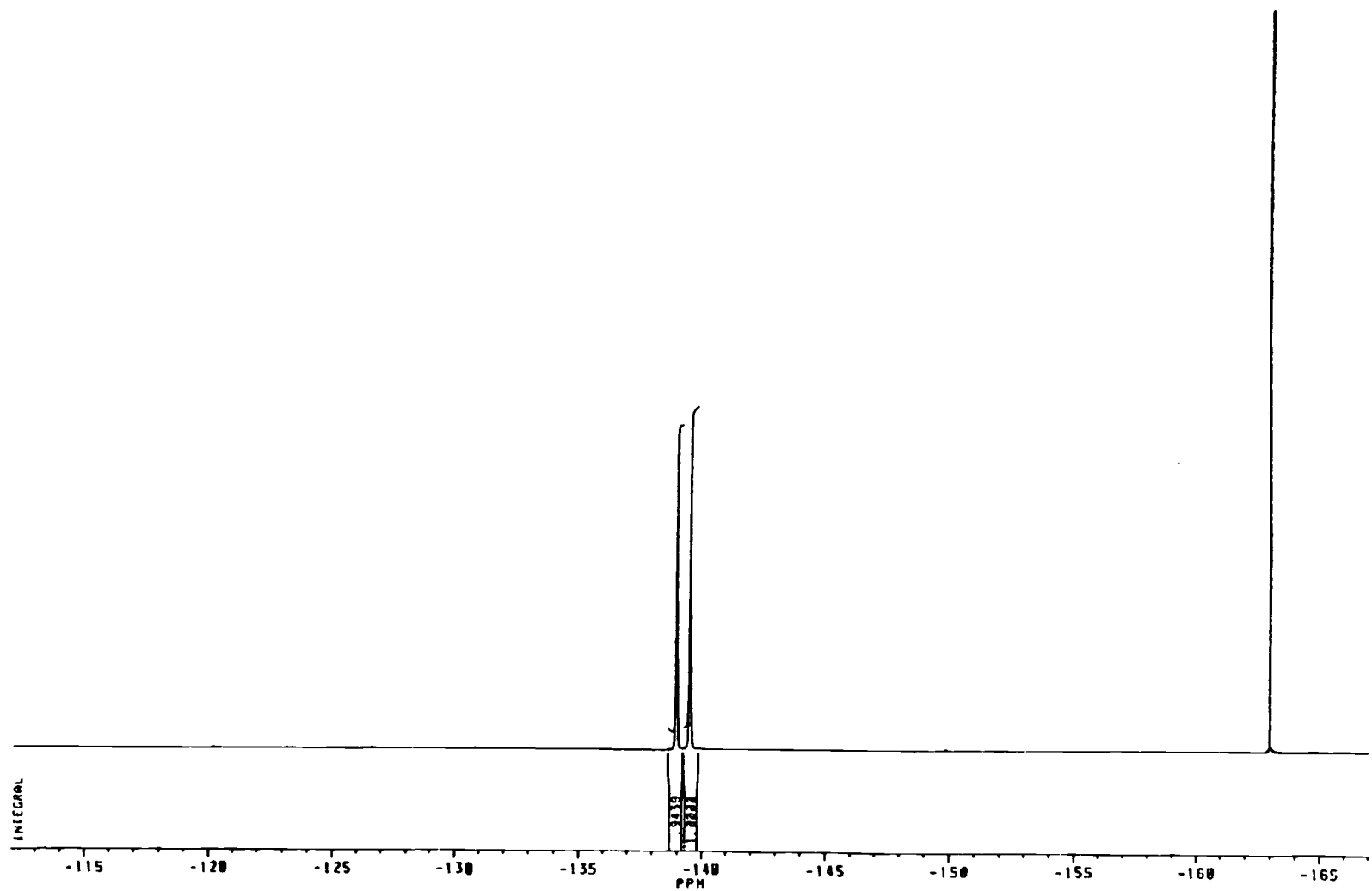


Figure 15. ^{19}F -NMR spectrum of 2,2',3,3',5,5',6,6'-octafluorobiphenyl (52).

List of chemical shifts (ppm from CFCl_3) and relative intensities for the ^{19}F -NMR spectrum of 52 (Fig. 15)

#	PPM	INTENSITY
1	-138.9448	1.128
2	-138.9489	1.236
3	-138.9531	1.169
4	-138.9655	1.759
5	-138.9740	2.243
6	-138.9789	2.676
7	-138.9826	2.632
8	-138.9903	2.146
9	-138.9975	2.068
10	-139.0045	4.157
11	-139.0072	4.340
12	-139.0229	2.378
13	-139.0292	3.601
14	-139.0320	3.577
15	-139.0404	2.202
16	-139.0474	1.984
17	-139.0603	1.608
18	-139.4927	1.441
19	-139.5043	2.121
20	-139.5114	2.962
21	-139.5206	2.314
22	-139.5322	3.614
23	-139.5543	4.325
24	-139.5662	2.346
25	-139.5741	3.365
26	-139.5873	1.657
27	-139.5956	2.010
28	-139.6030	1.447
29	-162.9999	18.079

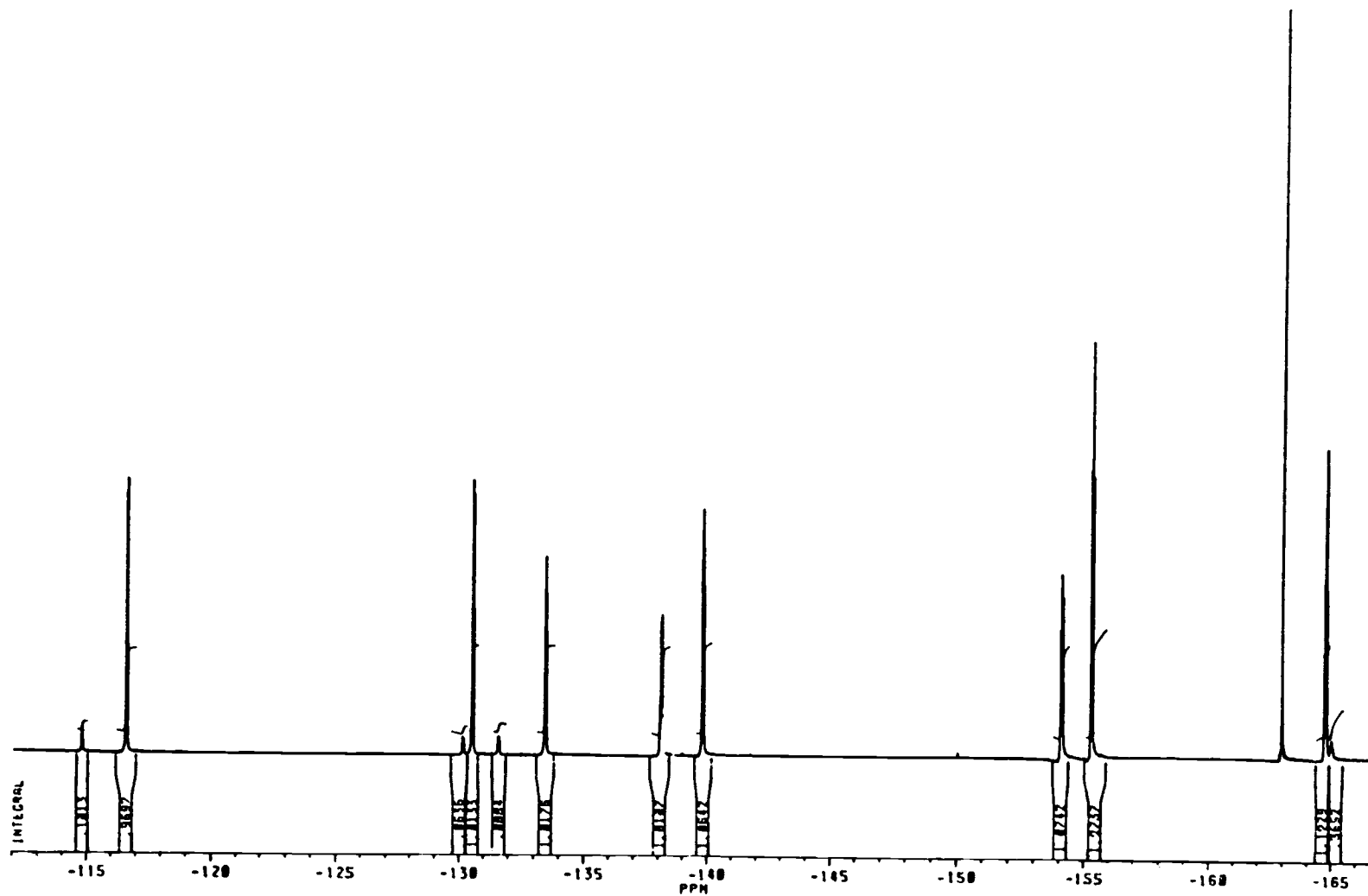


Figure 16. ^{19}F -NMR spectrum of 2,2',3,3',4,4',5,6'-octafluorobiphenyl (53).

List of chemical shifts (ppm from CFCl_3) and relative intensities for the ^{19}F -NMR spectrum of 53 (Fig. 16)

=	PPM	INTENSITY			
1	-116.5969	2.742	61	-139.8799	4.094
2	-116.6040	2.718	62	-139.8804	3.761
3	-116.6266	6.353	63	-154.0397	3.091
4	-116.6324	5.495	64	-154.0534	2.949
5	-116.6502	5.554	65	-154.0604	3.046
6	-116.6560	6.595	66	-154.0737	3.084
7	-116.6781	2.650	67	-154.0932	4.162
8	-116.6853	2.447	68	-154.1082	4.378
9	-130.4917	3.543	69	-154.1149	4.552
10	-130.4989	3.568	70	-154.1267	4.363
11	-130.5105	3.757	71	-154.1292	4.324
12	-130.5179	6.562	72	-154.1481	3.452
13	-130.5252	3.648	73	-154.1617	3.814
14	-130.5368	3.586	74	-154.1687	3.879
15	-130.5442	3.799	75	-154.1826	3.793
16	-130.5486	3.635	76	-155.2691	3.137
17	-130.5562	3.612	77	-155.2766	7.012
18	-130.5673	3.923	78	-155.2838	4.930
19	-130.5747	6.340	79	-155.3233	5.007
20	-130.5825	3.368	80	-155.3304	10.297
21	-130.5937	3.452	81	-155.3377	6.972
22	-130.6008	3.202	82	-155.3764	3.176
23	-133.4195	2.959	83	-155.3841	6.853
24	-133.4258	3.082	84	-155.3913	4.962
25	-133.4381	3.193	85	-163.0002	44.738
26	-133.4462	3.937	86	-164.7031	2.805
27	-133.4543	3.285	87	-164.7191	2.970
28	-133.4667	3.313	88	-164.7321	4.285
29	-133.4745	4.750	89	-164.7480	4.190
30	-133.4819	3.257	90	-164.7599	6.305
31	-133.4942	3.184	91	-164.7758	6.447
32	-133.5025	3.858	92	-164.7886	7.502
33	-133.5104	3.154	93	-164.8044	7.124
34	-133.5228	2.966	94	-164.8166	4.110
35	-133.5290	2.734	95	-164.8324	4.059
36	-138.0604	.782	96	-164.8450	4.119
37	-138.0751	1.358	97	-164.8609	3.778
38	-138.0894	2.378			
39	-138.1039	3.030			
40	-138.1184	3.225			
41	-138.1345	3.422			
42	-138.1448	3.352			
43	-138.1479	3.206			
44	-138.1588	3.470			
45	-138.1752	3.291			
46	-138.1893	3.107			
47	-138.2039	2.499			
48	-138.2181	1.414			
49	-138.2325	.831			
50	-139.7659	3.217			
51	-139.7741	4.685			
52	-139.7922	3.746			
53	-139.8001	5.540			
54	-139.8058	4.836			
55	-139.8223	5.627			
56	-139.8310	6.067			
57	-139.8482	4.823			
58	-139.8538	5.058			
59	-139.8564	4.778			
60	-139.8620	4.488			

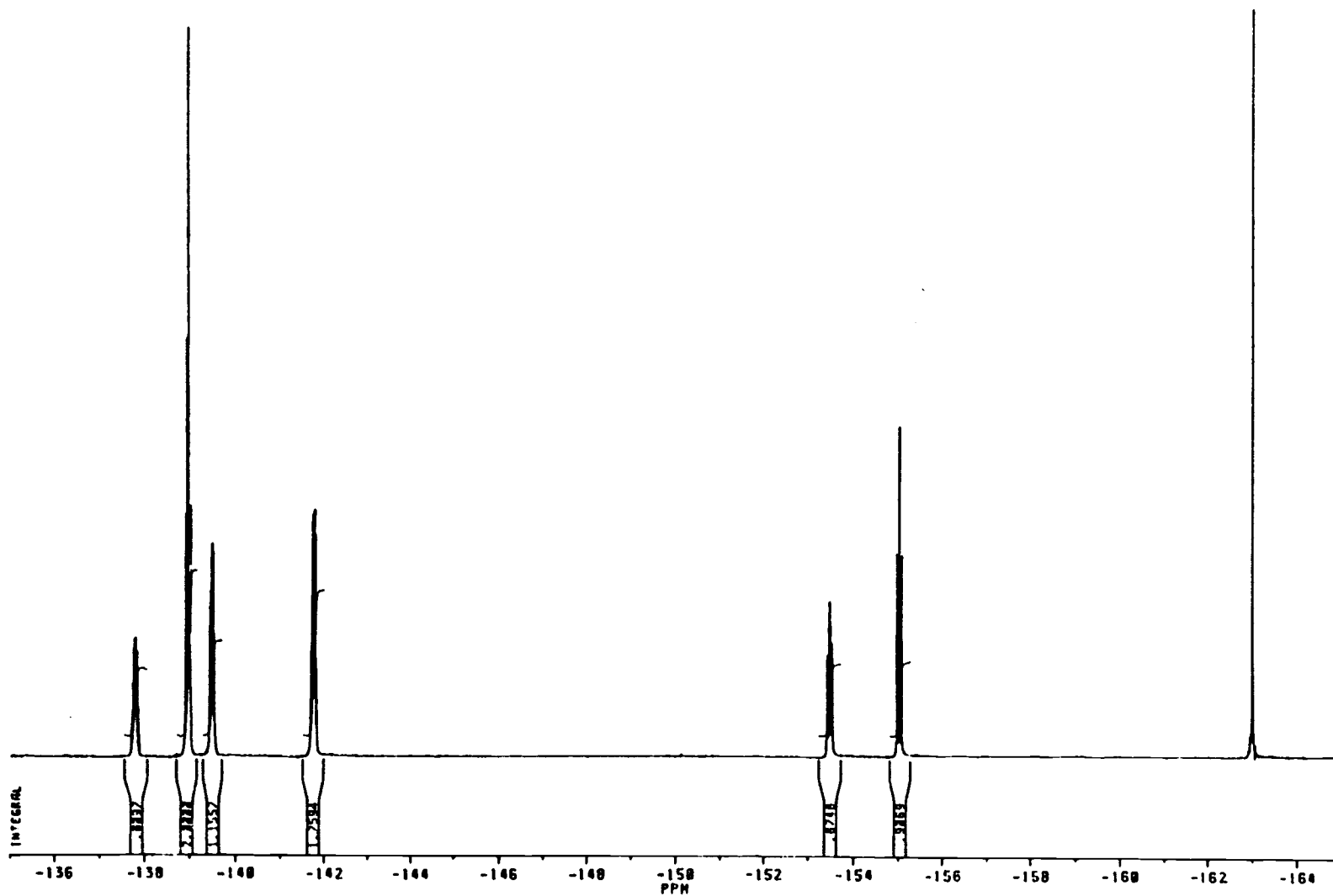


Figure 17. ^{19}F -NMR spectrum of 2,2',3,3',4,5,5',6'-octafluorobiphenyl (54).

List of chemical shifts (ppm from CFCl_3) and relative intensities for the ^{19}F -NMR spectrum of 54 (Fig. 17)

=	PPM	INTENSITY			
1	-137.7233	.657	61	-153.4563	2.398
2	-137.7384	1.164	62	-153.4749	3.303
3	-137.7528	1.873	63	-153.4890	3.622
4	-137.7673	2.700	64	-153.4932	3.849
5	-137.7825	2.680	65	-153.5100	3.303
6	-137.7983	2.971	66	-153.5298	2.552
7	-137.8084	2.470	67	-153.5443	2.704
8	-137.8123	2.531	68	-153.5502	2.819
9	-137.8219	2.961	69	-153.5646	2.479
10	-137.8372	2.657	70	-154.9685	3.048
11	-137.8529	2.685	71	-154.9758	5.063
12	-137.8673	1.960	72	-154.9835	2.868
13	-137.8816	1.231	73	-155.0222	4.611
14	-137.8963	.574	74	-155.0296	8.336
15	-138.9233	5.435	75	-155.0370	4.930
16	-138.9298	6.043	76	-155.0757	2.872
17	-138.9492	5.760	77	-155.0830	4.981
18	-138.9551	6.923	78	-155.0904	2.895
19	-138.9611	10.930	79	-162.9087	.205
20	-138.9858	18.935	80	-162.9231	.192
21	-139.0107	11.541	81	-162.9435	.537
22	-139.0163	7.962	82	-162.9555	.455
23	-139.0223	5.823	83	-163.0001	84.258
24	-139.0415	6.295	84	-163.0633	.310
25	-139.0480	5.635	85	-163.0811	.124
26	-139.0929	.131			
27	-139.4033	.167			
28	-139.4447	3.226			
29	-139.4533	3.224			
30	-139.4711	3.706			
31	-139.4770	4.279			
32	-139.4850	3.730			
33	-139.5016	5.118			
34	-139.5099	5.259			
35	-139.5273	3.954			
36	-139.5333	5.164			
37	-139.5408	3.297			
38	-139.5524	1.335			
39	-139.5589	3.095			
40	-139.5667	2.860			
41	-141.7012	2.197			
42	-141.7070	2.615			
43	-141.7209	2.487			
44	-141.7281	3.990			
45	-141.7375	5.835			
46	-141.7494	2.910			
47	-141.7573	6.161			
48	-141.7622	5.783			
49	-141.7835	5.402			
50	-141.7867	5.575			
51	-141.7912	6.151			
52	-141.7995	2.877			
53	-141.8111	5.453			
54	-141.8208	3.596			
55	-141.8281	2.425			
56	-141.8419	2.263			
57	-141.8477	2.034			
58	-153.4213	2.394			
59	-153.4356	2.544			
60	-153.4419	2.435			

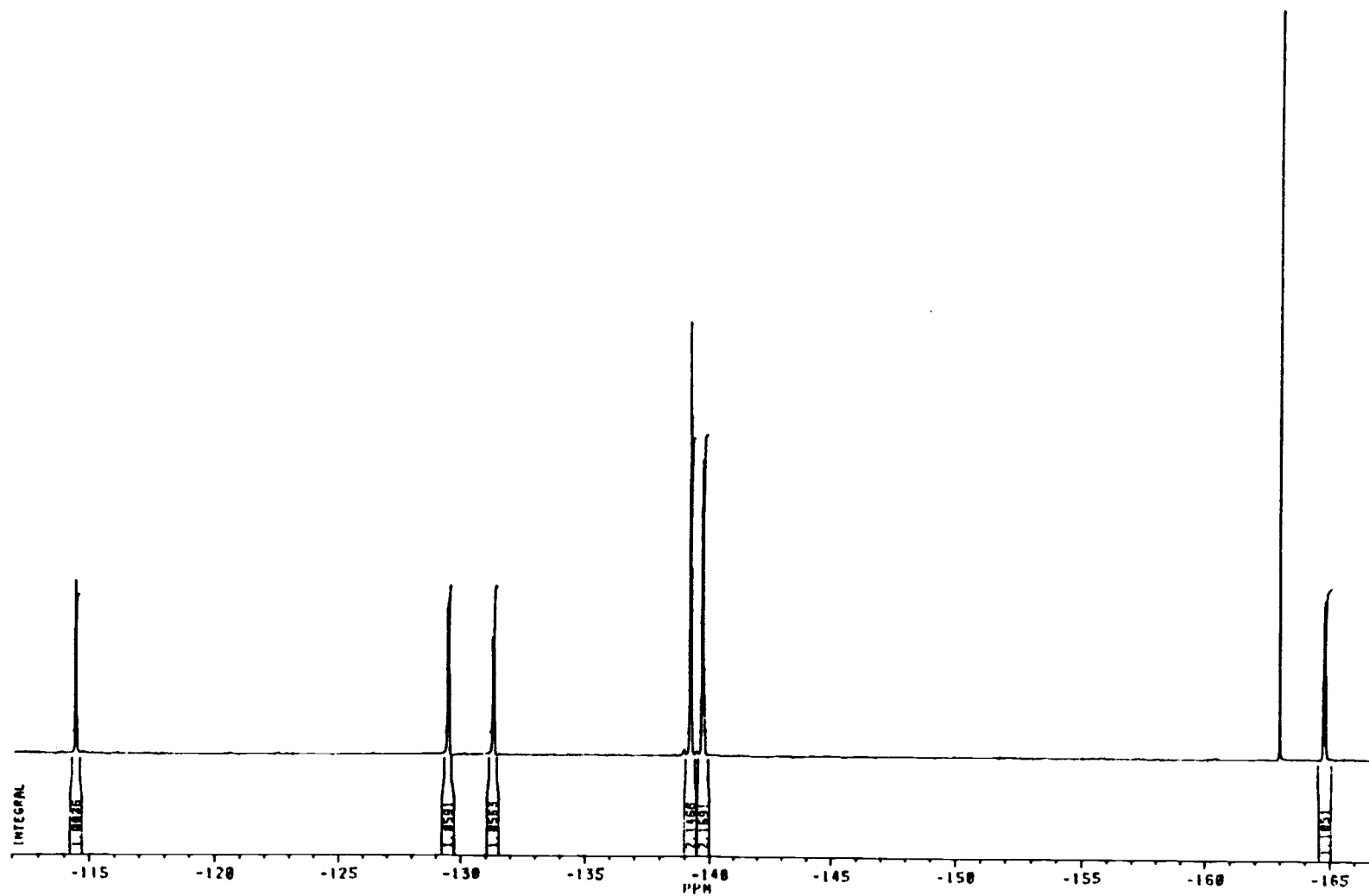


Figure 18. ^{19}F -NMR spectrum of 2,2',3,3',4,5',6,6'-octafluorobiphenyl (55).

List of chemical shifts (ppm from CFCl_3) and relative intensities for the ^{19}F -NMR spectrum of 55 (Fig. 18)

#	PPM	INTENSITY			
1	-114.4572	.917	61	-164.8458	2.267
2	-114.4657	1.012	62	-164.8616	2.169
3	-114.4802	2.484	63	-164.8742	2.113
4	-114.4872	2.988	64	-164.8899	2.027
5	-114.5090	4.184			
6	-114.5311	2.943			
7	-114.5381	2.317			
8	-114.5535	.869			
9	-114.5615	.783			
10	-129.4837	2.201			
11	-129.4922	2.257			
12	-129.5039	2.531			
13	-129.5113	3.614			
14	-129.5183	2.258			
15	-129.5302	2.327			
16	-129.5397	3.721			
17	-129.5490	2.248			
18	-129.5608	2.384			
19	-129.5682	3.556			
20	-129.5752	2.085			
21	-129.5869	2.016			
22	-129.5954	1.858			
23	-131.2780	1.136			
24	-131.2809	1.152			
25	-131.2961	2.780			
26	-131.2989	2.767			
27	-131.3171	2.796			
28	-131.3201	2.742			
29	-131.3371	1.909			
30	-131.3521	2.736			
31	-131.3733	2.523			
32	-131.3928	.840			
33	-139.1996	3.017			
34	-139.2259	3.775			
35	-139.2316	6.873			
36	-139.2585	10.472			
37	-139.2854	8.133			
38	-139.3137	4.508			
39	-139.3167	3.822			
40	-139.6776	1.397			
41	-139.6979	3.473			
42	-139.7100	3.581			
43	-139.7191	3.791			
44	-139.7294	5.929			
45	-139.7404	2.182			
46	-139.7507	7.075			
47	-139.7722	5.129			
48	-139.7867	2.419			
49	-139.7917	2.712			
50	-139.8071	2.107			
51	-139.8282	.735			
52	-163.0167	19.499			
53	-164.7334	1.952			
54	-164.7491	1.998			
55	-164.7620	2.051			
56	-164.7778	2.086			
57	-164.7897	3.827			
58	-164.8055	3.823			
59	-164.8183	3.897			
60	-164.8340	3.775			